Harnessing the interaction nanoparticle-protein for the design of smart carriers for drug delivery

Alba Balmori Pastor

UNIVERSITAT RAMON LLULL

DOCTORAL THESIS

Title	Harnessing the interaction nanoparticle-protein for the design of smart carriers for drug delivery
Presented by	Alba Balmori Pastor
Centre	IQS School of Engineering
Department	Bioengineering
Directed by	Dr. Salvador Borrós Gómez Dr. David Sánchez García

C. Claravall, 1-3 | 08022 Barcelona | Tel. 93 602 22 00 | Fax 93 602 22 49 | info@url.edu | www.url.edu

A mi familia

“Nothing in life is to be feared, it is only to be understood”

Marie Curie

Acknowledgments

Esta tesis es fruto del esfuerzo y apoyo que me han proporcionado mucha gente. Ante todo, me gustaría agradecer a mis directores de tesis, Dr. Salvador Borrós y Dr. David Sánchez, quienes han hecho este camino a mi lado y los cuales han hecho posible mi tesis doctoral. Salvador muchas gracias por abrirme la puerta y darme un sitio en tu familia y en disneyland. Gracias por brindarme la oportunidad de hacer el doctorado. ¡Alba! ¿Cuál es la pregunta?, ahora lo entiendo. Gracias por haberme enseñado tanto.

David, gracias por ayudarme y darme apoyo en todo momento, por tu disposición a resolverme dudas y tus ganas de sacar lo mejor de mí. Ha sido una suerte contar con tu codirección y tus consejos. Gracias por hacer ciencia siempre con una sonrisa.

Speranta Tanasescu, thanks for giving me the chance to work in your lab. I had a great time in Bucharest and I learnt a lot from the experience of working in a new and challenging environment. Thanks for your kindness and hospitality and for treating me so well.

Que gran suerte haber podido realizar la tesis en GEMAT. Un engranaje en el que todos aportan para siempre tirar hacia adelante. Os echaré tantísimos de menos mis tarados.

Primeros los doctores. AnnaMas, fuiste la primera, contigo empezó todo, me diste la mano y me ayudaste siempre que te necesité. Gracias por darme tu apoyo en los momentos de agobio y los buenos momentos que hemos vivido. Mi eterna presidenta, eres sencillamente increíble. Ai Robert… gracias por esa forma tan tuya de demostrar tu cariño en cada broma que haces y ser la alegría del laboratorio. ¿Uno callos para celebrarlo? Joan durante todo este tiempo hemos tenido momentos de todo tipo, pero siempre he sentido que podía contar contigo cuando lo necesitaba. Estoy tremendamente agradecida de haber podido coincidir contigo, Peri, qué gran orgullo. Gracias por darnos a todos una lección de cómo ser buen científico y mejor persona. Cris, el meu agraïment cap a tu és majúscul. Gràcies per contagiar-me del teu entusiasme per la ciència i per ajudar-me sempre que ho he necessitat sense esperar res a canvi. T'agraeixo moltíssim tot el que m'has solucionat, suggerit, respost i ensenyat aquests anys.

Mis queridos doctorandos… Nunu, el tiempo pone cada uno en su lugar, estos años me han dado la oportunidad de poder conocerte, gracias por aportarnos esa tranquilidad y dulzura. Cris, por demostrarnos lo fuerte que podemos llegar a ser y siempre con esa sonrisa en la cara, por ser una persona noble. Manu, lo prometido es deuda, por haberte hecho tu sitio en nuestro grupo por mérito propio, por haberte hecho querer por cómo eres y ser parte de nosotros. Mario, por ser una persona tan brillante y atenta a los demás, siempre dispuesto a ayudar. Polete, gracias por ese sexto sentido que hemos adquirido todos para esquivar tu falta de "psicomotricidad". Germanchitooo, gracias por habernos enseñado La Fira y por ser nuestro guía de antros. Tito, la Alba de hoy está super contenta de haber coincidido contigo estos años, pero la Alba de mañana…más. Patry, por enseñarnos tu

dualidad y que me haya encariñado con ambas. Antoñito, porque contigo somos más…pero mejor! El cierre de una preciosa época. Lopes, aunque ya no estés en el laboratorio, siempre tendrás tu sitio en nuestro corazón.

Muchas gracias al grupo de Sagetis por haberme enseñado tantísimas cosas, desde cultivos hasta facetas más sintéticas o como iba algún equipo o donde encontrar…cualquier cosa. Muchas gracias Miguel Ángel, Irene, Elena y Anna. Especialmente me gustaría darte las gracias a ti Marta, por haberme dedicado tantísimo tiempo y haberme dado todas las facilidades del mundo.

Gràcies al Lab Vell, a la Núria i a la Marina, per estar disposades a donar-me un cop de mà quan ho he necessitat.

Como no agradecer a los compañeros de mi otro laboratorio, los bioquímicos. Gracias por facilitarme cuanto necesité y amenizarme las dificultades con vuestras sonrisas y vuestro buen ambiente; gracias Sergi, Mire, Laia, Nuria, Marc y Bernat. Sergi ha sido un placer compartir mi última etapa contigo, ahora te tendrás que buscar a otra secretaria! Mire eres inspiración, quien quiere, puede, ¡no cambies nunca! Marc, qué bonito es aprender a tu lado al arte de vivir sin móvil. Bernat, gracias por tus clases magistrales de castellers, siempre tendrás una enxaneta cuando lo necesites. Mis compañeras de promoción, Laia y Nuria, muchas gracias por compartir conmigo este largo proceso y los ánimos que me daban fuerza para seguir adelante. Estela, aunque seas una emérita, has dejado huella, muchas gracias por tus consejos y por guiarme cuando lo he necesitado. Sois la muestra de lo bonita que puede ser la ciencia con el apoyo de amigos.

Dentro y fuera de IQS, gracias a mis compañeros de promoción y amigos más allá de la universidad: gracias Mariana, Anna, Marta, Sandra, Tess, Pocho, Sara, Sonia y Eric. Gracias por esta familia tan bonita que hemos creado durante tantos años.

A mis dos Vilapiscineros, Raul qué dos años más bonitos, he podido conocerte mejor y disfrutar de ti. Victor, gràcies per ser-hi sempre, quan se't necesita o quan simplement et vull veure. Gabi desde nuestras quedadas a las 7:30h para llegar a IQS te he podido conocer mejor, gracias por tu apoyo durante todos estos años.

Teta, qué gran descubrimiento, qué bonito que la vida te siga sorprendiendo con personas como tú.

En los buenos y en los malos momentos, no hubiese podido tener más suerte que tener amigos como vosotros. Mire y Marc, gracias por ser así, gracias por los vinitos, por los viajes y por los momentos de desconexión, gracias por las palabras de apoyo y las risas necesarias, gracias por ser una parte tan importante de mí. También me gustaría agradecer a Puxi y a Jaume por complementarlos tan bien y por todas las experiencias vividas y las que nos quedan por vivir juntos.

A ti, por ser tan especial, por ser el pilar de mi vida, por cuidarme y hacerme sentir tan bien, por hacerme ser mejor científica y lo más importante, mejor persona. Por haber llegado de una forma tan bonita a mí y por haberte convertido en la persona con la que quiero compartir el resto de mis días.

Llegados a este punto, me gustaría agradecer a quien debo de todo corazón esta tesis, quienes me han guiado desde siempre y a quienes me ha dado la oportunidad de llegar donde he llegado, a mi familia.

A mi madre. Mamá, tú has sido la inspiración que me ha llevado hasta aquí. Por enseñarme a luchar por mis sueños, por haber cuidado siempre de mí y haberme dado lo mejor.

A mi padre. Papá, eres mi ejemplo a seguir. El mundo sería tan bonito si todo el mundo fuera como tú. Gracias por haber confiado siempre en mí.

A mi hermana. Sara, persona fuerte que sabe lograr sus objetivos y la más dulce. Un orgullo que me hayas tocado como hermana. Gracias por todo lo que haces por mí.

A Óscar, mi hermano, gracias por haberme hecho ver lo friki que soy.

A mi abuela, por haberme criado y haberme dado todo el amor del mundo. Te quiero.

A mi Tita Paqui, por volver a ser quien éramos, por el cariño que nos hemos tenido siempre.

A mi Tita Jose, mi madrinita, por tantos momentos buenos vividos.

A mi Tío Jesús, por ser una persona tan desinteresadamente bondadosa.

Gracias a mis primos por todos los momentos vividos y por el calor de la familia, Andrea, Marc, Nira, Víctor y Óscar.

A mi abuelo, a mi yaya y a mi yayo, os llevaré siempre en mi corazón, porque sé lo orgullosos que os sentiríais de mí.

Muchas gracias a todos, por haberme dado un entorno tan bonito en el que crecer. Os quiero.

No tengo palabras suficientes para agradeceros todo lo que habéis hecho por mí. Los valores que me habéis inculcado y que me han hecho llegar donde me he propuesto. Sois mi referencia.

Abstract

HARNESSING THE INTERACTION NANOPARTICLE-PROTEIN FOR THE DESIGN OF SMART CARRIERS FOR DRUG DELIVERY

NPs have gained promise for its potential therapeutic applications as drug delivery systems. The common procedure for this purpose is dissolving, encapsulating, and finally adsorbing or adhering a drug on the NPs surface, avoiding the undesired damage to healthy cells and organs. In the same way, mesoporous silica nanoparticles (MSN) have recently attracted a lot of attention in the nanomedicine field due to their singular characteristics. However, the therapeutic efficiency of MSNs when used as drug delivery systems is often compromised by the pre-release of loaded drug molecules during the blood circulation and the lack of ability to do targeting. Considering these two problems, we propose in this doctoral Thesis the utilization of the widely known protein corona to avoid this premature release by fitting it into the pore. To achieve this, Human Serum Albumin-NP loaded with an antitumor drug for selective liver targeting MSN has been constructed. The main objective of this work is the development of a nanoparticle-protein complex capable of an efficient delivery of a therapeutic drug. This complex should simultaneously avoid premature release and be able to do liver targeting both by effect of the PC.

To reach this, first of all the synthesis of MSNs has been optimized, in order to obtain MSNs reproducible and with defined properties. Then, the corresponding characterization of their physicochemical traits showed that through the design of a DOE it is possible to elucidate which parameters have a higher influence on MSN synthesis. Furthermore, it has been here demonstrated that a qualitative and quantitative determination of the protein corona through an innovative use of analytical equipment is possible, the nanoDSC and ITC. This allows the deepening in the PC knowledge and control. It has also been assessed the effect of the protein corona in the release profile of an anti-tumor drug. Finally, the protein corona has been shown to provide a more sustained release of the drug to a liver tumor cell line, without affecting cell viability.

In conclusion, results have shown that the relationship between the pore size and the protein size in HSA-MSN systems determine the system's application. In this work it has been proposed the PC engineering according to the size ratio between the pore and the protein to use the same proteins that form the protein corona as gatekeepers while targeting the desired organ.

Resumen

HARNESSING THE INTERACTION NANOPARTICLE-PROTEIN FOR THE DESIGN OF SMART CARRIERS FOR DRUG DELIVERY

Las NP han surgido como prometedores sistemas de administración de fármacos por sus posibles aplicaciones terapéuticas. El procedimiento común para este propósito es disolver, encapsular y, finalmente, adsorber o adherir un medicamento a la superficie de la NP, evitando el daño no deseado a las células y órganos sanos. De la misma manera, las MSN recientemente han atraído mucha atención en el campo de la nanomedicina debido a sus características singulares. Sin embargo, la eficacia terapéutica de las nanopartículas de sílice mesoporosas (MSN) cuando se utilizan como sistemas de administración de fármacos a menudo se ven comprometidas por la liberación previa del fármaco cargado durante la circulación sanguínea y la falta de capacidad para llegar al destino deseado. Teniendo en cuenta estos dos problemas, proponemos en esta Tesis doctoral la utilización de la "protein corona" para evitar esta liberación prematura siendo ésta encajada en el poro. Para lograr esto, se han construido HSA-NP cargadas con un fármaco antitumoral para la dirección selectiva al hígado utilizando MSN. El objetivo principal de este trabajo es el desarrollo de un complejo de nanopartículas y proteínas, capaz de un suministrar eficientemente un fármaco terapéutico. Este complejo debe evitar simultáneamente la liberación prematura y ser capaz de atacar al hígado por efecto de la PC.

Para alcanzar esto, en primer lugar, se ha optimizado la síntesis de MSN, con el fin de obtener MSN reproducibles y con propiedades definidas. Luego, la caracterización correspondiente de sus rasgos fisicoquímicos mostró que, mediante el diseño de un DOE, es posible dilucidar qué parámetros tienen una mayor influencia en la síntesis de MSN. Además, en el presente trabajo se ha demostrado que es posible una determinación cualitativa y cuantitativa de la "protein corona" mediante un uso innovador de equipos analíticos; el nanoDSC y el ITC. Esto permite profundizar en el conocimiento y control de la PC. También se ha evaluado el efecto de la PC en el perfil de liberación de un fármaco antitumoral. Finalmente, se ha demostrado que la "protein corona" proporciona una liberación más sostenida del fármaco a una línea celular de tumor hepático, sin afectar la viabilidad celular.

En conclusión, los resultados han demostrado que la relación entre el tamaño de poro y el tamaño de la proteína en los sistemas HSA-MSN determina la aplicación del sistema. En este trabajo se ha propuesto que, mediante la ingeniería de la PC, según la relación de tamaño entre el poro y la proteína se pueden usar las mismas proteínas que forman la "protein corona" para bloquear la salida prematura del fármaco mientras se dirige al órgano deseado.

Resum

HARNESSING THE INTERACTION NANOPARTICLE-PROTEIN FOR THE DESIGN OF SMART CARRIERS FOR DRUG DELIVERY

Les NP han sorgit com prometedors sistemes d'administració de fàrmacs per les seves possibles aplicacions terapèutiques. El procediment comú per a aquest propòsit és dissoldre, encapsular i, finalment, adsorbir o adherir un medicament a la superfície de la NP, evitant el dany no desitjat a les cèl·lules i òrgans sans. De la mateixa manera, les nanopartícules de sílice mesoporoses (MSN) recentment han atret molta atenció en el camp de la nanomedicina per les seves característiques singulars. No obstant això, l'eficàcia terapèutica de les MSN quan s'utilitzen com a sistemes d'administració de fàrmacs sovint es veuen compromeses per l'alliberament previ del fàrmac carregat durant la circulació sanguínia i la manca de capacitat per arribar al destí desitjat. Tenint en compte aquests dos problemes, proposem en aquesta Tesi doctoral la utilització de la "protein corona" per evitar aquest alliberament prematura essent aquesta encaixada al porus. Per aconseguir això, s'han construït HSA-NP carregades amb un fàrmac antitumoral per a la direccionalitat selectiva del fetge utilitzant MSN. L'objectiu principal d'aquest treball és el desenvolupament d'un complex de nanopartícules i proteïnes, capaç de subministrar eficientment un fàrmac terapèutic. Aquest complex ha d'evitar simultàniament l'alliberament prematur i ser capaç de fer *targeting* al fetge per efecte de la PC.

Per assolir això, en primer lloc, s'ha optimitzat la síntesi de MSN, per tal d'obtenir MSN reproduïbles i amb propietats definides. Després, la caracterització corresponent dels seus trets fisicoquímics va mostrar que, mitjançant el disseny d'un DOE, és possible dilucidar quins paràmetres tenen una major influència en la síntesi de MSN. A més, en el present treball s'ha demostrat que és possible una determinació qualitativa i quantitativa de la "protein corona" mitjançant un ús innovador d'equips analítics; el nanoDSC i l'ITC. Això permet aprofundir en el coneixement i control de PC. També s'ha avaluat l'efecte de la PC en el perfil d'alliberament d'un fàrmac antitumoral. Finalment, s'ha demostrat que la "protein corona" proporciona un alliberament més sostingut del fàrmac a una línia cel·lular de tumor hepàtic, sense afectar la viabilitat cel·lular.

En conclusió, els resultats han demostrat que la relació entre la mida de porus i la mida de la proteïna en els sistemes HSA-MSN determina l'aplicació del sistema. En aquest treball s'ha proposat que, mitjançant l'enginyeria de PC, segons la relació de mida entre el porus i la proteïna es poden fer servir les mateixes proteïnes que formen la "protein corona" per bloquejar la sortida prematura del fàrmac mentre es dirigeix a l'òrgan desitjat.

Table of Contents

Index of Figures

Figures from Chapter I

Figures from Chapter II

Figures from Chapter III

Figures from Chapter IV

Index of Tables

Tables from Chapter II

Tables from Chapter III

List of Abbreviations

Å	Armstrong
AcONa	Sodium acetate
Al_2O_3	Aluminium oxide
AML12	Alpha mouse liver 12
APTES	(3-aminopropyl)triethoxysilane
AR	Aspect ratio
Au	Gold
Ag	Silver
BCA	Bicinchoninic acid assay
BET	Brunauer-Emmett and Teller theory
BI	Biological identity
BJH	Barrett-Joyner-Halenda method
BOC	*Tert*-butyloxycarbonyl
BrAcOEt	Ethyl bromoacetate
brs	Broad signal
ºC	Celsius Degrees
$CDCl_3$	Cloroform
CEN	European Committee for Standardization
CeO_2	Cerium (IV) oxide
CTAB	Cetyltrimethylammonium bromide
cm	Centimetres
Cu	Copper
^{13}C-NMR	Carbon nuclear magnetic resonance
CO_2	Carbon dioxide
CryoTEM	Cryogenic electron microscopy
d	Doublet
DCM	Dichloromethane
dd	Doublet of doublets
ddd	Doublet of doublets of doublets
df	Degrees of freedom
DLS	Dynamic Light Scattering
DMEM	Dulbecco's Modified Eagle Medium
DMSO	Dimethyl Sulfoxide
DNA	Deoxyribonucleic Acid
DOE	Design of experiments
DOX	Doxorubicin
Eq	Equivalent

EtOH	Ethanol
5-FU	5-Fluorouracil
FBS	Fetal Bovine Serum
FDA	Fluorescein diacetate
Fe	Iron
Fe_2O_4	Iron (IV) oxide
FE-SEM	Field Emission Scanning Electron Microscope
FITC	Fluorescein IsoTioCyanate
FT-IR	Fourier Transform Infrared Spectroscopy
g	Gram
GO	Glucose oxidase
H_2	Hydrogen
H_2O	Water
HCl	Chlorhydric Acid
HeLa	Human Cervical Carcinomal Cell Line
HepG2	Liver hepatocellular carcinoma
HSA	Human Serum Albumin
^{1}H-NMR	Proton Nuclear Magnetic Resonance
IR	Infrared
kDa	Kilo Dalton
Lys	Lysozyme
M	Molar
m	Complex multiplet
mBar	Milli Bar
MeOH	Methanol
$MgSO_4$	Magnesium sulphate
MHz	Mega Hertz
min	Minute
mL	Millilitre
MicroITC	Micro Isothermal Titration calorimeters
MW	Molecular weight
MSN	Mesoporous Silica Nanoparticle
MTT	3-(4,5-dimethylthiazol-2-yl)-2,5-duphenyltetrazolium bromide
mV	Millivolts
N_2	Nitrogen
NanoDSC	Nano Differential Scanning Calorimeter
NaOH	Sodium Hydroxide
NH_3	Ammonium
NH_4NO_3	Ammonium nitrate
Ni	Nickel

nm	Nanometre
NP	Nanoparticle
pBAEs	Poly(β-aminoester)s
PBS	Phosphate Buffered Saline
PC	Protein Corona
Pd/C	Palladium on carbon
PdI	Polydispersity Index
PEG	Polyethylene glycol
PI	Isoelectric Points
PVP	Polyvinylpyrrolidone
q	Quartet
RNA	Ribonucleic Acid
RPM	Revolutions per minute
s	Singlet
SCN	Isothiocyanate
SD	Standard deviation
SDS	Sodium Dodecyl Sulphate
SDS-Page	SDS Polyacrylamide Gel Electrophoresis
SEM	Scanning Electron Microscope
SI	Synthetic Identity
SiO_2	Silicon dioxide
Si-O-Si	Siloxane bones
SN	Supernatants
T	Triplet
TEOS	Tetraethlorthosilicate
TMS	Tetramethylsilane
THF	Tetrahydrofura**n**
TiO_2	Titanium oxide
T_m	Transition midpoint
TsCl	4-Toluenesulfonyl chloride
UV-Vis	Ultraviolet Visible
W/W	Mass fraction (weight/weight)
Zn	Zinc
µm	Micrometre

Chapter I. Motivations and aims

This page left blank intentionally

Introduction: Protein Corona

Nanotechnology is rapidly progressing as a tool for drug delivery systems allowing to solve several limitations of conventional drugs such as nonspecific biodistribution and targeting, lack of solubility, poor bioavailability and low therapeutic indexes. In this study, we describe the development of a nanoparticle-protein complex capable of an efficient delivery of therapeutic drugs[1].

1.1 State of the art

Nanotechnology is the modern multidisciplinary science which studies, understands and controls the manipulation of materials on a nanometric scale. It is based on the manipulation of individual atoms and molecules to produce materials from them for applications well below the sub-microscopic level. Nanotechnology includes many structures and techniques at a scale around 100 nm. One of the most popular structures which are object of study by nanotechnology are nanoparticles (NP). NPs can be classified in two broad families of nanobjects: organic nanoparticles including dendrimers, liposomes, polymer systems and micelles and inorganic nanoparticles, such as "quantum dots", carbon nantotubes and all kinds of transition metal nanoparticles and silica among others (Figure 1)[2,3,4,5].

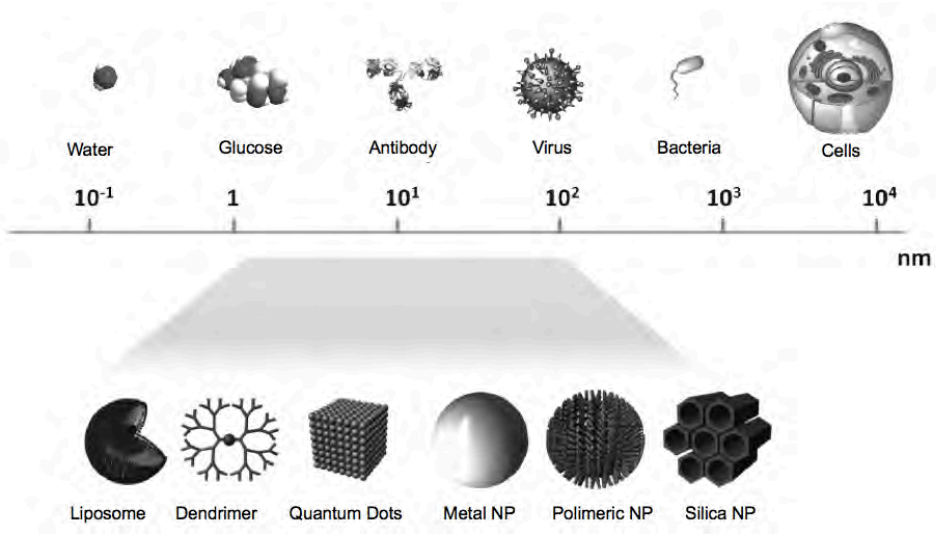

Figure 1: Size-comparison of nanoparticles at nanometer scale.

NPs are supposed a discovery of the XX century, however artisans in Mesopotamia were the first to use materials of this type as early as in the IX century BC, to obtain a glittering effect on the surface of ceramic vessels[6,7]. During the Renaissance and in later times, the development of visual arts and printing and engraving methods contributed to the technique of producing fine inorganic and organic dust particles used as dyes or ink[8,9,10,11]. Despite the usages of nanoparticles, Michael Faraday was the first to provide a scientific description of the optical properties of nanometric metal particles, in a paper he published in 1857[12]. Ten years later (1867), James Clark Maxwell[13], suggested a series of concepts of differentiation in nanotechnology, but without using the word "nanotechnology" to define thin, monomolecular layers[14]. Despite these early advances in nanotechnology it took almost 50 years more for the first accurate observations and measurements, from the hand of Richard Adolf Zsigmondy, who used dark field ultramicroscopy which allows the visualization of particles smaller than monochromatic light wavelength and was able to observe 1/1.000.000 mm particles (1914). He was the first author to apply the term "nanoparticles" explicitly to such particles[15]. In 1920, Irving Langmuir and Katharine B. Blodgett, dealing with nanoparticle characterization and related phenomena that define interface in colloid science, introduced the concept of monolayer, a layer of material one molecule thick[16,17].

In recent years, nanoparticles have helped to considerably improve, even revolutionize, many technology and industry sectors such as information technology, homeland security, medicine, transportation, energy, food safety, and environmental science, among many others[18]. Their application to medicine, known as nanomedicine, concerns the use of precisely engineered materials at this length scale, as nanoparticles, to develop novel therapeutic and diagnostic modalities[19,20].

NPs can be used to overcome some of the limitations found in traditional therapeutic and diagnostic agents: problems associated with the solubility, bioavailability, immunocompatibility and cytotoxicity. Some of these limitations have already been issued through the use of nanoparticles as drug delivery vehicles for increased circulatory persistence and targeted delivery to specific sites; transporters to promote their controlled release; adjuvants for vaccines; diagnostic tools and drug delivery devices[21,22,23,24].

One of the most exploited fields of nanoparticles' technology is precisely their application in drug delivery. The common procedure for this purpose is the following: the drug of interest is dissolved, encapsulated, and finally adsorbed or adhered on the nanoparticles. The advantages of the use of nanoparticles for the administration of drugs

are mainly due to their particular size, since in many cases they can cross easily the cellular membrane, get to inflammation sites, pass over the epithelium, and penetrate into tumours or microcapillaries[25,26]. Also, the small particles have a greater surface area-volume ratio, which favours a greater association of the drug with the molecules of the target organ (being more exposed) and therefore, a faster release of the drug. On the other hand, the larger particles have large nuclei, which allows a greater amount of drug encapsulated by the particles and make the release slower[27,28].

After systemic administration, NPs are exposed to fluids, mostly blood, that contain proteins and other biomolecules. The adsorption of proteins on NPs is so-called “protein corona” (PC). This adsorption can modify the physicochemical properties of NPs such as size, surface charge, and functionality, hence conferring a new biological identity to NPs. This PC determines various biological responses such as fibrillation, cellular uptake, circulation time bioavailability, and even toxicity, whence the physiological response[29,30,31,32,33].

The proteins in the corona can remain for a relevant time on the NP surface (hard corona), possibly preventing the adsorption of the other molecules. Other proteins, instead, dynamically exchange with those in solution (soft protein corona). Due to the important role that the evolution of the corona plays in the way that NPs interact with biological systems, it is crucial for any possible biological application to understand how the processes of the protein adsorption and exchange occur. The formation and kinetic evolution of the corona, depends on the nanoparticles’ synthetic identity (physicochemical properties), such as the size, shape, curvature and pore size, among the others [34,35,36,37,38,39].

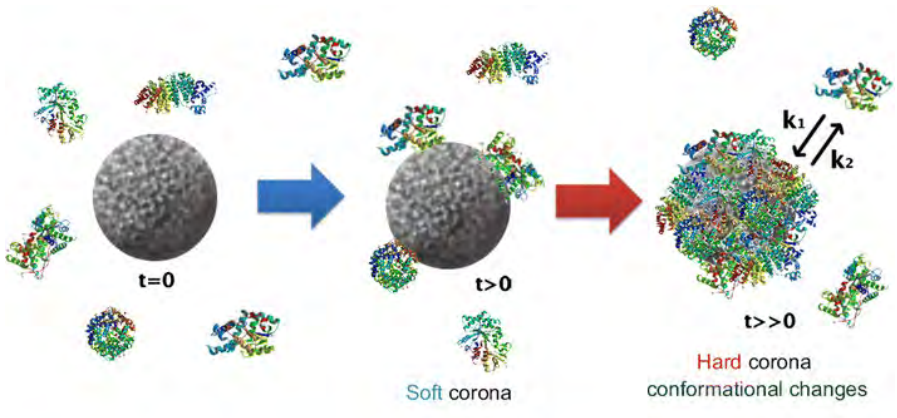

Figure 2: Schematic illustration of a hard and soft protein corona formation. Hard coronas are characterized by slow exchange and lower abundance, with a high affinity of proteins, whereas soft coronas are typed by rapid exchange and lower affinity of proteins with weakly bound outer layers on NPs.

Since the formation of PC coats the NP surface, some researchers focus on avoiding the formation of the PC in order to maintain the targeting abilities of the NPs after their incubation in biological fluids. Moreover, protein corona induces a reduction in the uptake of the targeted NPs. By contrast, some studies demonstrate that the PC does not significantly affect the targeting ability of functionalized NPs[40,41,42,43]. These contributions prompt two considerations, the first one being the importance of studying the physicochemical properties of NPs, and the second one the new NP identity provided by the PC that may result in the loss of targeting properties, thereby affecting the pharmacokinetics and its payload[44,45].

In spite of these scientific advances, which state that the PC formation affects negatively or does not affect targeting of the drug delivery system, some drug delivery systems effectively attach proteins for tumour targeting. For instance, the commercial complex of paclitaxel and albumin, so-called “Abraxane”, is used to treat pancreatic cancer[46,47,48]. In the same way, albumin is widely used for liver targeting. Some reports have demonstrated the liver cancer cells’ overexpression of specific human serum albumin receptors and their ability to internalize large amounts of HSA through the mechanism of caveolae-mediated endocytosis[49,50,51,52]. Also, albumin is the most abundant plasma protein involved in the natural transport of the nutrients within the body facilitated by its multiple ligand binding sites, cellular receptor engagement, and a long circulatory half-life of ~19 days due to interaction with the recycling neonatal Fc receptor. Exploitation of these properties promotes albumin as an attractive candidate for half-life extension and targeted intracellular delivery of drugs attached in the NPs’ surface. Thus, albumin is an interesting next-generation “self” drug delivery approach[53,54,55].

Considering all these advances, we propose the construction of a Human Serum Albumin-NP loaded with an antitumor drug for selective liver targeting using mesoporous silica nanoparticles (MSN)[56]. MSN have attracted a lot of attention in the nanotechnology field due to their characteristics, such as the high surface area that allows store a large amount of cargo, the high pore volume, good chemical and thermal stability, non-toxicity and biocompatibility, morphological ease of modification, among others[57,58,59,60]. Basically, the mesoporous form of silica has unique properties, particularly interesting for loading therapeutic agents at high quantities and their subsequent releases[61,62,63,64]. These MSNs are constituted by a matrix of silica and have pores of a diameter ranged between 2 and 50 nm[65]. This singularity provides these NPs with two differentiated domains: an external surface and an internal one inside the pores[66,67,68].

However, the therapeutic efficiency of MSNs used as drug delivery system is often compromised by the pre-release of physically loaded drug molecules during the blood circulation and a lack of ability to do targeting, which accounts for a low level of drug accumulation in the target cancer cells and undesired damage to healthy cells and organs[69]. To improve their therapeutic efficacy and minimize the side effects the block of the pore of MSNs with desirable sealants for controlled drug release is needed[70]. MSN systems have shown particular promising results in preventing premature release of drugs in physiological conditions[71,72,73]. Also, they have been used for controlling drug release at targeted sites when the pores of MSN are capped with various gatekeepers anchored to the surface such as metallic nanoparticles, quantum dots, and macromolecules those being responsive to the complex tumour microenvironment[74,75,76].

To address these issues, the approach detailed hereinafter is that the specific properties given by the pores allow both an internal space in the pore to load an antitumor drug and the formation of a PC on the MSN's surface. It is here proposed the study of the relationship between the pore size and the protein size, which will determine the system's application. That is, three scenarios are possible: proteins adsorbed on the NPs' surface, proteins fitted inside the pore and proteins that will enter the NP silica matrix. And this leads to different applications: organ or tissue targeting[49,50], blocking of the pores for controlled drug release[77] or release of the same protein from the nanoparticle[78].

Aimed at understanding the influence of the pore size in the behaviour of proteins and the necessity of blocking the premature release of the drug during the MSN circulation, in this work it is proposed the PC engineering according to the size ratio between the pore and the protein to use the **same proteins** that form the protein corona as **gatekeepers** while **targeting** the desired organ.

1.2 Aims

The main objective of this thesis is to develop a nanoparticle-protein complex capable of an efficient delivery of therapeutic drug.

In particular, the specifics objectives goals of the present thesis can be summarized as follows:

- Development of a methodology for the preparation of MSN through a DOE in order to obtain MSNs reproducible and with defined properties such as a size, shape and pore size; and the corresponding characterization of the physicochemical traits (**Chapter 2. Synthesis Identity).**

- Formation of a protein corona in the MSN's surface and correlation of the synthetic identity with the biological identity that the proteins provide. The quantitative and qualitative determination of the protein corona through an innovative use of some analytical equipment to go deep in the PC knowledge and control. (**Chapter 3. Biological Identity**).

- Assessment of the effect of the protein corona in the release profile of an anti-tumor drug, use of the protein corona to obtain a more sustained release of the drug for its use as a drug delivery system to a liver tumor; and the in vitro uptake and viability, i.e. the physiological response (**Chapter 4. Physiological response**)

1.3 Content of this Dissertation

The multiple important advances in the area of nanotechnology bring nanoparticles closer to their goal as drug delivery vehicles. Even so, the understanding of how their synthetic identity has an influence on their biological identity needs to improve in order to increase the control over the physiologic response of nanoparticles. This way, the treatment for some diseases could be addressed or enhanced.

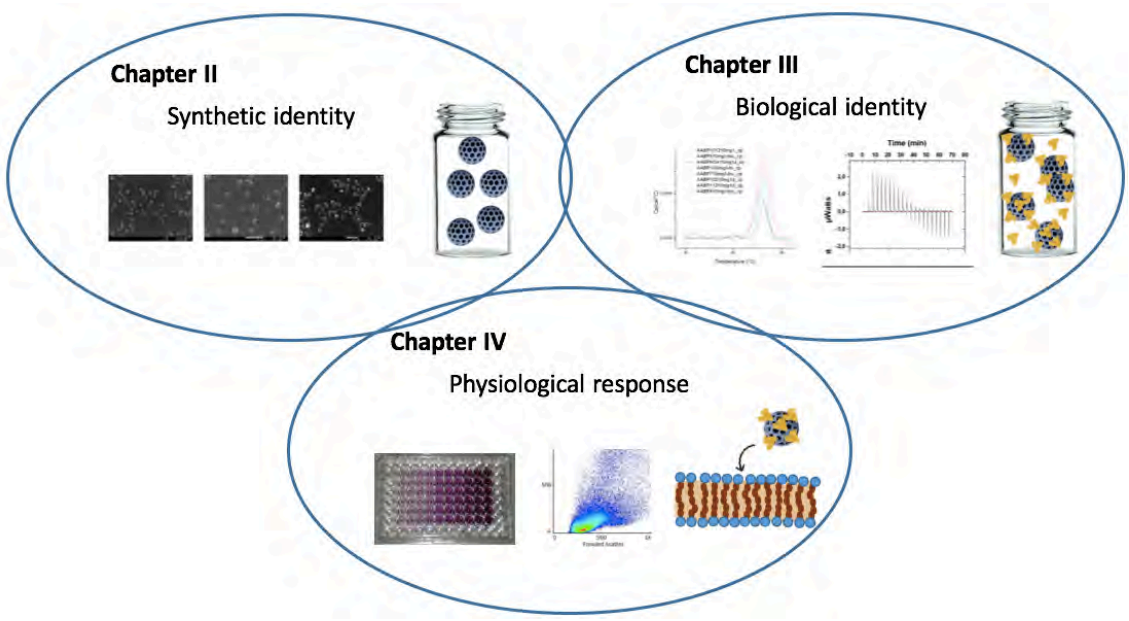

Figure 3: Structure of the different chapters.

In this doctoral thesis, it is proposed to prepare a set of MSN with a wide range of properties with the aim to assess the formation of PC. Therefore, different batches of MSNs will be synthesized in Chapter II, in order to have nanoparticles with different physicochemical properties. To do so, a DOE (Design Of Experiments) is designed to have differentiated physicochemical characteristics of the nanoparticles by changing the synthetic conditions. This way, it will be possible to tune the synthetic identity of the nanoparticles. Moreover, the resulting NP will be properly functionalized to introduce electrostatic charges and modulate their lipophilicity.

Then, with the aim of obtaining drug delivery systems, the protein corona that is formed after the systemic administration of nanoparticles will be studied. This protein corona will be characterized in the Chapter III through a newly application of a thermodynamic equipment. The different profiles of PC that are obtained are correlated with the synthetic identities described in Chapter II. In the Chapter III will be devoted to understand the relationship between the formation of the PC and the pore. Later, in Chapter IV, the

mentioned protein-nanoparticle complexes will be exposed to a cellular environment to evaluate their *in vitro* response. More specifically two hepatic cell lines are employed, one being from hepatic carcinoma and the other one healthy hepatic cells. Previously, it is needed the loading of a drug into the nanoparticle's pores. In this case, since it is the most widely employed anticancer drug, Doxorubicin is chosen. Due to the obtained results it was needed to change DOX by 5-Fluorouracil, an anti-cancer chemotherapeutic drug with a different molecular structure.

The deep knowledge of the relationship between synthetic identity, biological identity and the physiological response is key to reach the main aim of this thesis. A nanoparticle is safe and effective only when its physiological response is understood and can be controlled. For this reason, this thesis proposes an innovative way to control and understand the biological behavior of mesoporous silica nanoparticles that can lead to their use for hepatic cancer treatment.

1.4 References

(1) Vallet-Regí, M.; Colilla, M.; Izquierdo-Barba, I.; Manzano, M. Mesoporous Silica Nanoparticles for Drug Delivery: Current Insights. *Molecules* **2018**, *23* (1), 3–5.

(2) Ferrari, M. Nanovector Therapeutics. *Curr. Opin. Chem. Biol.* **2005**, *9* (4), 343–346.

(3) Mahmoodi, N. M.; Khorramfar, S.; Najafi, F. Amine-Functionalized Silica Nanoparticle: Preparation, Characterization and Anionic Dye Removal Ability. *Desalination* **2011**, *279* (1–3), 61–68.

(4) Albanese, A.; Walkey, C. D.; Olsen, J. B.; Guo, H.; Emili, A.; Chan, W. C. W. Secreted Biomolecules Alter the Biological Identity and Cellular Interactions of Nanoparticles. *ACS Nano* **2014**, *8* (6), 5515–5526.

(5) Llinàs, M. C.; Sánchez-garcía, D. Nanoparticulas de Sílice y Aplicaciones En Biomedicina. *Afinidad LXX!* **2014**, *565*, 20–31.

(6) Heiligtag, F. J.; Niederberger, M. The Fascinating World of Nanoparticle Research. *Mater. Today* **2013**, *16* (7–8), 262–271.

(7) Sitzman, B. B. Nanoparticles. How Small Are Nanoparticles? Open for Discussion. *Chem. Mater.* **2012**, No. October.

(8) You, A.; Be, M. A. Y.; In, I. Copper in Glazes of Renaissance Luster Pottery : Nanoparticles , Ions , and Local Environment. *J. Appl. Phys.* **2007**, *10058* (March 2003), 6–12.

(9) Pe, J.; Molera, J.; Larrea, A.; Pradell, T.; Vendrell-saz, M.; Borgia, I.; Brunetti, B. G.; Cariati, F.; Fermo, P.; Mellini, M.; et al. Luster Pottery from the Thirteenth Century to the Sixteenth Century : A Nanostructured Thin Metallic Film. *J. Am. Ceram. Soc* **2001**, *84*, 442–446.

(10) Berger, M. *Nano-Society: Pushing the Boundaries of Technology*; 2009.

(11) Seifert, M. Nanothechnology. The Future Is Tiny By Michael Berger. *Angew Chem* **2017**, *129*, 7457.

(12) November, R.; February, R. Experimental Relations o f Gold {and Other Metals) to Light. B Y. **1857**.

(13) Maxwell, J. C.; Nivin, W. D. *The Scientific Papers of James Clerck Maxwell*; 1890.

(14) J, D. R. No Title. *Eng. Physics, Tata McGraw-Hill Educ.* **2010**.

(15) Zsigmondy, R. A. Properties of Colloids, Nobel Lectures, Chemistry 1922-1941. *Amsterdam Elsevier Publ. Co.* **1966**.

(16) Langmuir, I. The Constitution and Fundamental Properties of Solids and Liquids. *Met. Chem. Eng.* **1916**, *468* (15).

(17) Greenspan, J.; Greenspan, J. An Extraction Method Fot the Determination of Acids and Its Application to Para-Hydroxybenzoic Acid. *J. Am. Chem. Soc.* **1935**, *57* (6).

(18) M. Rosenholm, J.; Sahlgren, C.; Linden, M. Multifunctional Mesoporous Silica Nanoparticles for Combined Therapeutic, Diagnostic and Targeted Action in Cancer Treatment. *Curr. Drug Targets* **2011**, *12* (8), 1166–1186.

(19) Rizvi, S. A. A.; Saleh, A. M. Applications of Nanoparticle Systems in Drug Delivery Technology. *Saudi Pharm. J.* **2018**, *26* (1), 64–70.

(20) Ming, X.; Li, F.; Zheng, C.; Xin, J.; Chen, F.; Ling, H.; Sun, L.; Webster, T.; Liu, J. Enhanced Tumor Delivery and Antitumor Response of Doxorubicin Loaded Albumin Nanoparticles Formulated Based on a Schiff Base. *Int. J. Nanomedicine* **2016**, *Volume 11*, 3875–3890.

(21) Baeza, A.; Castillo, R. R.; Torres-Pardo, A.; González-Calbet, J. M.; Vallet-Regí, M. Electron Microscopy for Inorganic-Type Drug Delivery Nanocarriers for Antitumoral Applications: What Does It Reveal? *J. Mater. Chem. B* **2017**, *5* (15), 2714–2725.

(22) Zhang, Y.; Yang, C.; Wang, W.; Liu, J.; Liu, Q.; Huang, F.; Chu, L.; Gao, H.; Li, C.; Kong, D.; et al. Co-Delivery of Doxorubicin and Curcumin by PH-Sensitive Prodrug Nanoparticle for Combination Therapy of Cancer. *Sci. Rep.* **2016**, *6* (January), 1–12.

(23) Agudelo, D.; Bourassa, P.; Bruneau, J.; Bérubé, G.; Asselin, É.; Tajmir-Riahi, H. A. Probing the Binding Sites of Antibiotic Drugs Doxorubicin and N-(Trifluoroacetyl) Doxorubicin with Human and Bovine Serum Albumins. *PLoS*

One **2012**, *7* (8), 1–13.

(24) Thao, L. Q.; Byeon, H. J.; Lee, C.; Lee, S.; Lee, E. S.; Choi, Y. W.; Choi, H. G.; Park, E. S.; Lee, K. C.; Youn, Y. S. Doxorubicin-Bound Albumin Nanoparticles Containing a TRAIL Protein for Targeted Treatment of Colon Cancer. *Pharm. Res.* **2016**, *33* (3), 615–626.

(25) Zhang, M.; Xu, C.; Wen, L.; Han, M. K.; Xiao, B.; Zhou, J.; Zhang, Y.; Zhang, Z.; Viennois, E.; Merlin, D. A Hyaluronidase-Responsive Nanoparticle-Based Drug Delivery System for Targeting Colon Cancer Cells. *Cancer Res.* **2016**, *76* (24), 7208–7218.

(26) Zhang, L.; Li, J.; Chen, T.; Deng, F.; Wan, J.; Tang, Y.; Yuan, P. Synthesis, Characterization, and in Vitro Evaluation of Curcumin-Loaded Albumin Nanoparticles Surface-Functionalized with Glycyrrhetinic Acid. *Int. J. Nanomedicine* **2015**, *10* (1), 5475.

(27) Gelperina, S.; Kisich, K.; Iseman, M. D.; Heifets, L. The Potential Advantages of Nanoparticle Drug Delivery Systems in Chemotherapy of Tuberculosis. *Am. J. Respir. Crit. Care Med.* **2005**, *172* (12), 1487–1490.

(28) Burke, T. G.; Mi, Z. The Structural Basis of Camptothecin Interactions with Human Serum Albumin: Impact on Drug Stability. *J. Med. Chem.* **1994**, *37* (1), 40–46.

(29) Lazarovits, J.; Chen, Y.; Sykes, A.; Chan, W. C. W. Nanoparticle – Blood Interactions : The Implications on Solid Tumour Targeting. *Chem. Commun.* **2015**, *51*, 2756–2767.

(30) Lesniak, A.; Campbell, A.; Monopoli, M. P.; Lynch, I.; Salvati, A.; Dawson, K. A. Serum Heat Inactivation Affects Protein Corona Composition and Nanoparticle Uptake. *Biomaterials* **2010**, *31* (36), 9511–9518.

(31) Shahabi, S.; Treccani, L.; Dringen, R.; Rezwan, K. Nanoparticles for Dual Drug Loading and Release †. *Nanoscale* **2015**, *7*, 16251–16265.

(32) Mahmoudi, M.; Lohse, S. E.; Murphy, C. J.; Fathizadeh, A.; Montazeri, A.; Suslick, K. S. Variation of Protein Corona Composition of Gold Nanoparticles Following Plasmonic Heating. *Nano Lett.* **2013**, *14* (1), 6–12.

(33) Casals, E.; Pfaller, T.; Duschl, A.; Oostingh, G. J.; Puntes, V. Time Evolution of the Nanoparticle Protein Corona. *ACS Nano* **2010**, *4* (7), 3623–3632.

(34) Flanagan, M. B.; Lundqvist, M.; Stigler, J.; Cedervall, T.; Bergga, T. The Evolution of the Protein Corona around Nanoparticles : A Test Study. *ACS Appl. Nano Mater.* **2011**, *5* (9), 7503–7509.

(35) Vilanova, O.; Mittag, J. J.; Kelly, P. M.; Milani, S.; Dawson, K. A.; Ra, J. O. Understanding the Kinetics of Protein − Nanoparticle Corona Formation. *ACS Appl. Nano Mater.* **2016**, *10*, 10842–10850.

(36) Lee, B. Protein Corona : A New Approach for Nanomedicine Design. *Int. J. Nanomedicine* **2017**, *12*, 3137–3151.

(37) Ritz, S.; Schöttler, S.; Kotman, N.; Baier, G.; Musyanovych, A.; Kuharev, J.; Landfester, K.; Schild, H.; Jahn, O.; Tenzer, S.; et al. Protein Corona of Nanoparticles: Distinct Proteins Regulate the Cellular Uptake. *Biomacromolecules* **2015**, *16* (4), 1311–1321.

(38) Docter, D.; Distler, U.; Storck, W.; Kuharev, J.; Wünsch, D.; Hahlbrock, A.; Knauer, S. K.; Tenzer, S.; Stauber, R. H. Quantitative Profiling of the Protein Coronas That Form around Nanoparticles. *Nat. Protoc.* **2014**, *9* (9), 2030–2044.

(39) Tenzer, S.; Docter, D.; Kuharev, J.; Musyanovych, A.; Fetz, V.; Hecht, R.; Schlenk, F.; Fischer, D.; Kiouptsi, K.; Reinhardt, C.; et al. Rapid Formation of Plasma Protein Corona Critically Affects Nanoparticle Pathophysiology. *Nat. Nanotechnol.* **2013**, *8* (10), 772–781.

(40) Corbo, C.; Molinaro, R.; Parodi, A.; Toledano Furman, N. E.; Salvatore, F.; Tasciotti, E. The Impact of Nanoparticle Protein Corona on Cytotoxicity, Immunotoxicity and Target Drug Delivery. *Nanomedicine* **2016**, *11* (1), 81–100.

(41) Xiao, W.; Gao, H. The Impact of Protein Corona on the Behavior and Targeting Capability of Nanoparticle-Based Delivery System. *International Journal of Pharmaceutics*. 2018, pp 328–339.

(42) Dobrovolskaia, M. A.; Neun, B. W.; Man, S.; Ye, X.; Hansen, M.; Patri, A. K.; Crist, R. M.; McNeil, S. E. Protein Corona Composition Does Not Accurately Predict Hematocompatibility of Colloidal Gold Nanoparticles. *Nanomedicine Nanotechnology, Biol. Med.* **2014**, *10* (7), 1453–1463.

(43) Karmali, P. P.; Simberg, D. Interactions of Nanoparticles with Plasma Proteins: Implication on Clearance and Toxicity of Drug Delivery Systems. *Expert Opin. Drug Deliv.* **2011**, *8* (3), 343–357.

(44) S.R., S.; A., D.; A.L., L. Interaction of Nanoparticles with Proteins: Relation to Bio-Reactivity of the Nanoparticle. *J. Nanobiotechnology* **2013**, *11* (1), 1–12.

(45) Mirshafiee, V.; Kim, R.; Park, S.; Mahmoudi, M.; Kraft, M. L. Impact of Protein Pre-Coating on the Protein Corona Composition and Nanoparticle Cellular Uptake. *Biomaterials* **2016**, *75*, 295–304.

(46) (EMA), E. M. A. Cetuximab; Erbitux®. Anexo I: Ficha Técnica o Resumen de Las Características Del Producto. *Agencia Eur. Medicam.* **2014**, 1–33.

(47) Green, M. R.; Manikhas, G. M.; Orlov, S.; Afanasyev, B.; Makhson, A. M.; Bhar, P.; Hawkins, M. J. Abraxane®, a Novel Cremophor®-Free, Albumin-Bound Particle Form of Paclitaxel for the Treatment of Advanced Non-Small-Cell Lung Cancer. *Ann. Oncol.* **2006**, *17* (8), 1263–1268.

(48) Trofe, J.; Wimberley, S. Solid Organ Transplant: Medication Management Issues. *J. Am. Pharm. Assoc. (Wash).* **2000**, *40* (5 Suppl 1), 99–106.

(49) Wang, H.; Thorling, C. A.; Liang, X.; Bridle, K. R.; Grice, J. E.; Zhu, Y.; Crawford, D. H. G.; Xu, Z. P.; Liu, X.; Roberts, M. S. Diagnostic Imaging and Therapeutic Application of Nanoparticles Targeting the Liver. *J. Mater. Chem. B* **2015**, *3* (6), 939–958.

(50) Surendran, S. P.; Thomas, R. G.; Moon, M. J.; Jeong, Y. Y. Nanoparticles for the Treatment of Liver Fibrosis. *Int. J. Nanomedicine* **2017**, *12*, 6997–7006.

(51) L.H., R.; P., C. Nanotechnology for Therapy and Imaging of Liver Diseases. *J. Hepatol.* **2011**, *55* (6), 1461–1466.

(52) Gun'ko, V. M.; Turov, V. V.; Krupska, T. V.; Tsapko, M. D. Interactions of Human Serum Albumin with Doxorubicin in Different Media. *Chemical Physics*. 2017, pp 26–34.

(53) Chicea, D.; Chicea, R.; Chicea, L. M. HSA Particle Size Characterization by AFM. *Rom. Reports Phys.* **2013**, *65* (1), 178–185.

(54) Chi, E. Y.; Krishnan, S.; Randolph, T. W.; Carpenter, J. F. Physical Stability of

Proteins in Aqueous Solution: Mechanism and Driving Forces in Nonnative Protein Aggregation. *Pharm. Res.* **2003**, *20* (9), 1325–1336.

(55) Bartczak, D.; Vincent, P.; Goenaga-Infante, H. Determination of Size- and Number-Based Concentration of Silica Nanoparticles in a Complex Biological Matrix by Online Techniques. *Anal. Chem.* **2015**, *87* (11), 5482–5485.

(56) Croissant, J. G.; Fatieiev, Y.; Almalik, A.; Khashab, N. M. Mesoporous Silica and Organosilica Nanoparticles: Physical Chemistry, Biosafety, Delivery Strategies, and Biomedical Applications. *Adv. Healthc. Mater.* **2018**, *7* (4), 1–75.

(57) Ruiz-Hernández, E.; Baeza, A.; Vallet-Regí, M. Smart Drug Delivery through DNA/Magnetic Nanoparticle Gates. *ACS Nano* **2011**, *5* (2), 1259–1266.

(58) Lu, J.; Liong, M.; Zink, J. I.; Tamanoi, F. Mesoporous Silica Nanoparticles as a Delivery System for Hydrophobic Anticancer Drugs. *Small* **2007**, *3* (8), 1341–1346.

(59) Argyo, C.; Weiss, V.; Bräuchle, C.; Bein, T. Multifunctional Mesoporous Silica Nanoparticles as a Universal Platform for Drug Delivery. *Chem. Mater.* **2014**, *26* (1), 435–451.

(60) Mora-Raimundo, P.; Lozano, D.; Manzano, M.; Vallet-Regí, M. Nanoparticles to Knockdown Osteoporosis-Related Gene and Promote Osteogenic Marker Expression for Osteoporosis Treatment. *ACS Nano* **2019**.

(61) Huang, Y. Functionalization of Mesoporous Silica Nanoparticles and Their Applications in Organo-, Metallic and Organometallic Catalysis. *Funct. mesoporous silica nanoparticles their Appl. organo-, Met. Organomet. Catal.* **2009**, 1-12; 37-42.

(62) Jiménez, C. S. Nanopartículas Mesoporosas Funcionalizadas Para Vehiculización de Fármacos y Vectorización En Terapia Antineoplásica. **2012**, *4* (10), 5003.

(63) Yu, M. K.; Park, J.; Jon, S. Targeting Strategies for Multifunctional Nanoparticles in Cancer Imaging and Therapy. *Theranostics* **2012**, *2* (1), 3–44.

(64) Petros, R. A.; Desimone, J. M. Strategies in the Design of Nanoparticles for Therapeutic Applications. *Nat. Rev. Drug Discov.* **2010**, *9* (8), 615–627.

(65) Knežević, N.; Durand, J. O. Large Pore Mesoporous Silica Nanomaterials for Application in Delivery of Biomolecules. *Nanoscale* **2015**, *7* (6), 2199–2209.

(66) Larsen, M. T.; Kuhlmann, M.; Hvam, M. L.; Howard, K. A. Albumin-Based Drug Delivery: Harnessing Nature to Cure Disease. *Mol. Cell. Ther.* **2016**, *4* (1), 3.

(67) Caracciolo, G. Liposome-Protein Corona in a Physiological Environment: Challenges and Opportunities for Targeted Delivery of Nanomedicines. *Nanomedicine Nanotechnology, Biol. Med.* **2015**, *11* (3), 543–557.

(68) Mahmoudi, M.; Sheibani, S.; Milani, A. S.; Rezaee, F.; Gauberti, M.; Dinarvand, R.; Vali, H. Crucial Role of the Protein Corona for the Specific Targeting of Nanoparticles. *Nanomedicine* **2015**, *10* (2), 215–226.

(69) Zhang, Y.; Ang, C. Y.; Li, M.; Tan, S. Y.; Qu, Q.; Luo, Z.; Zhao, Y. Polymer-Coated Hollow Mesoporous Silica Nanoparticles for Triple- Responsive Drug Delivery. **2015**.

(70) Thambi, T.; Ikram, M.; Kang, Y. M.; Yi, G.; Hyung, J. (Manuscript for Acta Biomaterialia) Zwitterionic Mesoporous Nanoparticles with a Bioresponsive Gatekeeper for Cancer Therapy School of Chemical Engineering , Sungkyunkwan University , Suwon 440-746 , Republic of School of Medicine , Kyungpook National U. **2016**.

(71) Maleki, A.; Kettiger, H.; Schoubben, A.; Rosenholm, J. M.; Ambrogi, V.; Hamidi, M. Mesoporous Silica Materials: From Physico-Chemical Properties to Enhanced Dissolution of Poorly Water-Soluble Drugs. *J. Control. Release* **2017**, *262* (June), 329–347.

(72) Mura, S.; Nicolas, J.; Couvreur, P. Stimuli-Responsive Nanocarriers for Drug Delivery. *Nat. Mater.* **2013**, *12*, 991.

(73) Chen, C.; Ke, J.; Zhou, X. E.; Yi, W.; Brunzelle, J. S.; Li, J.; Yong, E.-L.; Xu, H. E.; Melcher, K. Structural Basis for Molecular Recognition of Folic Acid by Folate Receptors. *Nature* **2013**, *500*, 486.

(74) Zhu, J.; Niu, Y.; Li, Y.; Gong, Y.; Shi, H.; Huo, Q.; Liu, Y.; Xu, Q. Stimuli-Responsive Delivery Vehicles Based on Mesoporous Silica Nanoparticles: Recent Advances and Challenges. *J. Mater. Chem. B* **2017**, *5* (7), 1339–1352.

(75) Liu, J.; Zhang, B.; Luo, Z.; Ding, X.; Li, J.; Dai, L.; Zhou, J.; Zhao, X.; Ye, J.; Cai, K. Enzyme Responsive Mesoporous Silica Nanoparticles for Targeted Tumor Therapy in Vitro and in Vivo. *Nanoscale* **2015**, *7* (8), 3614–3626.

(76) Kim, S. E.; Yun, Y. P.; Shim, K. S.; Park, K.; Choi, S. W.; Shin, D. H.; Suh, D. H. Fabrication of a BMP-2-Immobilized Porous Microsphere Modified by Heparin for Bone Tissue Engineering. *Colloids Surfaces B Biointerfaces* **2015**, *134*, 453–460.

(77) Liu, Y.; Ding, X.; Li, J.; Luo, Z.; Hu, Y.; Liu, J.; Dai, L.; Zhou, J.; Hou, C.; Cai, K. Enzyme Responsive Drug Delivery System Based on Mesoporous Silica Nanoparticles for Tumor Therapy in Vivo. *Nanotechnology* **2015**, *26* (14).

(78) Tu, J.; Boyle, A. L.; Friedrich, H.; Bomans, P. H. H.; Bussmann, J.; Sommerdijk, N. A. J. M.; Jiskoot, W.; Kros, A. Mesoporous Silica Nanoparticles with Large Pores for the Encapsulation and Release of Proteins. *ACS Appl. Mater. Interfaces* **2016**, *8*, 32211–32219.

Chapter II. Synthetic Identity

This page left blank intentionally

2.1 Introduction

Although several pieces of legislation in the European Union (EU) and USA have specific references for nanoparticles[79], a single internationally accepted definition for NPs does not exist. However, nanoparticles can be described as materials with length of 1–1000 nm in at least one dimension although they are commonly defined to be of diameter in the range of 1 to 100 nm[80,81,82,83]. Many different criteria can be applied in order to classify NPs, being one of this the presence or absence of intentionally designed modifications performed onto nanometric materials. According to this benchmark, the European Committee for Standardization (CEN) divides NPs in two types: non-engineered and engineered NPs[84].

Nowadays, the modern multidisciplinary science studies, understands and controls the manipulation of materials on a nanometric scale engineer NPs for its intentional using application on modern knowledges, both for their synthesis and characterization. These nanoparticles can be classified in different categories according to their bulk material, i.e. if they are made of metals (including Au, Ag, Zn, Ni, Fe, and Cu), metal oxides (TiO_2, Fe_2O_4, SiO_2, CeO_2, and Al_2O_3)[85,86], nonmetals (quantum dots)[87], carbon (graphene and fullerene), polymers (alginate, chitosan, hydroxyethylcellulose, polyhydroxyalkanoates and polyhydroxyalkanoates, poly-E-caprolactone and pBAEs)[88], or lipids (soybean lecithin and stearic acid)[89,90].

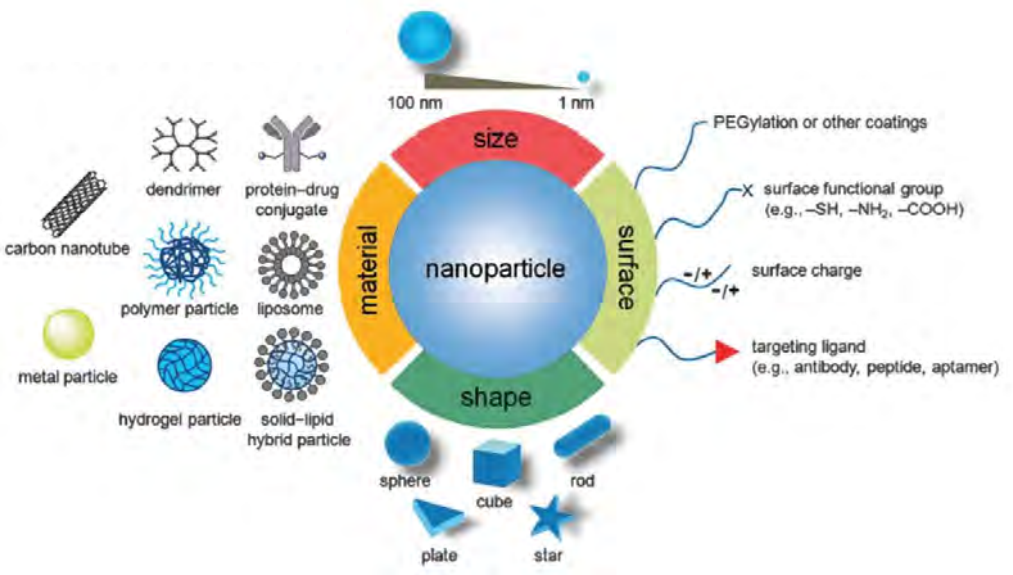

Figure 4: Nanoparticles for drug delivery. The mechanisms of the engineered nanoparticles for drug delivery in cancer stem cell therapy. A summary of nanoparticles that have been explored as carriers for drug delivery in cancer stem cell therapy, together with illustrations of biophysicochemical properties[91].

Regardless of the material used for the synthesis of the nanoparticles, the most important aspect of NP for drug delivery are their physicochemical properties[92,93], i.e. shape, size, surface charge and functional groups[94], affect the way cells in the body "see" NPs and thus dictate their distribution, toxicity and targeting ability[95,96,97,98] (Figure 4).

Among the nanoparticles reported, mesoporous silica nanoparticles (MSN) are probably the most extensively studied for "smart" drug delivery[99,100,101]. Specifically, MSN offer appealing inherent properties including biocompatibility, controllable uniform particle size, high mechanical strength and stability, as well as high drug loading capacities[102,103,104,105]. The advances on MSNs, exploding their unique structural for drug carriers, have been well established in pharmaceutical research over the recent decade[106,107]. Typically, MSNs used as drug delivery systems are featured by their ordered arrays of 2D hexagonal mesopore structure, uniform particle sizes[108] (80-500 nm), large surface areas[82,83] (>1000 $m^2 \cdot g^{-1}$), high pore volumes (0.5-2.5 $cm^3 \cdot g^{-1}$), tunable pore diameters (1.3-30 nm), controllable particle morphology[109] and both exterior and interior surfaces that could be independently modified with a variety of functional groups[61,110]. The main special feature when using this type of nanoparticles for drug delivery is the presence of the porous and the controllable morphology of the NPs[111,112]. This singularity provides these NPs with two differentiated domains, that will be exploited for the goals of the work here presented: an external surface and an internal one inside the pores, which provides the NP with an added value[113]. The presence of the pores arranged in the whole matrix of the nanoparticle allows a high loading of the drug due to the large surface area. In turn, this porous matrix allows the drug's ease of release at the time of need due to the ease with which the drug passes through the rigid structure and it accesses to the outside. To sum up, this type of NPs gives a high loading capacity of drug, an ease release of the same and the capacity of differentiation of the two domains (an external surface and an internal one), on which the capacity of drug release depends. In addition, by modifying the synthetic methodology slightly, MSNs can be obtained nanoparticles with well-defined and uniform shapes and sizes will determine their physiologic response[114]. For that reason, they have optimal characteristics for their use as a drug delivery.

The synthetic methodology for MSN is based on the condensation of silica precursors, typically sodium silicate or tetraethylorthosilicate, in the presence of cationic surfactants under basic conditions [4]. In fact, this procedure is an adaptation of the method described by Stöber in 1968 for obtaining silica nanoparticles. In particular, the standard preparation consists of mixing a silicate precursor, usually

tetraethylorthosilicate (TEOS), with a cationic surfactant, such as a cetyltrimethylammonium bromide (CTAB), at a temperature between 30 and 80 °C and pH = 11. The nanoparticles are formed by the sol-gel process catalyzed in basic medium[115,94].

In the first stage of the process, the hydrolysis of the alkoxide takes place. Then, the silanol groups polymerize by condensation, forming three-dimensional structures linked by siloxane bonds (Si-O-Si). In the following step, the presence of cylindrical micelles formed by the surfactant is critical, since they act as a template and will give rise to the formation of the pores. The cationic surfactant attracts the negative charges of the silica species, which are concentrated around the micelles forming a tubular silica structure. The nanoparticle increases in size until the negative charge, introduced by the silica species, is so high that it stops growing. It should be noted that the size, hexagonal shape, regularity of the particles and the pore size, i.e. the synthetic identity depend on various variables such as temperature, rate of addition, agitation, pH and the amount of catalyst used with respect to that of TEOS[115,94], which are studied through a design of experiment.

Finally, the surfactant should be removed from the inside of the pores. To do so, three methods have been recommended: reflux in acidified alcohol with hydrochloric acid, treatment with ammonium nitrate or by calcination. These treatments allow the rupture of the electrostatic interaction that exists between the groups of the cationic surfactant head and the anionic silicates, which facilitates the elimination of the surfactant in the mesoporous and the final formation of the particles[115,116,117].

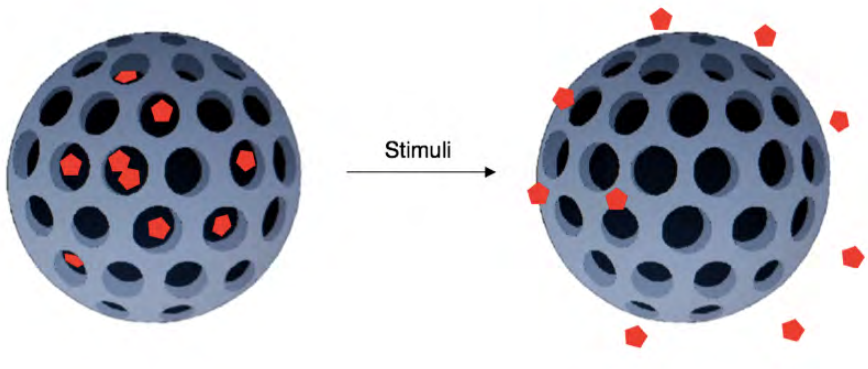

Figure 5: Schematic representation of mesoporous silica nanoparticles for drug delivery by stimuli.

MSN with different properties can be obtained by altering the factors of its synthesis. The main objective of this chapter is the obtaining of MSNs with physicochemical characteristics differences, that is to say with differentiated synthetic identities for its later

application as a drug delivery for improve the safety and efficacy of the drugs[118,119,120,121,122,123]. This requires cross-disciplinary research opportunities to design and develop multifunctional devices that can target, diagnose, and treat devastating disease such as cancer[124 125]. In addition, the characterization of the parameters will be studied hereafter, both for the DOE study and for the correlation in chapters to come (Figure 22).

2.1.1 Objectives

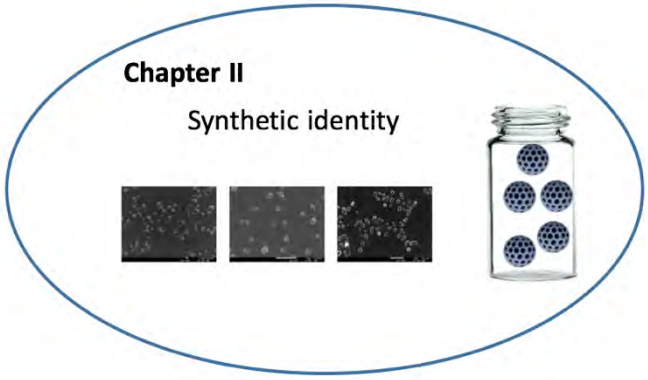

Figure 6: Graphical abstract of the Chapter II.

In order to achieve this objective, the following tasks were proposed:

- To optimize a synthetic methodology for obtaining mesoporous silica nanoparticles with different synthetic identity (size, shape, pore sizes…) and adequate properties for its use as a drug delivery.
- To use and analyse a Design Of Experiment for the obtaining of nanoparticles with different physicochemical properties.
- To use different equipment to assess the characteristics of the obtained nanoparticles and correlate them with the factors studied in the DOE
- To characterize the MSNs' physicochemical properties, and evaluate the DOE.
- To obtain new synthetic identities through the addition of functional groups for the future study of MSN as drug delivery systems.

2.2 Materials and Methods

2.2.1 Synthesis of MSNs

A solution of 0.2 g of CTAB in 48 mL of **A** M NH_4OH was allowed to rise to **B** ºC during 30min at **C** rpm. Then 1 mL of TEOS at **D** ml/h was added dropwise by an automatic injector, followed by the addition of **E** ml of APTES. The solution was stirred at the same temperature for another 3 h. Solid samples were collected via centrifuging at 13000 rpm for 13 min, washing and dispersing with deionized H_2O and EtOH twice. Surfactant templates were removed by extraction in acidic ethanol, 0.5 ml of HCl in 20 mL of EtOH at 65 ºC for 24 h. Again, samples were collected via centrifuging at 13000 rpm for 13 min, washing and dispersing with deionized H_2O and EtOH twice. Then, they were lyophilized.

Sample	A (M)	B (ºC)	C (rpm)	D (mL/h)	E (mL)
1	0.2	60	1100	2	3.85
2	0.2	80	1100	4	20
3	0.2	80	1100	2	12.8
4	0.2	60	1100	7	20
5	0.5	60	1100	4	12.8
6	0.5	80	1100	7	3.85
7	0.2	60	550	7	12.8
8	0.5	60	550	2	20
9	0.2	60	550	4	3.85
101	0.5	80	550	7	12.8
102	0.5	80	550	7	3.85

2.2.2 Synthesis of S112

A solution of 3 g of PVP and 30 mL of 1-pentanol were sonicated during 2 hours at room temperature. Then, 3 mL of absolute ethanol, 0.84 mL of ultrapure water and 0.2 mL of 0.18M sodium citrate dihydratate (0.5294g/10mL) were added. The solution was shaken by hand and 0.675 mL of ammonia (30% p/p) were added. The solution was shaken again and finally 0,3 mL of TEOS were added. Then, the solution was aged, without stirring for 24 h. Solid samples were collected via centrifuging at 1500 g for 15

min, washing and dispersing with deionized H_2O and EtOH twice. Then, they were lyophilizated.

2.2.3 Characterization of MSNs

2.2.3.1 DLS

Particle size and surface charge measurements of the NPs were determined by Dynamic Light Scattering (DLS) at room temperature with a Zetasizer Nano ZS (Malvern Instruments Ltd, United Kingdom, 4-mW laser) using a wavelength of 633 nm. Samples were prepared at a concentration of 5 $mg \cdot mL^{-1}$ in MilliQ (pH 6.3) water or PBS 1x buffer solution (pH 7.4). Better results are obtained if MSNs have just been sonicated during 15 minutes. Sometimes, samples need to be filtered in a 0.45 µm nylon filter. Normally, in order to adjust concentration range, the initial concentration must be diluted 1/10 or 1/3. Results were plotted as mean and standard deviation of triplicates analysed by intensity.

2.2.3.2 SEM

The images were done with the microscope J-7100F (Jeol). Samples were ultrasonically dispersed in H_2O at a concentration of 1 mg of MSN in 20 ml. The sample were deposited on an amorphous, porous carbon grid. In order to make the sample conductive a layer of graphite was made.

2.2.3.3 BET

The analysis of adsorption/desorption of nitrogen was carried out with the micromeritic gemini V Surface area and pore size. Prior to conduct adsorption experiments, 17 mg of the samples were lyophilized at 0,05 mBar, -0,759 ºC, 24 h, directly inside BET tubs to remove the solvent at a reduced pressure and low temperature. Pore size distribution curves were obtained from analysis of the absorption portion of the isotherms using the BJH (Barrett-Joyner-Halenda) method.

2.2.4 Synthesis of different superficial chemistry

2.2.4.1 Isothiocyanate group

200 mg of MSN with the surface aminated were treated with toluene at 50 ºC for 24 h. 40 mg of the resulting MSN-(NH_2) were suspended in 35 mL of toluene and 95 mg of thiocarbonyldi-2(1*H*)-pyridone (**5**) (0.409 mmol, 12 eq.) in 15 mL of dry DCM were added. The suspension was stirred for 24 h at room temperature. Solid samples were collected by centrifugation at 13000 rpm for 13 min and then were washed and dispersed with

DCM and EtOH. This procedure was repeated six times and finally MSN-(NCS) were rotary evaporated under reduced pressure and stored dry.

2 mg of MSN (S1) were suspended in 2 mL of EtOH, then 1.075, 0.5375, 0.268 and 0.054 mg of FITC were added in order to obtain the 20%, 10%, 5% and 1% of fluorescein in the surface. The mixture was allowed to react for 24 hours in the orbital shaker at room temperature in the dark. Finally, it was collected via centrifuging at 13000 rpm for 13 min, washing and dispersing with deionized H_2O and EtOH twice. Then, they were lyophilized.

2.2.4.2 BOC group

The differentiation between the functionalization of the surface and the pores was made through the addition of the BOC group when the pore remain with the surfactant. For that, prior to the elimination of the CTAB from the pore, 180 mg on MSN with the surfactant were dispersed in 88 ml of H_2O and 62 mg of $(BOC)_2O$ were added. 1 mL of triethylamine was added to the solution and it is heated to 30-35 ºC and stirred at 600 rpm during 6 hours. Then, MSNs were collected via centrifuging at 13000 rpm for 13 min, washing and dispersing with deionized H_2O and EtOH twice. Finally, in order to remove the surfactant, nanoparticles were dispersed in 15 mL of EtOH and 200 mg of ammonium nitrate were added and stirred at room temperature overnight. The utilization of NH_4NO_3 versus HCl is to not remove the BOC on the surface. Samples were washed and lyophilized as previously described.

2.2.4.3 PEG chains

*2.2.4.3.1 Synthesis of 2-(2-(2-(2-hydroxyethoxy)ethoxy)ethoxy)ethyl 4-methylbenzenesulfonate (**2**)*

The first step was the obtaining of 2-(2-(2-(2-hydroxyethoxy)ethoxy)ethoxy)ethyl 4-methylbenzenesulfonate (2). For that, 2.2360 g (11.5 mmol) of tetraetilenglicol was dissolved in 5 mL of THF. To this solution was added another one of 1.85 M of NaOH, and it was stirred at 0 ºC while 20 mL of a solution 0.57 mM of TsCl in THF was added. After 2 hours stirring at 0 ºC the reaction was quenched adding 100 mL of cold water. Then the resulting mixture was extracted three times with DCM. The combined organic layers were wash twice with H_2O and dried with $MgSO_4$ anhydrous and evaporated under reduced pressure.

*2.2.4.3.2 Synthesis of 1-azido-3,6,9,12-tetraoxatetradecane (**3**)*

2.45 g (7 mmol) of the product **2** were dissolved in 85 mL of EtOH and 4.87 g (75 mmol) of NaN_3 were added and the solution is stirred at 70 ºC overnight using a reflux.

To the reaction, 62 mL of water were added, and two thirds were evaporated under reduced pressure. Finally, the mixture was extracted three times with AcOEt. The combined organic layers were dried with $MgSO_4$ anhydrous and evaporated under reduced pressure.

*2.2.4.3.3 Synthesis of 2-(2-(2-(2-azidoethoxy)ethoxy)ethoxy)ethanol (**4**)*

To 1 g of product **3** (4 mmol), 18 mL of a 1 M of NaH in THF anh. were added slowly at 0 ºC while stirring. Then, the solution was heated for 2 hours at 50 ºC, until it turns brown. 1.5 mL (9 mmol) of BrAcOEt were then added and it was allowed to react in the microwave during 1 hour at 125 ºC. The formed precipitate was filtered, and the solvent was evaporated under reduced pressure. To the product was added pentane and it was stirring at room temperature overnight. After 24 hours, 50 mL of water were added and it was extracted with AcOEt three times. The organic phase was wash with brine twice, and it was dried with $MgSO_4$ anh. and evaporated under reduced pressure.

*2.2.4.3.4 Synthesis of 3,6,9,12-tetraoxatetradecan-1-amine (**5**)*

10 mL of MeOH and 10 mg of Pd/C were added in to a two-neck round-bottom glass flask. The system was purged three times with H_2. Then, 100 mg of **4** (0,45 mmol) dissolved in 10 mL of MeOH were added into the flask, and it was allowed react during 30 min. Then, it was filtered with a celite filter (to prevent the degradation of the product). The PEG was evaporated under reduced pressure without temperature, due it was extremely unstable.

2.2.4.3.5 Characterization by ^{1}H-RMN

PEG n=4 was characterized by ^{1}H-RMN (Nuclear Magnetic Resonance). The spectra were recorded on a Varian 400-NMR spectrometer with frequency generators for ranges ^{1}H-^{19}F and ^{15}N-^{31}P, temperature control system, automatic tuning probe and sample introduction robot 50 positions (^{1}H-NMR at 400 MHz and ^{13}C-NMR at 100.6 MHz Chemical shifts are reported in part per million (ppm) on the δ scale, and are referenced to tetramethylsilane (TMS) in ^{1}H-NMR spectra and to solvent signal of $CDCl_3$ (77.0 ppm), DMSO-d_6 (39.5 ppm), or methanol-d4 (49.0 ppm) in 13C-NMR spectra. Coupling constants were reported in Hertz (Hz). Spectral splitting patterns were designed as: s (singlet), d (doublet), t (triplet), q (quartet), dd (doublet of doublets), ddd (doublet of doublet of doublets), m (complex multiplet) and brs (broad signal).

- ✓ TEG-TsCl

^{1}H NMR (400 MHz, Chloroform-*d*, TMS) (ppm): δ 7.80 – 7.76 (m, 2H), 7.33 (dddd, *J* = 7.2, 2.8, 1.4, 0.7 Hz, 2H), 4.17 – 4.12 (m, 2H), 3.71 – 3.62 (m, 10H), 3.59 (s, 2H), 3.55 (q, *J* = 1.1 Hz, 2H), 2.43 (dd, *J* = 1.8, 0.8 Hz, 3H)

- ✓ EtO-N_3

^{1}H NMR (400 MHz, Chloroform-*d*, TMS) (ppm): δ 4.36 – 4.06 (m, 4H), 3.66 (dd, *J* = 4.0, 1.2 Hz, 10H), 3.38 (t, *J* = 5.2 Hz, 2H), 1.87 – 1.76 (m, 2H), 1.32 – 1.20 (m, 3H)

- ✓ OH-N_3

^{1}H NMR (400 MHz, Chloroform-*d*, TMS) (ppm): δ 3.76 – 3.70 (m, 1H), 3.69 – 3.65 (m, 11H), 3.62 – 3.59 (m, 1H), 3.39 (td, *J* = 5.1, 3.6 Hz, 2H), 2.17 (s, 2H).

2.2.4.3.6 Anchoring of the PEG onto the surface of the nanoparticle

To a 10 mg of MSN-SCN (S1) 4,5 mL of EtOH were added and sonicated for the correct dispersion. It was added 2,5 mg of the product **5** (0,03668 mmol) dissolved in 0.5 mL of EtOH with two drops of triethylamine. The reaction was stirred at room temperature during 48 hours. Then, it was collected via centrifuging at 13000 rpm for 13 min, washing and dispersing with deionized H_2O and EtOH, twice. Then, they were lyophilized.

Regarding the addition of C12, it was used the same procedure with the same quantity of nanoparticles and 5.7 mg of C12 (0.03668 mml).

2.2.4.4 Oleylamine funtionalization

The same methodology was followed as in the anchoring of the PEG using 2.45 g of oleylamine (0.0366mmol).

2.3 Results and discussion

2.3.1 Synthesis of mesoporous silica nanoparticle

Mesoporous silica nanoparticles were synthesized according to the co-condensation methodology in three synthetic steps The methodology followed was reported by Victor S.-Y. Lin *et. al.*[109], and afforded MSN with good characteristics to be used inas a drug delivery at the same time as reached different morphologies. In this procedure, the first condensation TEOS acts as a silica precursor and the second reagent, APTES introduces the functional groups in both inner and outer surface, in this case a surface aminated. Finally, in the last step the surfactant is removed from the porous, through consecutives washes.

In order to prepare MSN with suitable with a wide range of physicochemical properties (size, shape,…) a Design Of Experiment (DOE) is proposed to respect the original methodology varying some parameters, which the literature revealed that affect the most the NPs' physicochemical characteristics[126,127,128]. The factors that can be controlled are:

- (A) Temperature (Cº)
- (B) Stirring (rpm)
- (C) pH (NH_2 M)
- (D) Flow rate (ml / min): the rate in which the reagents are added
- (E) % TEOS / APTES: the proportion of the reagents

Finally, five factors are proposed: temperature, stirring and the pH of the reagents at level 2 and flow time and the % at level 3 represented on Table 1. The level is chose depending on the importance of the effect that each factor has on literature.

Table 1: Factors and levels of the DOE

Factors	Level 1	Level 2	Level 3
Temperature (ºC)	60	80	-
Stirring (RPM)	550	1100	-
Concentration	0.2 M	0.5 M	-
Flow rate (ml/h)	2	4	7
% TEOS/APTES	3,85	12,8	20

In order to delimit the DOE's matrix, the degrees of freedom are defined through the factors and levels. Three factors are obtained at 2 levels, 3 degrees of freedom (df), and two factor at 3 levels, 4 df. In global, the design reach 7 df, for that reason a Taguchi method matrix $L_9(3^4)$ is proposed for the design of experiences, represented in Table 2. Consequently 9 experiments are needed to develop this DOE.

Table 2: Matrix of the DOE

	T	*Stirring*	*pH*	*Flow*	*% T/A*
Exp.	**A**	**B**	**C**	**D**	**E**
1	1	2	1	1	1
2	1	2	2	2	2
3	1	2	1	3	3
4	2	2	1	2	3
5	2	2	2	3	1
6	2	2	1	1	2
7	1	1	1	3	2
8	1	1	2	1	3
9	1	1	1	2	1

2.3.2 Characterization of the MSN

The realization of the DOE rendered 9 different type of MSN. To these nanoparticles must be added two types that were synthesized to optimize the methodology prior to the DOE, that they are named S101 and S102. To these samples it is also added the sample S112, which is a type of nanoparticle without pores, as a control sample. Each MSN batch was characterized by means of Dynamic Light Scattering (DLS), Scanning Electron Microscope (SEM) and N_2 adsorption and desorption isotherms (BET, BJH), in order to be able to correlate it with the properties of the biological identity and to know in depth the synthetic identity in the next chapter.

2.3.2.1 Determination of the MSN size and zeta potential via Dynamic Light Scattering

Dynamic light scattering (DLS) of NP in solution offer the most frequently used technique for accurate estimation of the particle size and size distribution. In this technique solution of spherical particles in Brownian motion causes a Doppler shift when they are exposed against shining monochromatic light (laser). Such monochromatic light

exposure hits the moving particle which results in changing the wavelength of the incoming light. Extent of this change in wavelength determines the size of the particle. This parameter assists in evaluation of the size distribution, particle's motion in the medium, which may further assists in measuring the diffusion coefficient of the particle and using the autocorrelation function. [129]

Nanoparticles size analysis using DLS measurements relate particles movement with their hydrodynamic radius. Differences in functional groups and media, among other factors, can result in variations in DLS results. In this case, because of the synthetic methodology, the surfaces of all samples were aminated in order to be able to compare their sizes. Moreover, MSN were characterized by measuring their zeta potential in order to estimate the charge on the surface of the nanoparticles. The zeta potential is extremely related with the cellular uptake. Positively charged NPs are taken up more easily by cells than negatively charged ones[130].

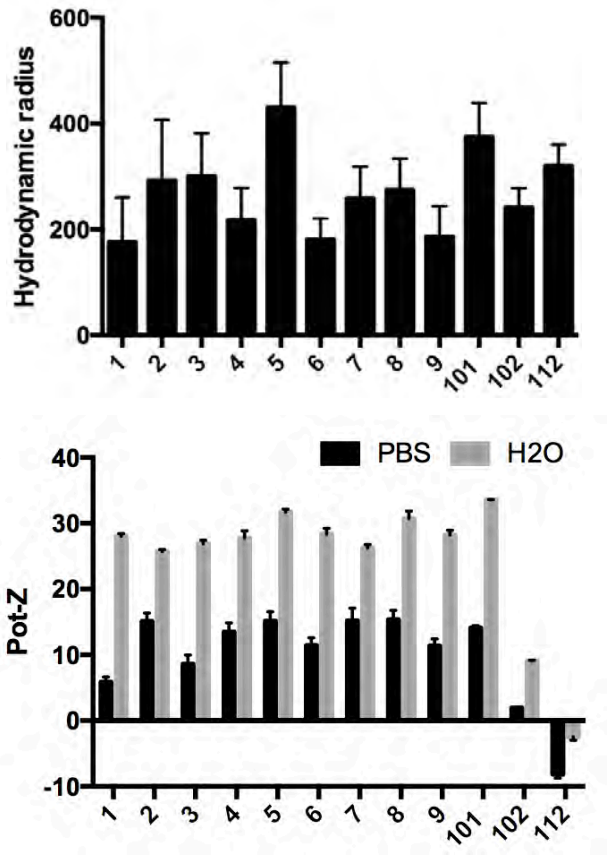

Figure 7: Results of the DLS analysis of each sample. Top: Hydrodynamic radius, Bottom: zeta potential (black in PBS and grey in H_2O). Results correspond to mean ± SD values of at least three replicates.

Regarding the hydrodynamic radius measured in water, the samples show a Z-average, which is the mean value of MSNs size, between 200 nm and 400 nm. On the other hand, the zeta potential was measured in both water and PBS, due to the fact that the medium is a determinant factor for these measurements. In water, the pH of the medium causes the amines to be protonated and the zeta potential of the nanoparticles to be around 30 mV positive; in the case of PBS the pH decreases the zeta potential to an average of 13 mV.

Here, the homogeneity of the NPs' samples regarding the size and the zeta potential was demonstrated. The values of the NPs' sizes were reported to be influential in the formation of PCs. In the next chapter will be determine if the different between the sample were enough to observed different in the composition or quantity of the proteins which form the PC.

2.3.2.1 Analysis of the image from scanning electron microscope

Another property of the synthetic identity that influences the PC formation is the shape of the nanoparticle. Thus, characterizing this property will be key to relate the synthetic identity with the biological one in chapter III. This will allow the design of MSN with defined physical properties for the obtaining of a desired PC. Here, in this work, the shape was referenced using the Aspect Ratio. The Aspect Ratio (AR) is defined as the relationship between its width (A) and its height (B). Hence, nanoparticles spherical have an aspect ratio equal to 1, while rod shape MNPs show higher values of AR. To do that, needed images are taken with a FE-SEM.

Also, using the SEM it can obtained the radius of the NPs. Due to the hydrodynamic ratius effect, there ir a pronounced difference between the size obtained by either DLS or SEM. In fact, in the case of MSN, DLS size is always higher than SEM, superficial amines make the measurement obtained by the DLS greater.

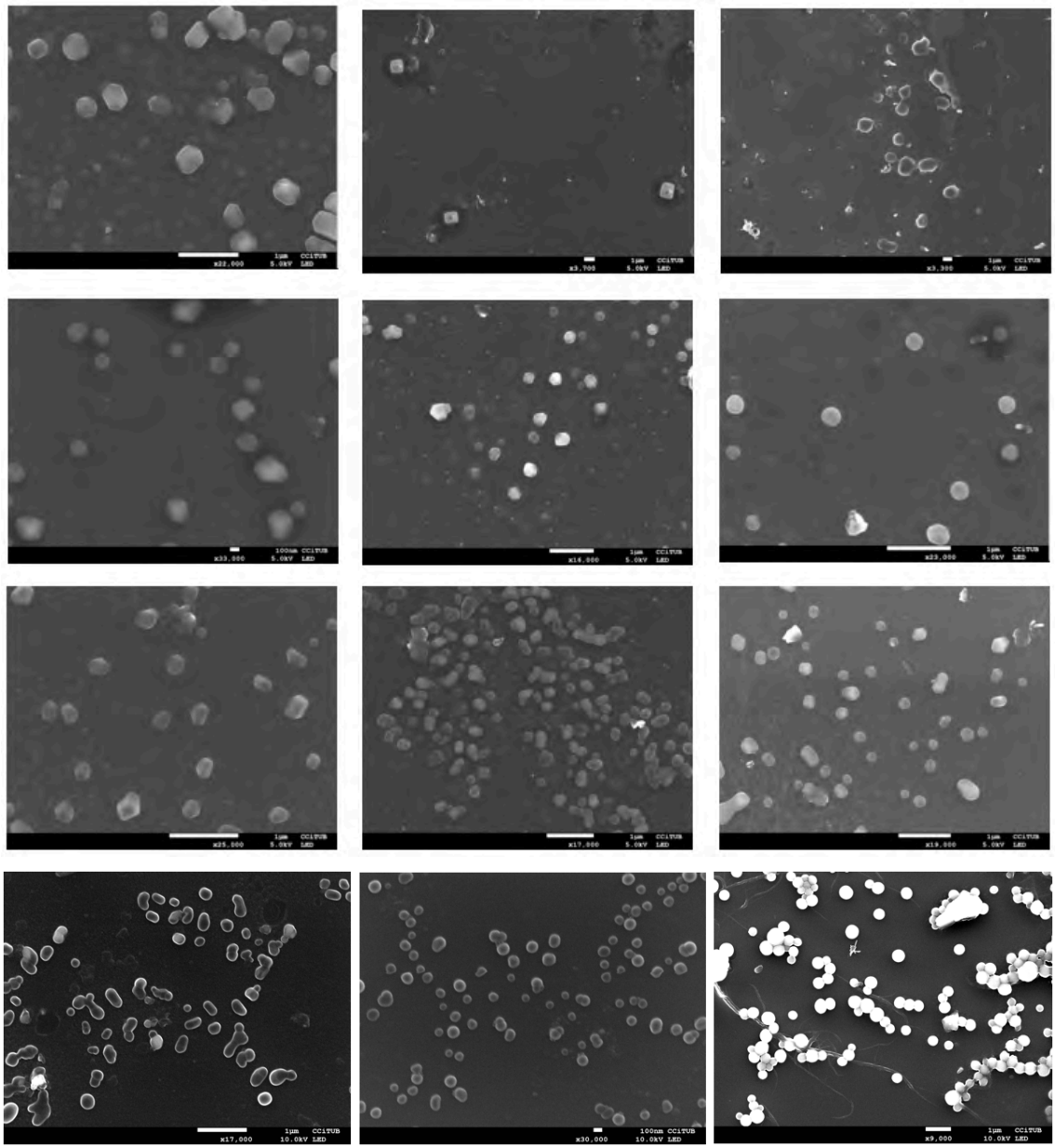

Figure 8: SEM images. From left to right, and from top to bottom: S1, S2, S3, S4, S5, S6, S7, S8, S9, S101, S102 and S112.

The images were analysed with a digital image processing program called ImageJ, with the purpose of valuing the properties of the nanoparticles. In Figure 9, the difference between the AR in the samples can be observed.

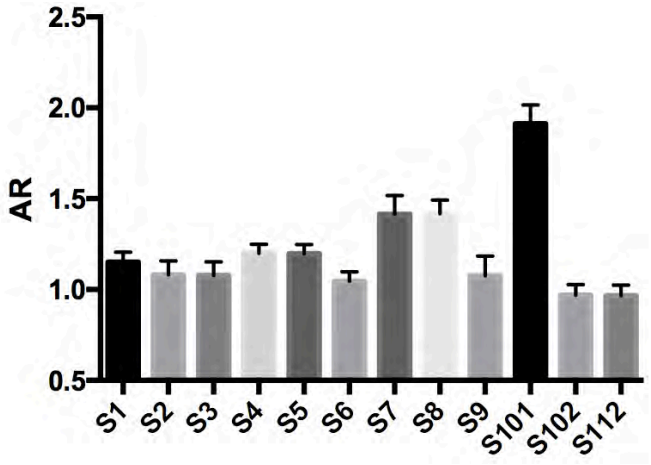

Figure 9: Aspect Ratio obtained from the SEM images.

In Figure 9, three mains groups can be differentiated: the first one being composed of the nanoparticles with a rod-shape which were S101 with an AR of 1.9; the second one composed of NPs with an elongated-spherical shape S5 which have an AR of 1.3 and S8 of 1.5; and the last one composed of the nanoparticles with a spherical shape, samples with an AR lower than 1.2.

Thanks to the utilization of the DOE, some MSN with different shapes were obtained. The influence in the PC formation will be determined in the next chapter. The three groups will be studied under the effect of the MSN incubation in different biological medium.

2.3.2.2 Surface Area and pore size characterization

The last parameter to complete the MSN characterization for their next correlation with the PC is the pore size. The pore is the most distinguished feature of the MSN and it also affects the PC formation. This parameter was studied using the adsorption/desorption technique. The main objective of this assay is obtaining of the nanoparticle's specific surface. The adsorption/desorption technique consists in impregnating a sample with nitrogen at a constant temperature to determine the specific surface of a material. The specific surface of the particles is the sum of the areas of the exposed surfaces by unit of mass. The method developed by Brunauer, Emmett and Teller (BET) is the most used to determine the total area surface. This method is based on the ability of the solids to absorb gases in their surface. The BET method provides essential information about solid porosity. The results obtained through this method are translated as adsorption-desorption isotherms. In the case of mesoporous nanoparticles,

the curve obtained, as it shown in Figure 10 is as isotherm of type IV, which presents a cycle of hysteresis associated of a characteristic of mesoporous materials (pore diameter between 2-50 nm). Regarding the study of the porosity, the most accepted and used method is the one proposed by Barrett, Joyner and Halenda (BJH) for the information on the porosity of the particle in the mesoporosity range. The characterization of the pores using the BJH method can be determined from the adsorption-nitrogen desorption.

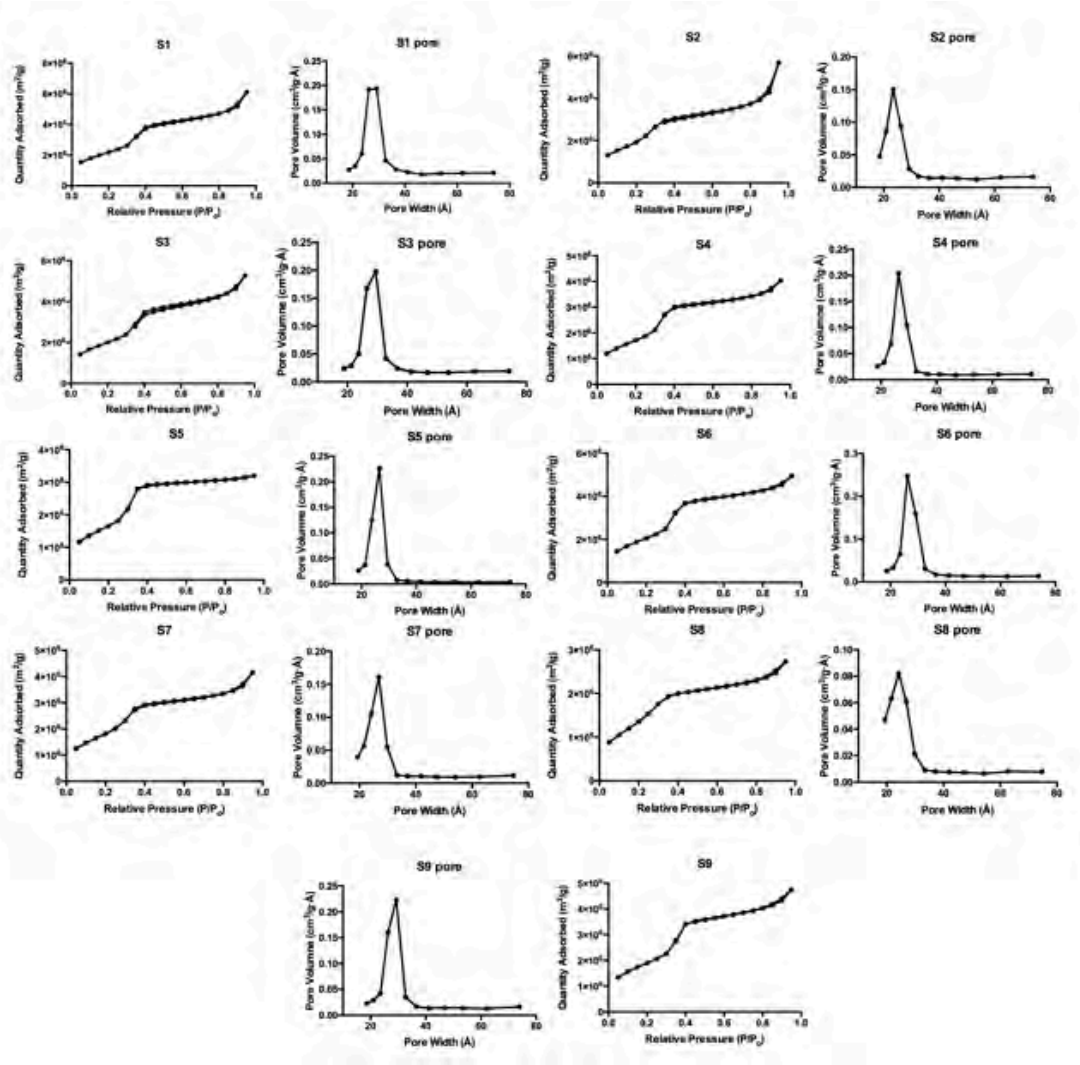

Figure 10: N_2 adsorption-desorption and BJH pore size distribution plots of MSN.

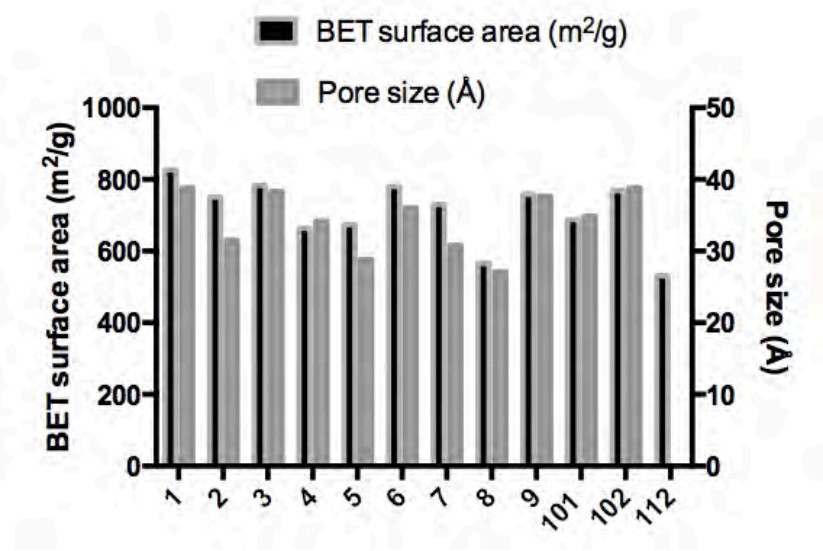

Figure 11: Results from BET analysis. In black the BET surface area and in grey the pore size.

In Figure 11, it can be observed the difference between the surface area (m^2/g) and the pore size (Å) among samples. No significant differences are shown in the surface area of nanoparticles. On the other hand, regarding the pore size, it is possible to make a classification into three groups. Large pore group is composed of the samples S1, S3, S9 and S102, which have a pore size bigger than 37.7 Å. Samples S5 and S8 have the pore smaller, lower than 30 Å. Samples that are between a pore size less than 37.7 Å and greater than 30 are: S6 with a pore size of 36 Å; S101 of 34.9 Å; S4 of 34.2 Å; S2 of 31.5 Å and S7 of 30.9 Å. The last nanoparticles are S112 which do not have pore.

2.3.2.3 Analysis of the DOE

Once the nanoparticles have been characterized, the design of experiment can be analysed in order to know which factor affects more in the studied physicochemical properties. The analysis is done through the results from the DLS, both size and zeta potential, the SEM, using the AR value, and the BET surface area and pore size. The characterization is summarised in Table 3:

Table 3: Table analysis of the DOE

	T	*Stirring*	*pH*	*Flow*	*% T/A*	*Results*				
Exp.	**A**	**B**	**C**	**D**	**E**	**Size**	**Pot-Z**	**AR**	**BET**	**Pore**
1	1	2	1	1	1	175.6	28.8	1.162	827.3	38.8
2	1	2	2	2	2	292.4	25.7	1.094	750.0	31.5
3	1	2	1	3	3	360.0	26.9	1.083	783.0	38.3
4	2	2	1	2	3	217.0	27.7	1.199	663.7	34.2
5	2	2	2	3	1	430.1	31.7	1.19	674.0	28.8
6	2	2	1	1	2	180.8	28.3	1.039	780.7	36.0
7	1	1	1	3	2	258.9	26.2	1.442	730.1	30.8
8	1	1	2	1	3	274.0	30.7	1.353	566.0	27.1
9	1	1	1	2	1	185.8	28.2	1.025	757.6	37.7
101	2	3	2	2	1	374.1	33.6	1.9	688.0	34,9
102	1	3	2	2	1	241.0	9.1	1.002	769.0	38,6

In the Pareto ANOVA graph shown in Figure 12, the percentage of the contribution is represented with respect to each of the factor in every MSN's characteristic. From this graph, it can be deduced that 56% of the variability of the results is attributed to the influence of the media pH factor for the values obtained from DLS for the size and 50% for the zeta potential. The 38% of the variability comes from the rpm of the reaction for the aspect ratio. Lastly, the reagents flow addition has the higher influence for surface area values, 43% and a 75% for the pore size.

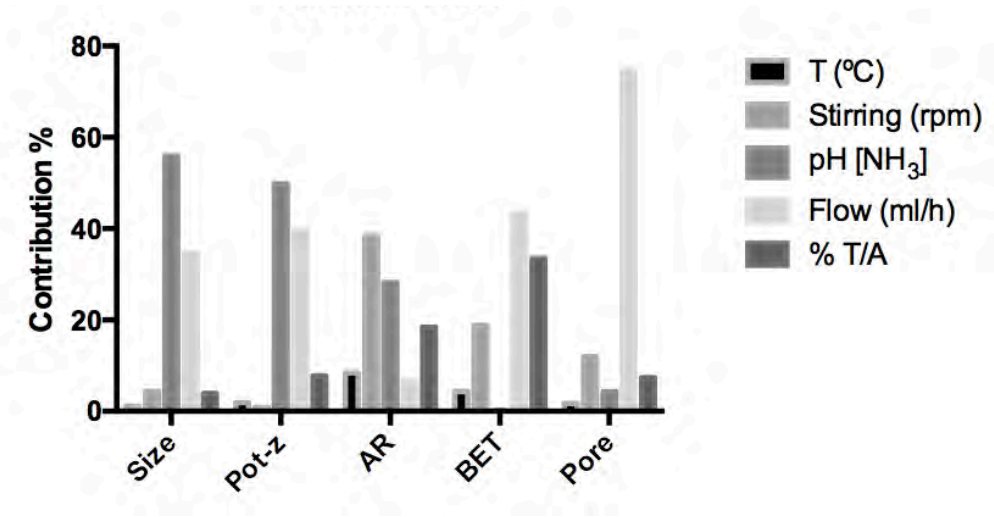

Figure 12: Contribution of the different DOE factors.

Pareto ANOVA method was used to analyse the results for the optimization, in this case, of the MSN's physicochemical characteristics. It is a simplified ANOVA method which uses Pareto principles, in order to determine how the factor that has a higher contribution affects. From the Pareto ANOVA method, the results of shows that the media pH have strong influence on the MSN's size and on the zeta potential, and it is a positive effect, a basic media results in the formation of bigger and positive nanoparticles. Thus, for the formation of small MSNs and less positive, the concentration of NH_3 must be decreased. Regarding the AR, the agitation of the reaction has a positive effect, what means that the faster the agitation, the more spherical the nanoparticles will be. By last, flow addition of the reagents has the strongest influence on the values obtained from the BET. The flow addition has a positive effect on the surface area: the faster reagents are added the more surface area will be obtained. On the contrary, this factor has a negative effect on the pore size. When the flow addition is more controlled, the MSNs get a larger pore size.

Based on the results it can be concluded that nanoparticles with favourable characteristics can be obtained at a higher concentration of NH_3, stirring at high agitation and, the most important, using a controlled flow addition. That is the optimal combination to get MSNs with some of the desired characteristics for MSN to be used as drug delivery carriers.

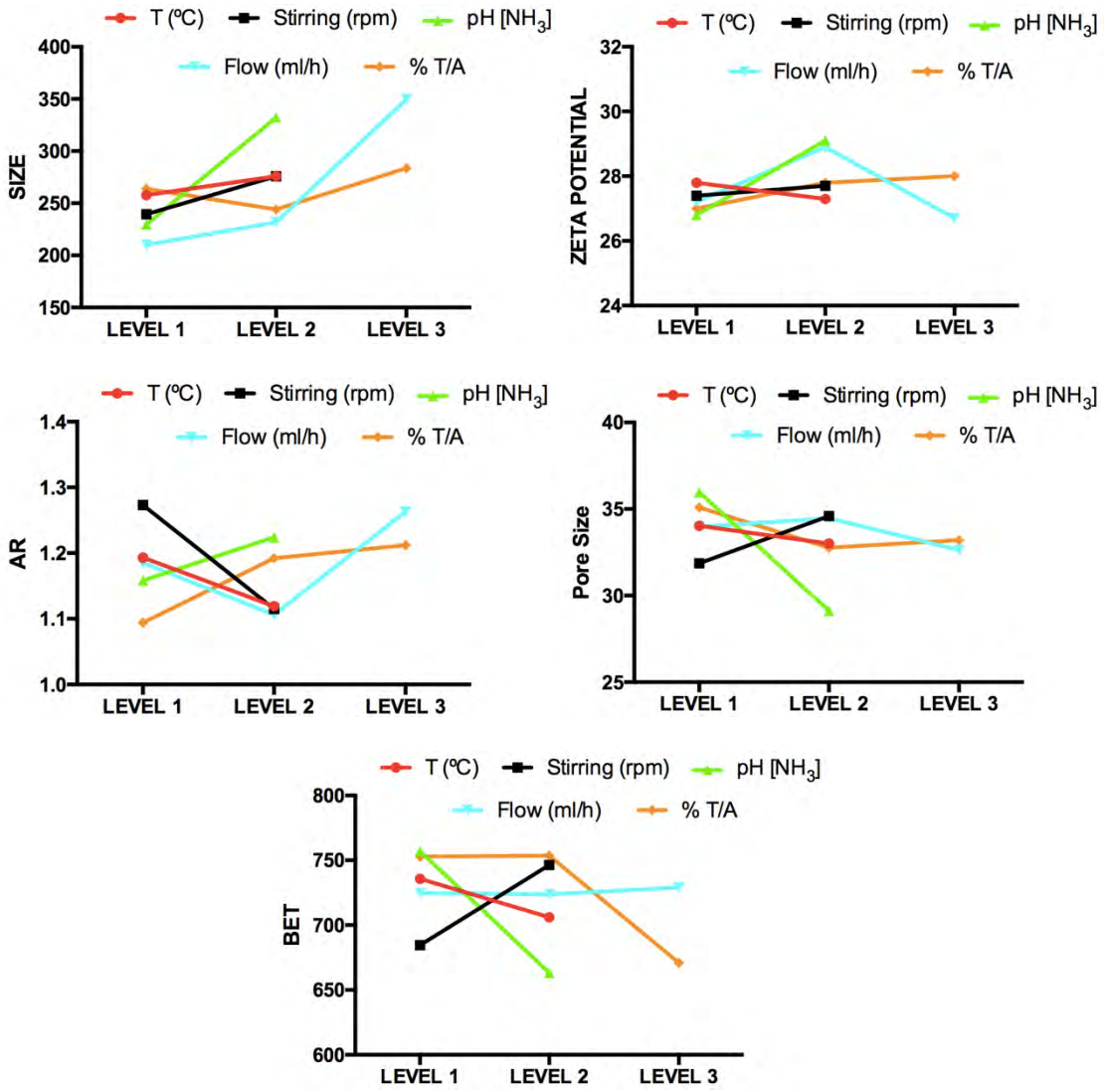

Figure 13: Effect of the DOE levels.

2.3.3 Synthesis of functionalized MSN

Once the intrinsic characteristics of the nanoparticles have been studied and it can be tuned through the DOE, modifications of the chemical surface are proposed to give a new synthetic identity. The different SIs allow the study of how they affect the biological identity when used as drug delivery systems. In this work, it is proposed the addition of isothiocyanate groups, BOC (tert-Butyloxycarbonyl) groups (on the surface or inside the pore or both in the surface and inside the pores) and finally the incorporation of PEGs of different lengths and oleylamine for the study of the influence of the adsorption of proteins[68,37,36,39]

2.3.3.1 Isothioyanate groups onto the MSN surface

The first modification was adding isothiocyanates. The highly selectivity of the SCN to amines groups allows the easy modification because of their presence on the MSN's surface, both the surface and the pore, as previously detailed in their synthesis. In addition to the study of the difference adsorption of the proteins on the surface, it is used for the rapidly incorporation of other functional groups. As is the case of the PEGs and oleylamine. For this, nanoparticles were dispersed in toluene and left for 24 hours at 50 °C and stirring. After the time, toluene is changed and thiocarbonyldi-2-(1*H*)-pyridone is added in DCM and it was left overnight at 50 ºC.

Figure 14: Schematic representation of the isothiocyanate groups' synthesis.

Rapidly, the white colourful of the MSN's surface was replace for a deep brown, while the capacity of dispersity and the others visual properties remain inalterable. By monitoring FTIR spectrum of the surface modified, MSN-SCN, it can be observed the formation of the new band at ≈ 2100 cm^{-1} corresponding to the isothiocyanate group (Figure 15).

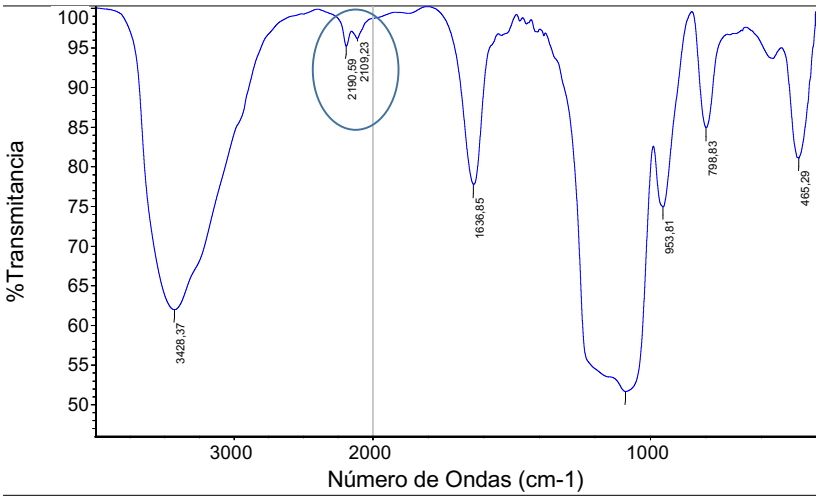

Figure 15: Infrared spectroscopy of the SCN

Another isothiocyanate groups addition is carried out through the conjugation of the isothiocyanate fruorescein (FITC), that is widely used as a bioconjugation through the formation of a isothiourea. This addition is useful for the monitoring of the nanoparticles in the followings of vitro assays. In the same way, its effect on the formation of the protein

corona will be studied, although in this case no change in the protein corona of MSN with and without FITC is expected. For that, two methods of anchoring are studied. The first one is adding FITC during the own synthesis of the MSN, and the second one is the anchoring once the nanoparticles have already been synthesized. It can be observed qualitatively in Figure 16 that all the nanoparticles are enough fluorescently labelled.

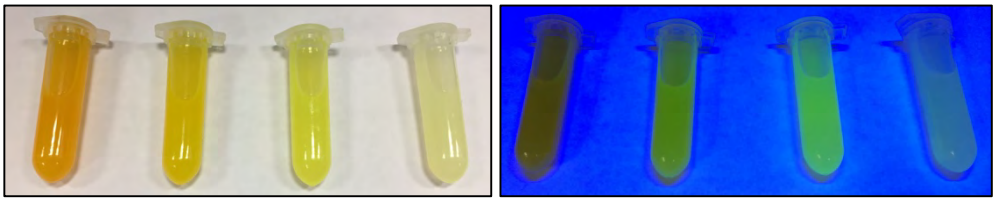

Figure 16: MSN covered post-synthesis with fluorescein at four different concentrations. The surface is covered with 20%, 10%, 5% or 1% of FITC for its study.

Also, the optimization of the obtaining of different concentration of FITC in the surface is studied for minimizing the change that have on the protein corona. Four different concentration are synthesized: 20%, 10%, 5% and 1% of FITC.

2.3.3.2 BOC group introduction

The previous modification of the amino groups by different groups is carried out indistinctly to the groups that are on the surface and in the pores. The differentiation of the two zones is very interesting for the use of the nanoparticles in drug delivery. For this, prior to the elimination of the surfactant in its synthesis, the surface groups are protected with BOC, so that when the subsequent elimination is carried out, the amino groups have been differentiated. This protection is accomplished by adding $(BOC)_2O$ in DCM. The reaction is left stirring for 4 hours at room temperature. Subsequently, the MSN are suspended in water and ammonium nitrate is added for the elimination of the surfactant, as detailed in materials and methods. HCl is changed to ammonium nitrate, since with the strong acid the conditions would be too extreme and the BOC would also be eliminated. In this way, it is possible to react the amines of the pores, having the pores protected with BOC; the amines of the surface can be reacted when the pore is clogged with the surfactant; and lastly, it can be reacted indistinctly inside and outside the pore using the primary amines.

To determinate the differentiation of the existing amino groups in the pores it cannot be done through an IR due to no well-defined bands of the BOC group are observed, since the proportion of BOC groups on the surface respect the amines of the nanoparticle is too small. Therefore, it can be analysed through the addition of ninhydrin. Ninhydrin

reacts with the amino groups, binds two ninhydrin for each amino, replacing the two protons of the amine and making an aromatic group with lilac coloration.

The resulting colours can be seen in Figure 17. From left to right are the nanoparticles with the pore uncovered without BOC group, having amino groups both on the surface and in the pore; the nanoparticles with the uncovered pore and BOC group on the surface, would only present amino groups in the pores; and finally the nanoparticles with BOC group and clogged pore, does not present exposed amino groups. It is observed how many more amino groups have exposed more intense is the colour, due to the reaction of ninhydrin. On the other hand, it is also determined through the zeta potential. The zeta potential of the initial MSN is 30 mV, after incorporation of the BOC group the zeta potential is 19.1 mV. Corroborating the correct addition.

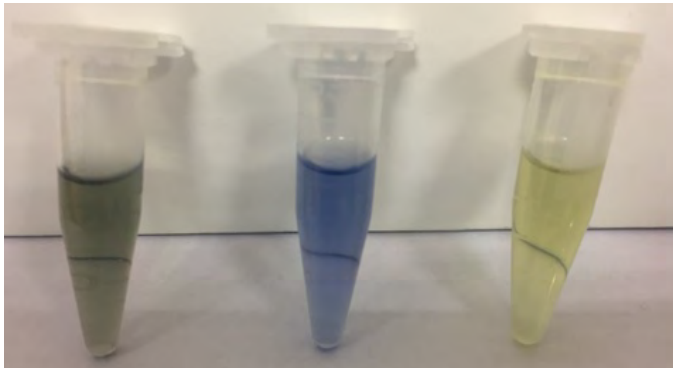

Figure 17: BOC both surface and pore, only pore and without BOC. From left to right are the nanoparticles with the pore uncovered without BOC group, the MSNs with the uncovered pore and BOC group on the surface, and the MSNs with BOC group and clogged pore.

2.3.3.3 PEG chain decoration

Poly(ethylene glycol) (PEG) has a wide variety of applications, which often involve its capacity to limit protein adsorption. PEG, immobilized to surfaces, greatly retards protein adsorption and shows antifouling activity[29,121]. Two lengths were chosen for this study, PEG n=4 (C4) and n=12 (C12). For this purpose, the synthesis of a C4 with an amine head and an ethyl ester tail is carried out. The synthetic route is shown in Figure 18, and the products are characterized through a ^{1}H-RMN (see Materials and Methods). Once the C4 has been synthesized it is easily added to the MSN, with the previous surface modification to SCN. The amine head reacts with the isothiocyanate group forming the isothiourea.

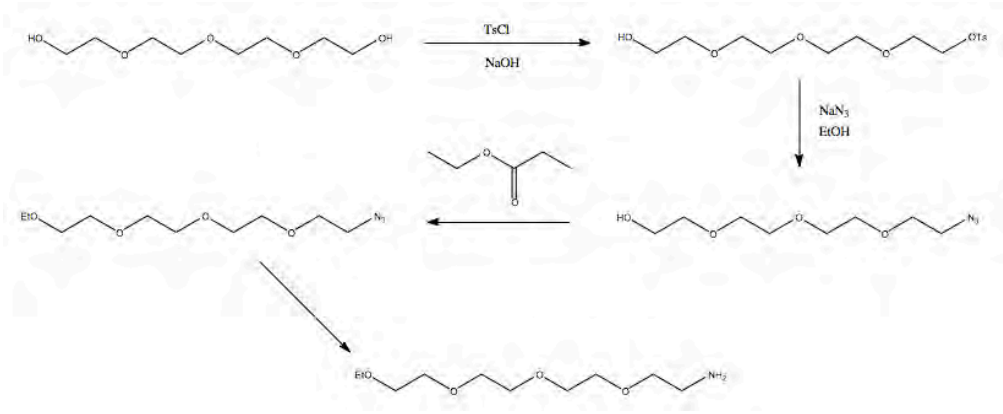

Figure 18: Synthetic route of PEG n=4.

On the other hand, the incorporation of the PEG n=12 is done. To test the surface anchoring a FTIR has been done of the two types of PEG's lengths. The FTIR are shown in Figure 19 obtaining the typical band around 1500 cm^{-1}, confirming the properly union. It is observed in the IR how the higher is the length of the PEG's chain, the greater its characteristic band results.

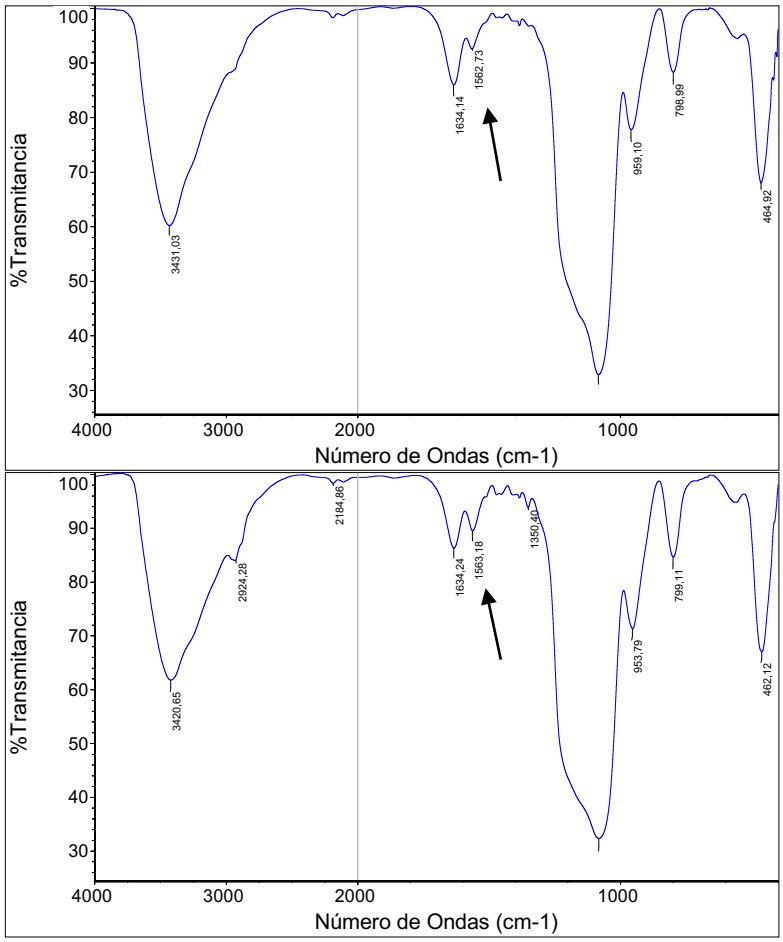

Figure 19: IR of the incorporation of the C4 and C12 to the MSN. On the top C4's IR, on the bottom the respective of the C12.

2.3.3.4 Oleylamine functionalization

It is reported in the literature that Oleic acid forms a complex with albumin[63,131,132]. Because of this complex, it can increase the ratio of albumin respect others proteins that form the PC, yielding a different and interesting for the study of the correlation between the synthetic identity and the biological identity fingerprint. For that reason, nanoparticles with isothiocyanate bonds are used to add oleylamine in the same way as the PEGs.

The FTIR of the nanoparticles with the incorporation of the oleyl group is shown in Figure 20, where appears the typical band at ≈1560 cm^{-1}

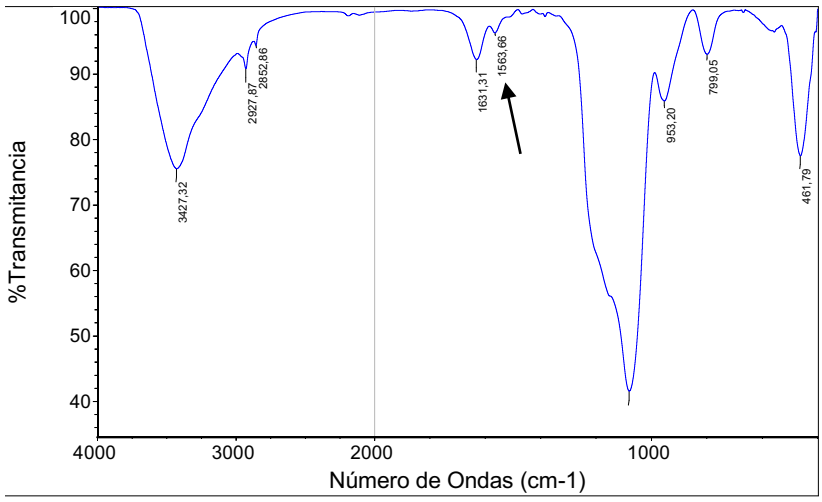

Figure 20: IR of the incorporation of the oleyl group

2.4 Concluding remarks

The results of this chapter show that mesoporous silica nanoparticles can be designed with different physiochemical properties. The optimization of a synthetic method and the application of a design of experiments renders twelve nanoparticles with different synthetic identity.

It is proposed a DOE varying the temperature, stirring, pH, flow rate and the % of the reagents (TEOS/APTES), which renders the synthesis of nine samples plus the two nanoparticles synthesized for optimized the synthetic method. After the analysis of the size and zeta potential of the MSNs through the DLS, the AR using the image from the SEM and the surface area and pore size with the BET, it is possible the analysis of the DOE. The DOE allows the study of the different parameters' influence in the MSN‘s SI. The pH of the media has a positive effect on the size and the zeta potential, also have a positive effect the agitation of the reaction on the pH size and the zeta potential. Finally, the flow addition has a positive effect on the surface area, opposite that on the pore size, where its effect is negative. Neither temperature nor the percentage of the reagent has any influence on the parameters of study.

Regarding the characterization of the physicochemical properties, in this chapter mesoporous silica nanoparticles with different sizes around 200 nm, and a zeta potential of +30 mV in water measure with the DLS, and +10mV in PBS have been obtained. At the same time, using a SEM it is possible the determination of the shape through the aspect ratio. Samples are composed by nanoparticles with a rod-shape (samples S5, S8 and S101 have an AR higher than 1.3) and the majority with a spherical shape (the other sample have an AR lower than 1.2). Lastly, regard the BET results, the nanoparticles present different pore size, which will be interesting for the next chapter. The samples can be classified into three groups: bigger than 37.7 Å (S1, S3 and S102), smaller than 30 Å (S5 and S8), and which is included between these groups, a pore size less than 37.7 Å and greater than 30. (S6, S101, S4, S2 and S7). On the other hand, silica nanoparticles without pores were synthesized as a control group. These NP ha 320 nm, a zeta potential of -8mV in water and -3mV in PBS, a spherical shape (AR equal to 1) and do not have pore.

Finally, for the study of the surface chemical’s influence, it has been synthesized some new synthetic identity. From the aminated surface of the sample S1 are obtained some different groups as an isothiocyanate, BOC (both an external surface and an internal one inside the pores), PEG and oleylamine. The analysis is done through IR.

Consequently, once the nanoparticles have been synthetized and characterized, the next chapter goes a step further and through the incubation of the MSN with biological media which allow the adsorption of the proteins, due to its future use as a drug delivery, the correlation between the synthetic identity and the adsorbed proteins will be performed.

2.5 References

(79) Nanoscience and Nanotechnologies : Opportunities and Uncertainties. *R. Soc.* **2004**, No. July.

(80) Croissant, J. G.; Fatieiev, Y.; Khashab, N. M. Degradability and Clearance of Silicon, Organosilica, Silsesquioxane, Silica Mixed Oxide, and Mesoporous Silica Nanoparticles. *Adv. Mater.* **2017**, *29* (9).

(81) Jeevanandam, J.; Barhoum, A.; Chan, Y. S.; Dufresne, A.; Danquah, M. K. Review on Nanoparticles and Nanostructured Materials : History , Sources , Toxicity and Regulations. *J. Nanotechnol.* **2018**, *9*, 1050–1074.

(82) Désert, A.; Tache, O.; Spalla, O.; Thill, A. SAXS Exploration of the Synthesis of Ultra Monodisperse Silica Nanoparticles and Quantitative Nucleation Growth Modeling. *J. Colloid Interface Sci.* **2010**, No. February.

(83) Fouilloux, S.; Daillant, J.; Thill, A. Colloids and Surfaces A : Physicochemical and Engineering Aspects Single Step Synthesis of 5 – 30 Nm Monodisperse Silica Nanoparticles : Important Experimental Parameters and Modeling. *Colloids Surfaces A Physicochem. Eng. Asp.* **2012**, *393*, 122–127.

(84) Miles, J. Metrology and Standars for Nanotechnology. New Global Frontiers in Regulation: The Age of Nanotechnology; 209AD; p 333.

(85) Balcells, L.; Fornaguera, C.; Brugada-Vilà, P.; Guerra-Rebollo, M.; Meca-Cortés, Ó.; Martínez, G.; Rubio, N.; Blanco, J.; Santamaría, J.; Cascante, A.; et al. SPIONs ' Enhancer Effect on Cell Transfection: An Unexpected Advantage for an Improved Gene Delivery System. *ACS Omega* **2019**, *4*, 2728–2740.

(86) Fern, M. Metal Oxide Nanoparticles. *Encycl. Inorg. Bioinorg. Chem.* **2011**.

(87) Mai, W. X.; Meng, H. Integrative Biology Mesoporous Silica Nanoparticles : A Multifunctional Nano Therapeutic System. *Integr. Biol.* **2013**, *5*, 19–28.

(88) Lo, A.; Arcos, D.; Terasaki, O. Aerosol-Assisted Synthesis of Magnetic Mesoporous Silica Spheres for Drug Targeting. *Chem. Mater.* **2007**, *19*, 3455–3463.

(89) Khan, I.; Saeed, K.; Khan, I. Nanoparticles : Properties , Applications and Toxicities. *Arab. J. Chem.* **2017**.

(90) Christian, P.; Kammer, F. Von der; Baalousha, M.; Hofmann, T. Nanoparticles : Structure , Properties , Preparation and Behaviour in Nanoparticles : Structure , Properties , Preparation and Behaviour in Environmental Media. *Ecotoxicology* **2008**.

(91) Jang, G.; Lee, H. Targeting Cancer Stem Cells by Using the Nanoparticles. *Int. J. na* **2015**.

(92) Dasgupta, S.; Auth, T.; Gompper, G. Wrapping of Ellipsoidal Nano-Particles by Fluid Membranes. *Soft Matter* **2013**, *9*, 5473–5482.

(93) Dasgupta, S.; Auth, T.; Gompper, G. Shape and Orientation Matter for the Cellular Uptake of Nonspherical Particles. *Nano Lett.* **2014**, *14*, 687–693.

(94) Hoffmann, F.; Cornelius, M.; Morell, J.; Fröba, M. Silica-Based Mesoporous Organic-Inorganic Hybrid Materials. *Angew. Chemie - Int. Ed.* **2006**, *45* (20), 3216–3251.

(95) Chithrani, B. D.; Ghazani, A. A.; Chan, W. C. W. Determining the Size and Shape Dependence of Gold Nanoparticle Uptake into Mammalian Cells. *Nano Lett.* **2006**, *4*.

(96) June, S.; Wu, S.; Lu, F.; Wu, S.; Hung, Y.; Mou, C. Size Effect on Cell Uptake in Well-Suspended , Uniform Mesoporous Silica Nanoparticles Size Effect on Cell Uptake in Well-Suspended , Uniform Mesoporous Silica Nanoparticles **. *small-journal* **2009**, No. June.

(97) Huang, X.; Teng, X.; Chen, D.; Tang, F.; He, J. The Effect of the Shape of Mesoporous Silica Nanoparticles on Cellular Uptake and Cell Function. *Biomaterials* **2009**, *31*, 438–448.

(98) Vivo, B.; Huang, X.; Li, L.; Liu, T.; Hao, N.; Liu, H.; Chen, D.; Tang, F. The Shape E Ff Ect of Mesoporous Silica Nanoparticles on Biodistribution ,. *ACS Appl. Nano Mater.* **2011**, *5* (7), 5390–5399.

(99) Hench, L. L. The Story of Bioglass®. *J. Mater. Sci. Mater. Med.* **2006**, *17* (11), 967–978.

(100) Vallet-Regi, M.; Rámila, A.; Del Real, R. P.; Pérez-Pariente, J. A New Property of MCM-41: Drug Delivery System. *Chem. Mater.* **2001**, *13* (2), 308–311.

(101) Izquierdo-Barba, I.; Ruiz-González, L.; Doadrio, J. C.; González-Calbet, J. M.; Vallet-Regí, M. Tissue Regeneration: A New Property of Mesoporous Materials. *Solid State Sci.* **2005**, *7* (8), 983–989.

(102) Vallet-Regí, M. Bioceramics: From Bone Substitutes to Nanoparticles for Drug Delivery. *Pure Appl. Chem.* **2019**, *91* (4), 687–706.

(103) Vallet-Regí, M.; Ruiz-Hernández, E. Bioceramics: From Bone Regeneration to Cancer Nanomedicine. *Adv. Mater.* **2011**, *23* (44), 5177–5218.

(104) Lai, C. Y.; Trewyn, B. G.; Jeftinija, D. M.; Jeftinija, K.; Xu, S.; Jeftinija, S.; Lin, V. S. Y. A Mesoporous Silica Nanosphere-Based Carrier System with Chemically Removable CdS Nanoparticle Caps for Stimuli-Responsive Controlled Release of Neurotransmitters and Drug Molecules. *J. Am. Chem. Soc.* **2003**, *125* (15), 4451–4459.

(105) Tarn, D.; Ashley, C. E.; Xue, M.; Carnes, E. C.; Zink, J. I.; Brinker, C. J. Mesoporous Silica Nanoparticle Nanocarriers: Biofunctionality and Biocompatibility. *Acc. Chem. Res.* **2013**, *46* (3), 792–801.

(106) Huang, W. Functionalized Mesoporous Silica Nanoparticles (MSNs) for Applications in Drug Delivery and Catalysis. **2012**.

(107) Caruso, F.; Hyeon, T.; Rotello, V.; Vivero-escoto, J. L.; Huxford-phillips, R. C.; Lin, W. Silica-Based Nanoprobes for Biomedical Imaging and Theranostic Applications. *Chem. Soc. Rev.* **2012**, No. 7.

(108) Nooney, R. I.; Thirunavukkarasu, D.; Chen, Y.; Josephs, R.; Ostafin, A. E. Synthesis of Nanoscale Mesoporous Silica Spheres with Controlled Particle Size. *Chem. Mater.* **2002**, No. 17, 4721–4728.

(109) Jerzy, W. W.; Yoo, J. C.; Pruski, M.; Lin, S. Organic Functionalization and Morphology Control of Mesoporous Silicas via a Co-Condensation Synthesis Method. *Chem. Mater.* **2003**, *15*, 4247–4256.

(110) Jong, W. H. De; Borm, P. J. Drug Delivery and Nanoparticles: Applications and Hazards. *Int. J. Nanomedicine* **2008**, *3* (2), 133–149.

(111) Yanagisawa Tsuneo, Shimizu Toshio, Kuroda Kazuyuki, K. C. The Preparation of Alkyltriinethylaininonium–Kaneinite Complexes and Their Conversion to

Microporous Materials. *The Chemical Society of Japan*. 1990, pp 988–992.

(112) C. T. Kresge; M. E. Leonowicz; W. J. Roth; J. C. Vartuli; J. S. Beck. Ordered Mesoporous Molecular Sieves Synthesized by a Liquid-Crystal Template Mechanism. *Nature* **1992**, *359* (22), 710–712.

(113) Trewyn, B. G.; Slowing, I. I.; Giri, S.; Chen, H.; Lin, V. S. Synthesis and Functionalization of a Mesoporous Silica Nanoparticle Based on the Sol – Gel Process and Applications in Controlled Release. *Acc. Chem. Res.* **2007**, 846–853.

(114) Huang, X.; Li, L.; Liu, T.; Hao, N.; Liu, H.; Chen, D.; Tang, F. The Shape Effect of Mesoporous Silica Nanoparticles on Biodistribution, Clearance, and Biocompatibility in Vivo. *ACS Nano* **2011**, *5* (7), 5390–5399.

(115) Llinas, M. C.; Sánchez, D. Nanopartículas de Sílice: Preparación y Aplicaciones En Biomedicina. *Affinidad* **2014**, *LXXI* (565), 20–31.

(116) Bourquin, J.; Milosevic, A.; Hauser, D.; Lehner, R.; Blank, F.; Petri-Fink, A.; Rothen-Rutishauser, B. Biodistribution, Clearance, and Long-Term Fate of Clinically Relevant Nanomaterials. *Adv. Mater.* **2018**, *30* (19), 1–31.

(117) Markovsky, E.; Baabur-Cohen, H.; Eldar-Boock, A.; Omer, L.; Tiram, G.; Ferber, S.; Ofek, P.; Polyak, D.; Scomparin, A.; Satchi-Fainaro, R. Administration, Distribution, Metabolism and Elimination of Polymer Therapeutics. *J. Control. Release* **2012**, *161* (2), 446–460.

(118) Illum, L. Nanoparticulate Systems for Nasal Delivery of Drugs : A Real Improvement over Simple Systems ? *J. Pharm. Sci.* **2007**, *96* (3), 473–483.

(119) Mudshinge, S. R.; Deore, A. B.; Patil, S.; Bhalgat, C. M. Nanoparticles : Emerging Carriers for Drug Delivery. *Saudi Pharm. J.* **2011**, *19* (3), 129–141.

(120) Krutzke, L.; Prill, J. M.; Engler, T.; Schmidt, C. Q.; Xu, Z.; Byrnes, A. P.; Simmet, T.; Kreppel, F. Substitution of Blood Coagulation Factor X-Binding to Ad5 by Position-Speci Fi c PEGylation : Preventing Vector Clearance and Preserving Infectivity. *J. Control. Release* **2016**, *235*, 379–392.

(121) Saraiva, C.; Praça, C.; Ferreira, R.; Santos, T.; Ferreira, L.; Bernardino, L. Nanoparticle-Mediated Brain Drug Delivery : Overcoming Blood – Brain Barrier

to Treat Neurodegenerative Diseases. *J. Control. Release* **2016**, *235*, 34–47.

(122) Dayanand, S.; Group, D. Nanoparticles : Nasal Delivery of Drugs International Journal for Pharmaceutical Research Scholars (IJPRS). *Int. J. Pharm. Res. Sch.* **2016**, *3* (3).

(123) Hamidi, M.; Azadi, A.; Ra, P. Hydrogel Nanoparticles in Drug Delivery. *Adv. Drug Deliv. Rev.* **2008**, *60*, 1638–1649.

(124) Singh, R.; Lillard, J. W. Nanoparticle-Based Targeted Drug Delivery. *Exp. Mol. Pathol.* **2009**, *86* (3), 215–223.

(125) Martínez-Edo, G.; Balmori, A.; Portón, I.; Martí del Rio, A.; Sánchez-garcía, D. Functionalized Ordered Mesoporous Silicas (MCM-41): Synthesis and Applications in Catalysis. *Catalysts* **2018**, *8*, 617.

Chapter III. Biological Identity

This page left blank intentionally

3.1 Introduction

In recent years, significant efforts have been made to progress in the use of nanotechnology for targeted drug delivery, focusing on formulate therapeutically active agents in biocompatible nanoforms such as NPs. These systems offer many advantages in drug delivery, mainly focusing on improved efficacy, biosafety and stability of the drugs[123,133,119,85].

Nanoparticles used for drug delivery can be administrated *via* three main routes: direct injection, inhalation and oral intake. Regardless of the way, once NPs were administered, they were exposed to blood, that is composed of several thousand biomolecules, mainly proteins, being each of whom at considerably different concentrations[63]. It has been demonstrated in lots of reports that nanoparticles can adsorb immediately proteins on their surface. Thus, when a NP enters a biological medium a competition between different biological molecules to adsorb on the surface of the nanoparticles begins immediately. This coating that was formed around on the NP's surface was known as the protein corona (PC).

To some extent, the nature of the PC determines the biological response, such as the cellular uptake, the circulation time, bioavailability, and even toxicity, and it was crucial to achieve the goal as a drug delivery. For that reason, it was highly important to understand and control the PC[134,135]. Protein corona could be schematically represented as a double-layer coating wrapping the NP. This two layers are differentiating according to both the speed at which the proteins in the medium begin to form part of the protein corona and the affinity of the proteins for the NPs' surface. In the initial stage, most abundant proteins were adsorbed on the surface; however, over the time they will be replaced by proteins with higher affinity. Thus, the part that forms a "fast" protein corona, that was built on a time scale of seconds, but it has a lower affinity and thus a higher turnover of loose interactions between proteins and NPs was known as the "soft" protein corona. On the other hand, the other part that forms a "slow" protein corona, which was formed in minutes or even hours and have a high affinity for the NPs' surface, was known as the "hard" protein corona. The proteins that forms the hard protein corona slowly replace the protein that form the soft corona. For this reason, the protein corona was determined by the kinetic and equilibrium binding, depending on the composition of the medium and on the properties of the NP[32,34,35,37,36].

The formation of the protein corona was governed by the "Vroman effect"[136]. Although this effect remains one of the quintessential mysteries of the biomaterials surface science and the exact mechanisms underlying this process have not yet been resolved, this effect proposes that the adsorption of the proteins from plasma occurs through a complex series of adsorption-displacement steps. This continuous state of dynamic exchange concomitantly occurs with the displacements of the low molecular-weight (MW) proteins, that arrive first in the NP surface, for the relatively higher MW proteins, that arrive later. At any time, a protein may desorb, allowing other proteins to interact with the nanoparticle's surface, until a stable corona was established (hard corona)[137].

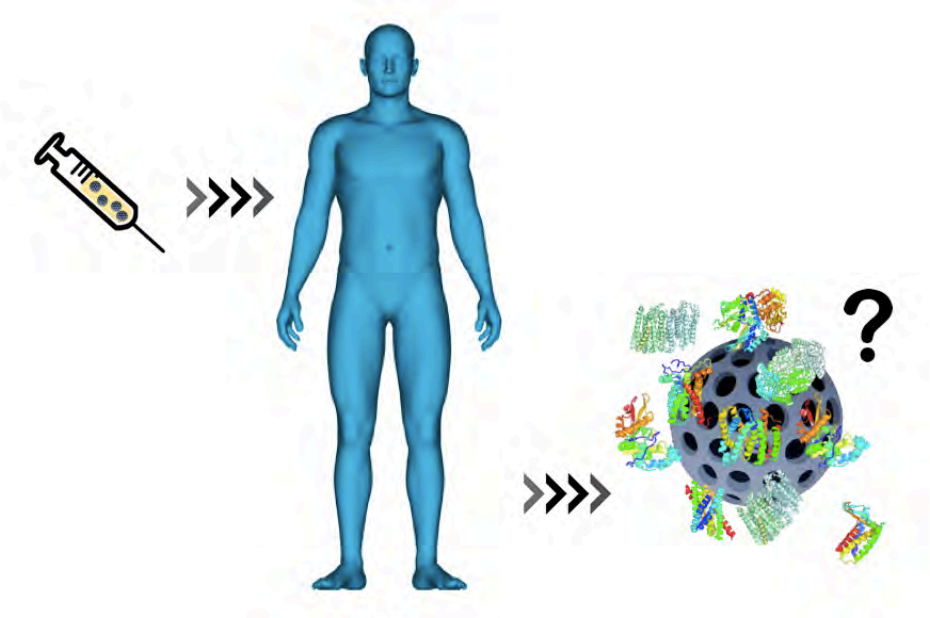

Figure 21: Schematic representation of the formation of the protein corona.

In the previous chapter (Chapter II) have been studied the geometrics parameters, nanoparticle shape (curvature) and roughness (pore size), among others. The pores distributed along the matrix of the porous nanomaterial are designed for the diffusion and desorption of the drug in a controlled and homogeneous way once NPs have been internalized in the cell, suitable for its use in drug delivery[4]. The blood enters into the NP structure and slowly dissolves the drug while releasing it to the medium. NP's structural integrity is kept intact thanks to their matrix[138].

However, the importance of the pores in the use of MSN for drug delivery has not been widely studied. Despite the extensive studies and the known influence of the physicochemical properties in the formation of the PC, only a few reports pay attention and focus on the influence of the nanoparticle roughness in the formation of the PC,

which will be key in the final physiological response of the nanoparticle[139,140]. Some researchers show the importance of the PC in the biodistribution[141] or in the targetability of the MSN[138,142], among others effects, but regardless of the relationship with the pore. The biocompatibility is also related with the pore size, even though it has yet not been elucidated, due to the diversity of engineered MSNs, to which extent this parameter has an influence on biocompatibility by itself[143].

The relationship between the pore size and the protein size determines the NPs application. Proteins in these systems can be used for targeting some organs[49,50], for blocking the pores for controlled drug release as a gatekeeper[77] or for being released from the nanoparticle[78]. The function of the protein will be determined according to the ratio between the protein and pore size.

Aimed at studying these three possible applications, in this chapter the use of nanoDSC and ITC is proposed. In order to understand how the pores' characteristics, affect the formation of the PC, finding one optimal protein is needed to interact with MSNs and form a pure PC. To do so, Human Albumin Serum (HSA), the most abundant protein, which is an always-found component in the plasma was chosen. This election was inspired by the non-specific interaction and the great potential of albumin in the field of drug delivery[144].

The enormous influence of the pore size on the PC formation has been demonstrated and it has been extracted as an independent geometric parameter. Even so, the mechanism of the PC formation in relation to the pore is not known. To analyse the soft corona of the MSN, the adsorption processes of HSA will be analysed by means of MicroITC measurement. This technique allows the characterization of the PC performing titrations of HSA solutions into suspensions of different MSN, while monitoring the interaction in situ. MicroITC will be used in order to analyse the formation of the protein corona regarding the pore size, as a dynamic study where the protein is fitted in the pore during the analysis. On the other hand, to analyse of the hard corona will be performed by using nanoDSC[29,145]. This technique enables the study of the denaturation of the hard corona and provides a static information[146]. In this assay, the cell is filled with the formed at the MSN surface, the denaturalization process of this system will depend on the pore size. Therefore, the complementarity of this two techniques allows an entire insight of the PC formation related to the pores of the MSN[29,147,148,149,145,2,150,64].

To summarize, having MSN characterized in the previous chapter, now an explanation to the behavior of proteins once it was formed the protein corona around MSN because of their purpose according to their pore size was here proposed in Chapter III. For this purpose, two thermodynamic equipment were used: the nanoDSC and the ITC.

3.1.1 Objectives

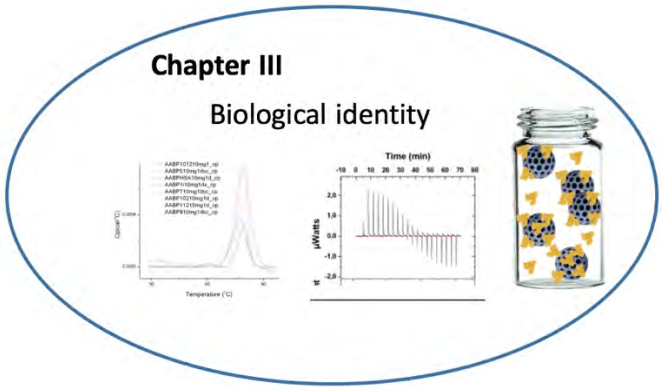

Figure 22: Graphical abstract of the Chapter III.

In order to achieve this objective, the following tasks were proposed:

- To characterize the protein corona of the different samples in quantity, composition and thermodynamic characteristics using nanoDSC and MicroITC.
- To correlate the properties of the protein corona with the nanoparticle's synthetic identity, in order to determine how the SI affects in the BI and be allow to design the MSN with defined properties in function of the wanted purpose.
- To postulate a mechanism through which the protein corona is formed, to understand, finally, which process take place during PC formation.

3.2 Materials and Methods

3.2.1 BCA

BCA quantification assays were performed by using PierceTM BCA Protein Assay Kit, by following instructions of the manufacturer. Rapidly, a calibration curve was prepared for subsequent quantification (125 µg/mL – 2 mg/mL in PBS). Analyses were performed in 96 micro-well plates (SPL), and 10 µL of standards and 20 of samples were charged, per triplicate, in each well. 200 µL of BCA reagent were added to standards and samples, and incubated at 37 °C during 30 minutes. After incubation, samples were allowed to cool and finally absorbance was measured at 562 nm.

For the subsequent protein quantification in the corona of MSNs, different nanoparticles were incubated with human serum albumin (≥96% purity, Sigma Aldrich). MSN were incubated with 10 mg of HSA in a total volume of 1 mL (PBS). Samples were mixed carefully, to avoid protein denaturation due to mixing, and incubated 24 hours at 37 °C. Purification of hard corona was carried out by centrifuging samples at 13000 rpm for 13 minutes and including three washing steps in the purification procedure. Samples were first centrifuged and supernatants (SN) were discarded and 1 mL of fresh PBS was added to suspend nanoparticles. Procedure was repeated 3 additional times, in order to wash nanoparticle solution from non-attached protein present in solution. Finally, 100 µL of 10% SDS were added to the washed pellet; samples were mixed and heated at 95 °C for 10 minutes to allow corona proteins desorb from NP surface. Samples were centrifuged under same conditions to separate the MSN of the PC.

For the PC formation with FBS, 100 µL were added to MSN solution to a final volume of 1 mL. For the Lys and GO were added also 10 mg of each protein. To the samples S1 with oleyl, PEG, SCN and FITC were add also 1 mg of sample.

3.2.2 SDS-Page

Protein corona were formed and removed of the nanoparticles with the same protocol as for the BCA for the SDS-Page analysis. Gels were reticulated with a 7% of acrylamide. Each gel run included one lane of a molecular weight ladder standard (BIO-RAD).

3.2.3 DSC

The hard corona was formed with the method described previously (without the washes), for HSA, FBS, Lys and GO coronas. Then, the cell was filled with the solution formed with 1 mg of MSN and 10 mg of HSA. Three temperature cycles between 25 to

98 ºC were performed. The baseline was obtained, subtracting each third cycle from the respective first one using Origin® software.

3.2.4 ITC

The calorimetric measurements were performed using a ITC200 Microcalorimeter (MicroCal). Injection parameters were specific for each sample, depending on the BCA assay: the range of MSN concentration was in the range from 2 mg/mL to 3 mg/mL of MSN in the sample cell, and HSA was charged at 7 mg/mL in the syringe. The reaction started by HSA titration over NPs suspension and in the end a total volume of 400 µL (2 µL x 20) was titrated. The time between the titration steps was 150 s and was chosen to reach an equilibrium state. During all experiments the temperature of the ITC device was kept constant at 37 °C. The nanoparticles inside the sample cell were permanently stirred at 500 rpm. Sample data was analysed by Origin® software.

3.2.5 Suspension stability

The suspension stability was made in H_2O due to in PBS the PdI was 1 in the studied concentrations. 5 mg on nanoparticle were sonicated in 1 mL of H_2O and they were added to a solution of different concentration of HSA. The concentrations studies were:

	0	**1**	**10**	**20**	**50**	**100**	**200**
H_2O (µL)	1000	955	950	900	850	500	0
HSA (1g/mL) (µL)	0	5	50	100	150	500	100

3.2.6 Aggregation regard the size (DSL)

The kinetics in the plate reader was run during 1 hour with a read every 10 seconds at a 300 nm. For the measurement of the NP without PC, 2.5 mg of S1 were sonicated in 1 mL of PBS, then it was placed in the cuvette. Regarding the sample with PC, 2.5 mg of S1 were incubated in 1mL of PBS with 50 µL of FBS, then it was filled the cuvette with the sample.

3.2.7 Proteomics

Nanoparticles were incubated and the protein corona was removed of the surface with the usual method. Then the solution of 10% of SDS with the PC.

3.2.8 Deconvolution program

The peaks of the DSC were deconvolved using OriginPro 9.0.0.0 (64-bit) SR2 software.

3.2.9 CryoTEM

Negative-staining TEM to image MSN. 8 µL of MSN were placed on a TEM grid and full evaporated at room temperature. Then, the TEM grid was submerged with 8 µl of uranyl acetate 2% was placed on the grid for 1 min before draining it off. The equipment used was JEOL JEM (2011).

3.3 Results and discussion

3.3.1 Study of the influence of the SI on the PC.

To determine how differences in the SI lead to the formation of different protein coronas, MSNs were incubated with HSA in PBS during 24 h at 37 ºC, in order to simulate the physiological conditions. Afterwards, the MSN were recollected via centrifugation, at 13000 rpm for 13 min, and the supernatant was discarded. Nanoparticles were then dispersed in 1 mL of PBS and centrifuged, discarded the supernatant again, three times in order to remove the free proteins that were not part of the hard protein corona for its correct characterization, including the quantification of the proteins.

As has been discussed before, the biomolecular interface can be divided into the "hard" and "soft" protein corona, even in the case that PC it is composed only by a single protein, understanding it as a dynamic layer, as in this case HSA. The "hard" protein corona consists of proteins with an irreversible protein binding (adsorption). On the other hand, there are proteins with a lower affinity which are reversibly bound to MSNs or are connected with the hard protein corona (protein–protein interactions), these proteins form the so called "soft" protein corona. Hard corona is responsible for the interaction pathways, for that reason in this work we study this PC. It is crucial to understand how the processes of protein adsorption and exchange occur in the corona[34,35,36,31]. In practice, the "hard" corona can be defined as the proteins which were not removed from the MSN's surface during preparation procedures such as washing and centrifugation, which that can interrupt the relatively weak protein–protein interactions which would remove the soft protein corona.

Two nanoparticle were chosen to check that the characteristics defined in the chapter II render different PC. The properties were summarized in Table 4.

Table 4: Synthetic properties of the S101 and S102.

	DLS		*SEM*		*BET*	
Exp.	**Size**	**Pot-Z**	**Size**	**AR**	**Area**	**Pore**
S101	374	33,6	320x130	1,9	688	34,9
S102	241	9,1	120	1	763	38,8

To analyze if the PCs were indeed different, the nature of the two fingerprints formed of the protein corona on the S101 and S102 nanoparticles were analyzed. For this purpose, a SDS-Page was carried out, which although the resolution in the protein separation was not very high, will give an idea of the protein profile. Sodium dodecyl sulphate polyacrylamide gel electrophoresis, SDS-Page, is a very common method for separating proteins by electrophoresis (separation of macromolecules in an electric field) that uses a discontinuous polyacrylamide gel as a support medium and sodium dodecyl sulphate (SDS) to denature the proteins. This system is also called the Laemmli method after U.K. Laemmli, who was the first to publish a paper employing SDS-PAGE in a scientific study[151].

The SDS-Page result (Figure 23) shows (the last lane of each gel) that the proteins that form the protein corona. For both gels, the first lane after the lane for the standard protein marker was the supernatant and the following lanes were the washes until there were no proteins in the medium. It can be clearly observed how the PC profile was different between the different samples.

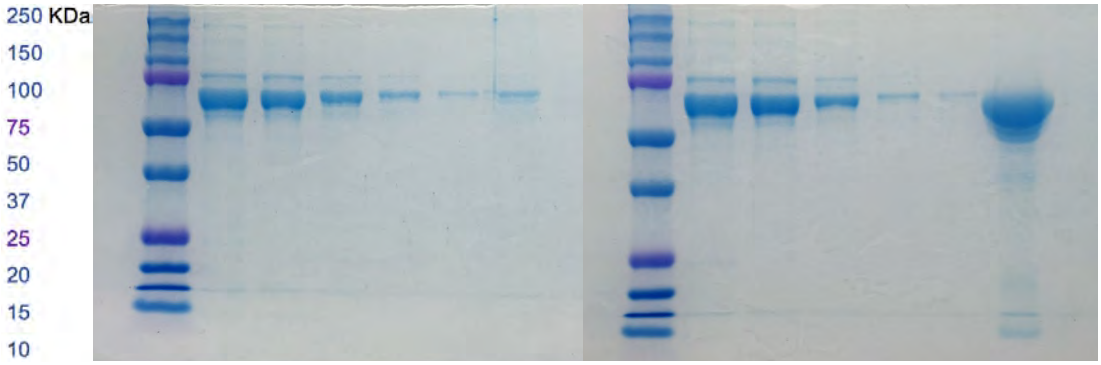

Figure 23: SDS-Page of S101 and S102, respectively. From left to right: marker, washes 1 to 5 and final protein corona of the MSN.

It was also studied the change in the zeta potential of the nanoparticle through the DLS. The MSN's zeta potential in PBS of S1 was + 5,8 mV, while the zeta potential of the MSN when were incubated in a medium with HSA was -10 mV.

3.3.2 Behavior of the nanoparticles with protein corona

3.3.2.1 Suspension stability

The suspension stability is also dependent on the surface nature. The behavior of nanoparticles when they have an aminated surface and when they are surrounded by proteins affects their capacity to remain in suspension or to fall to the bottom by gravity. The time that nanoparticles, with or without protein corona, remain in suspension can be

determined by a kinetic study using the absorbance plate reader. The MSN in the cuvette in suspension will absorb light whereas if they fall to the bottom they will not absorb.

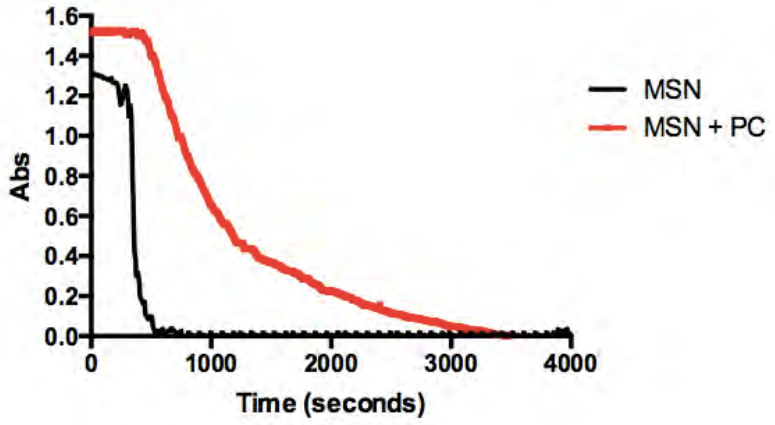

Figure 24: Suspension stability of MSN in PBS (black) and MSN with protein corona of HSA in PBS (red).

Nanoparticles without PC fall abruptly to the bottom by gravity in 4.3 minutes. Whereas, the same nanoparticles with protein corona needed 9.7 minutes to fall down. In turn, the deposition of nanoparticles with protein corona was more prolonged in time, more progressive. For the purpose of drug delivery, the colloidal stability of the NP's is a mandatory requirement.

3.3.2.2 Aggregation regarding the size

The aggregation of nanoparticles due to electrostatic processes is an important factor for their use as drug delivery systems. If nanoparticles get aggregated during the circulating time in the body, the biological system could collapse. Nanoparticle's increase in size can be monitored as HSA is added. Increasing amounts of albumin were titrated onto a constant quantity of nanoparticles and size was measured through DLS.

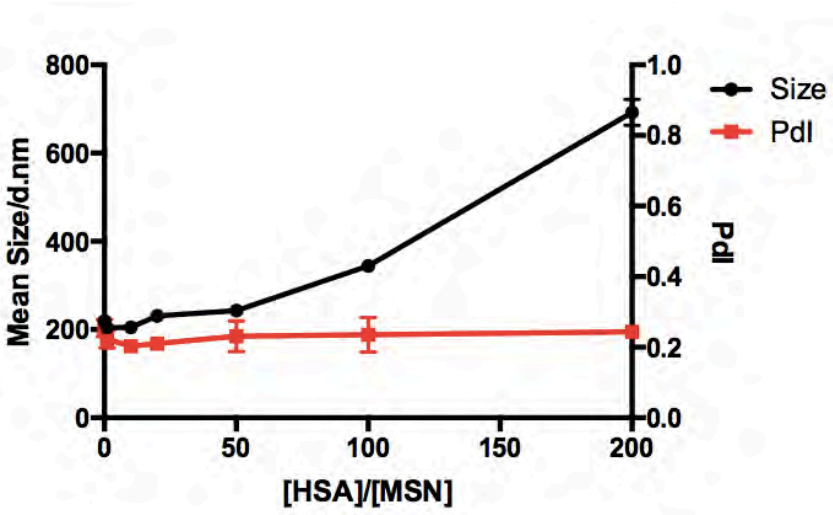

Figure 25: Relationship of the increase in size with the addition of protein of the size. Albumin was titrated over the sample of MSN in PBS and the size was monitored.

It can be observed in Figure 25 how, from a ratio of HSA and MSN was 100 [HSA]/[MSN] on, the size of the nanoparticles begins to grow exponentially. This increase was not due to the presence of the protein corona but to the aggregation. From the experiment it can be concluded that, the nanoparticles were not aggregated until a ratio of 100 [HSA]/[MSN].

3.3.3 Characterization of the protein corona

3.3.3.1 Quantification of the protein corona using BCA assay

Nanoparticles were incubated with a solution of human serum albumin (HSA). This protein corona could be considered part of the soft corona because in a real biological media, albumin and its derivatives belong to the more abundant proteins in plasma, which form firstly the PC but with a low affinity[152]. However, in this work it was taken as hard protein corona, due to the fact that some researchers assert that the incubation conditions allow the formation of strong bindings since the long incubation times confer extra stability. Furthermore, the washes for the treatment of the samples allow the elimination of proteins that do not have a strong enough binding to be considered hard corona[33].

Once the four washes and the extraction of the PC were performed (see Materials and methods), a quantification of the protein corona was done. The quantification was carried out *via* Bicinchoninic acid assay (BCA), which consist of a method for colorimetric detection and quantification of total protein[153]. The protein corona was given as the total weigh of protein that form the PC per weigh of nanoparticle (µg prot/mg NP). It can be

observed that different types of nanoparticles yield different amounts of proteins that form the protein corona (Figure 26).

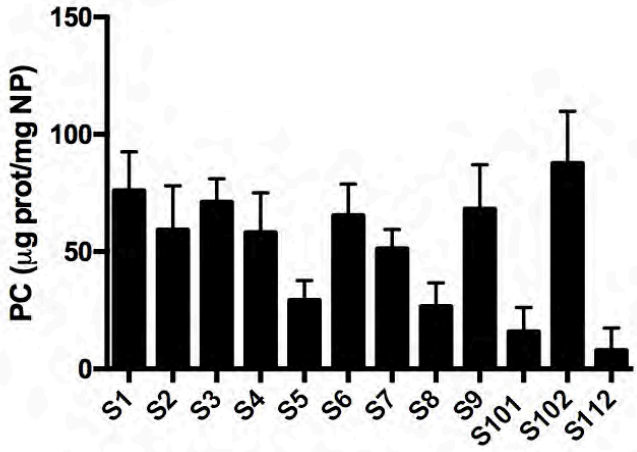

Figure 26: BCA quantification of the Hard Protein Corona incubated with HSA.

On the other hand, nanoparticles were also incubated with fetal bovine serum (FBS). The diversity of proteins in FBS with different concentrations, sizes, Isoelectric points (pI) and behaviors allow the formation of hard PCs composed by different proteins. The amount of the PC on the MSN were similar between the protein corona composed of FBS and only of HSA. That means that the characteristics of the nanoparticles influences the quantity of proteins absorbed in their surface.

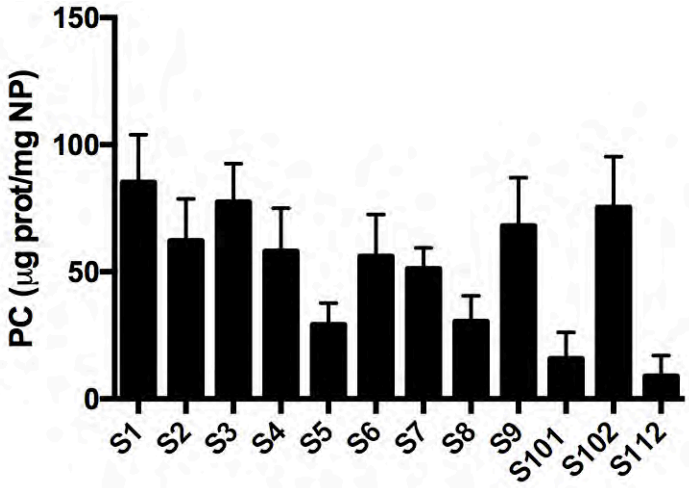

Figure 27: BCA quantification of the Hard Protein Corona incubated with FBS.

In Chapter II some new chemical identities adding oleyl group, PEG (C4 and C12) and SCN were synthetized. To these samples were also added MSN with oleyl groups on the surface, maintaining the NH_2 groups inside the pore (oleyl-NH_2). Using the BCA assay it can be analyzed the effect of the surface nature on the PC formation.

Table 5: BCA quantification of the Hard Protein Corona incubated with HSA and nanoparticles with surface modifications (Oleyl, C4 and SCN) compared to NH_2.

	S1	*C4*	*C12*	*Oleyl*	*Oleyl-NH_2*
PC	85,7	42,9	38,9	52,3	101,3

It can be observed in Table 4 how the quantity of proteins that form part of the PC decreases regarding the surface modification. Compared to S1, which was the unmodified MSN, when adding to these S1 nanoparticles PEG, both C4 and C12, the PC decreased to the half. Although bibliographically it is considered that the PEG groups avoid the formation of protein corona, the presence of oleyl does practically the same function. Finally, MSNs with the pore aminated and the surface with oleyl group show more proteins forming their PC. To know the identity of the proteins that form the PC, a SDS-PAGE has to be carried out.

3.3.3.2 Influence of the FITC in different media on the formation of the protein corona

The preliminary study of the addition of FITC for following *in vitro* assays was made. In this chapter, it was corroborated the no-influence of FITC in the amount of protein corona. No change in the PC was desired since the study and the optimization of the PC properties have to be maintained with the FITC.

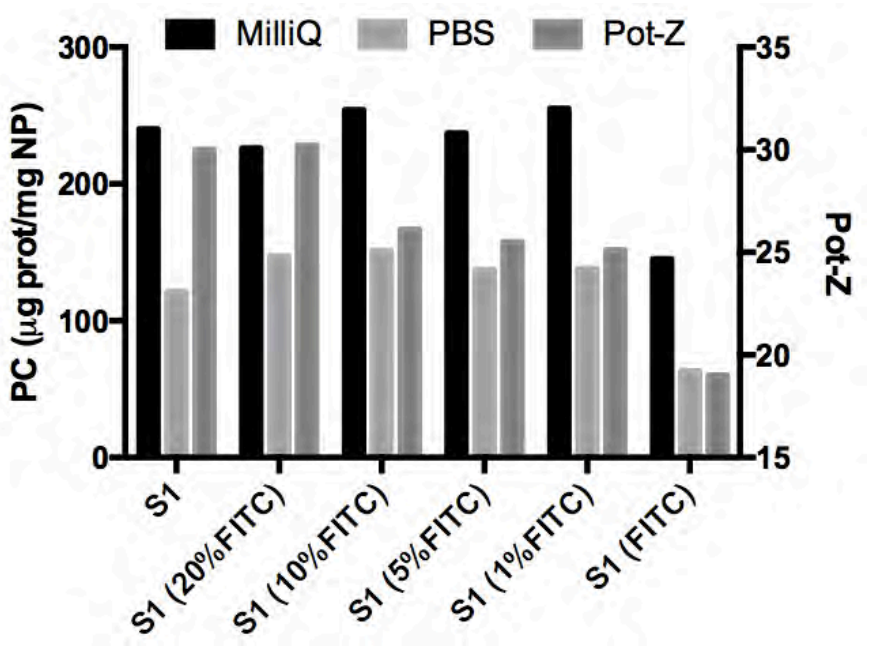

Figure 28: pH depending on the PC formation. S1, MSN without modification; S1 (20% FITC), S1 with a 20% of FITC, S1 (10% FITC), S1 with a 10% of FITC; S1 (5% FITC), S1 with a 5% of FITC; S1 (1% FITC), S1 with a 1% of FITC, S1 (FITC), S1 with 20% FITC added during the formation.

In Figure 28 it can be observed that the PC both in H_2O (MilliQ) and PBS was the same with any quantities of FITC. Conversely, when FITC was added during the nanoparticle formation cause changes that will change the protein corona. This addition changes the synthetic properties of the MSN causing a SI change and irretrievably a BI change. On the other hand, the zeta potential was also the same.

3.3.3.3 PC fingerprint characterization through SDS-Page

Once it was determined that changes in the synthetic identity have an influence on the protein corona formation regarding the quantity of proteins, and it had been seen that the fingerprints of two sample were different, SDS-Page was used to know the fingerprint of the hard protein corona of every sample incubated in HSA and in FBS solutions.

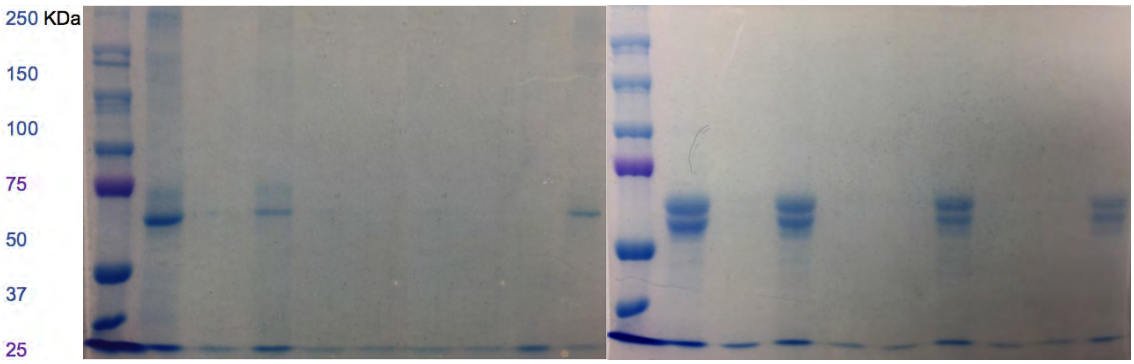

Figure 29: SDS-Page on the left MSN incubated in HSA and on the right MSN incubated in FBS. Every lane matches with the number of the sample: S1, S2, S3, S4, S5, S6, S7, S8, S9, S101 and S102.

Figure 29 shows the fingerprints of the PC, on the left with HSA and on the right with FBS. In the acrylamide gel it can be observed that three samples present protein enough to appear in the gel. At the same time, the band of S1 was greater than S3 and S9, which corroborates the BCA results, where they were the three samples that had more PC. On the other hand, in the gel of the MSN incubated with FBS (right) it can be observed four bands, S1, S3, S6 and S9. Regarding the composition of the PC it seems to be formed by the same proteins, but SDS-Page was not accurate enough to be conclusive.

It was also analyzed the fingerprint of the nanoparticles with the surface modified with PEG, both C4 and C12, and with oleyl and oleyl-NH_2.

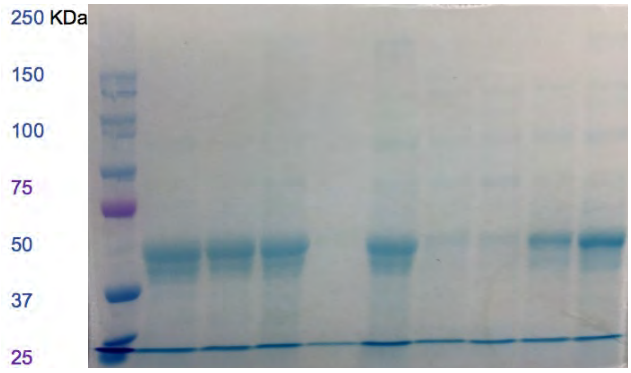

Figure 30: SDS-Page from the left to the right S1, S6, S9, S101, S102, C4, C12, Oleyl, NH_2-Oleyl. PC: 87.7, 71.2, 88, 23.3, 82.3, 42.9, 38.9, 52.3 and 101.3 µg FBS/mg MSN.

The first five lanes correspond to the naked samples S1, S6, S9, S101 and S102. Comparing the sample S1 to MSN with PEG in the surface, it can be observed how the proteins that form the PC decreased considerably. On the other hand, it was corroborated that the proportion of albumin in the PC was increased in the samples with oleyl, being more notably with the aminated pores.

3.3.3.4 Thermal study of the hard protein corona using nanoDSC

Although, nanoDSC is a technique commonly used for thermal studies of biomolecules (conformational transition of biological macromolecules)[154], biochemical reactions[155] or characterization of nanoparticles[156,157,158,159], only recently, nanoDSC has emerged as a standard technique for the characterization of the protein corona. It should be noted that this technique studies both hard PC and soft PC, due to the absence of previous washes during sample preparation to remove weakly bound proteins. In nanoDSC while heating or cooling a sample, thermal changes in the same sample are accompanied by an exchange of heat; hence the temperature of these transformations and heat flow can be determined.

During the incubation, some of the proteins in the media begin to form the protein corona. Consequently, after the protein corona formation, the amount of free proteins decreases. During adsorption on the nanoparticles, proteins may undergo structural rearrangements called “conformational changes”. The nature of a protein is different if the protein is part of the protein corona or if it is a free (unbound) protein. It is possible to differentiate the proteins’ stability according to the binding state of the protein. The major part of proteins that form protein corona are less stable than the free proteins (soft PC). It has been reported that the binding of proteins to planar surfaces often induces significant changes in secondary structure. Study of a variety of NP surfaces and proteins will allow the demonstration that the perturbation of protein structure appear. For

instance, serum albumin adsorbed on NPs surfaces shows a rapid conformation change at both secondary and tertiary structure levels[160].

More in detail, in the present work, the T_m of the protein corona was compared to the T_m of the albumin. This temperature (T_m) is known as transition midpoint and it is considered as the temperature at which 50% of the protein is in its native conformation, while the rest is denatured. The proteins denatured undergo the destruction of both the secondary and tertiary structures, only the primary structure (sequence of amino acids) remaining the same. Higher T_m values would be representative of more stable molecules[154,155].

Firstly, the HSA protein corona was formed in the MSN surface following the usual methodology (see materials and methods) but without the washes and centrifuges. After the necessary formation of PC, the cell of the nanoDSC was filled with this suspension. Three temperature cycles were performed, between 25 and 98 ºC (melting point of HSA depending on literature and conditions is between 59.7 and 79.5 ºC)[161]. During the first cycle the denaturation of the protein that form the protein corona occurred and therefore the melting point (T_m) can be calculated in this cycle. The second one was to cool down the cell. Finally, the third cycle, where all protein was denatured, was to obtain the baseline.

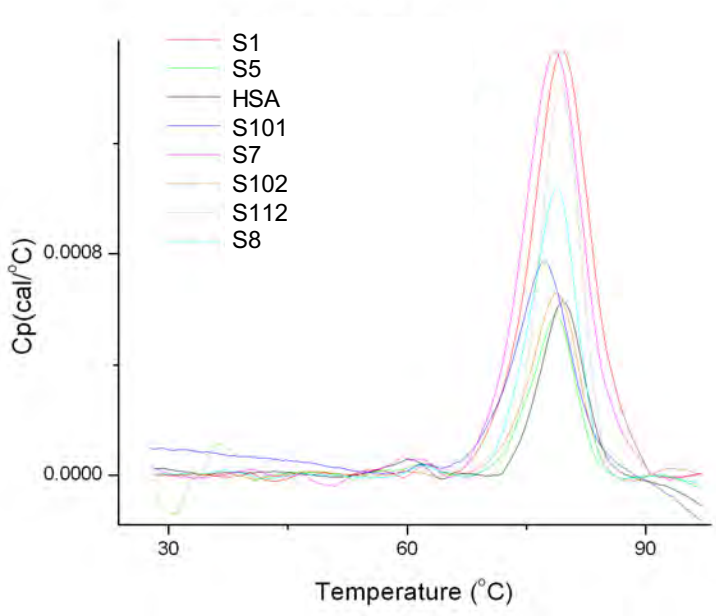

Figure 31: Thermograms of the different MSN incubated with HSA.

Figure 31 shows the peak displacement, corresponding to the change in T_m. That means that the nature of the protein corona formed was dependent on the characteristics of the nanoparticle. Due to, each MSN's SI have one thermodynamic profile.

The reproducibility of these experiments was demonstrated by running each sample twice. Figure 32 shows some of the repetitions of the thermograms (for samples S1, S5, S7 and S102).

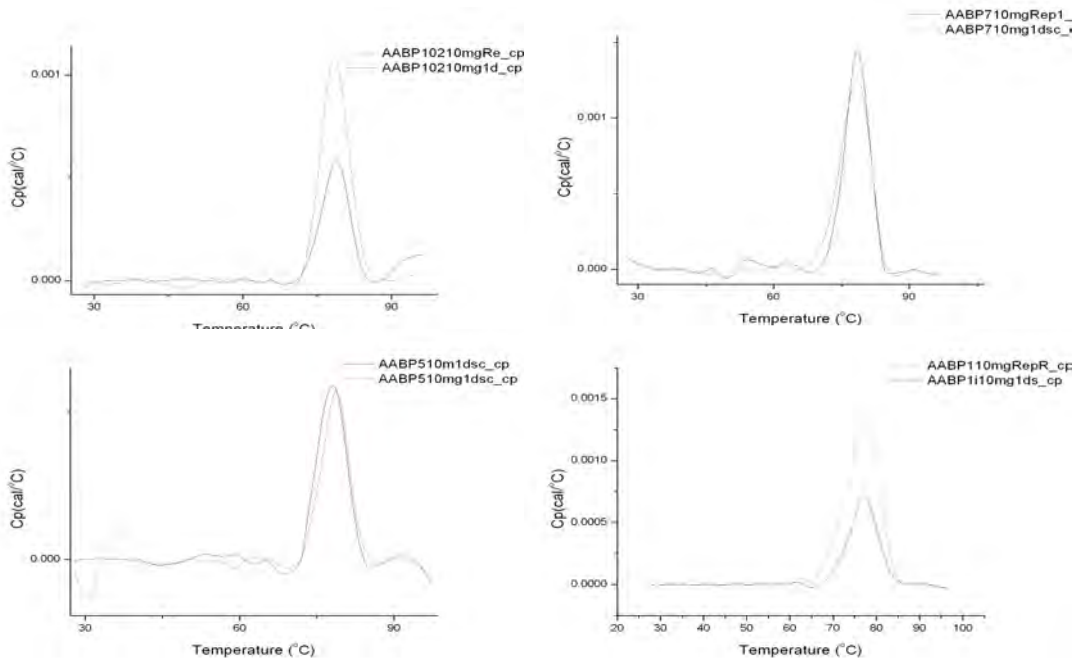

Figure 32: Example of reproducibility of the DSC results.

The DSC assay was also carried out with the PC formed with FBS (S1). The comparison was done with the same FBS batch, since the composition can change among different lots. There can be observed two major proteins. The first one was the albumin with a T_m of 79 ºC, which suffers the same effect as when incubating NPs with the albumin alone, and the second one was hemoglobin with a T_m of 59 ºC[162].

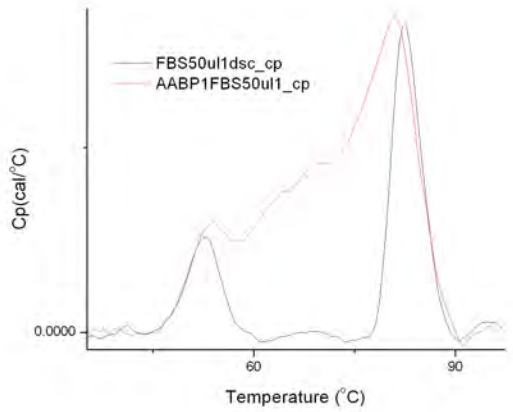

Figure 33: Thermogram obtained of the DSC with MSN incubated in FBS.

As stated previously, the goal of this work is the advantageous use of mesoporous silica nanoparticles as vehicles for drugs (inside their pores) and at the same time the employment of protein corona to protect these drugs from the outside (environment).

In order to be able to compare the behavior of the protein corona of the different mesoporous NPs, two blanks were made using silica nanoparticles without pores (S112) and gold nanoparticles (Au NP) (Figure 34). Comparing this NPs without pore in relation to MSNs, it can be isolated the specific impact of the pore property.

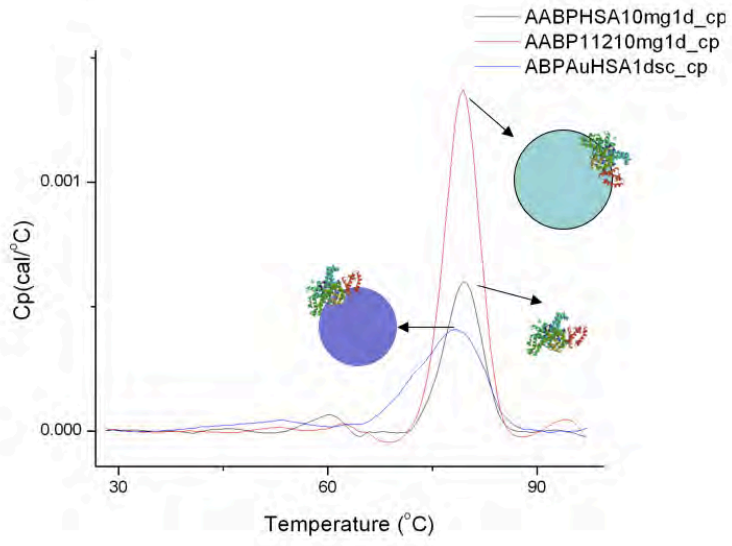

Figure 34: DSC thermograms of nanoparticles incubated with HSA without pore (Au NP and S112).

The thermogram of the NP without pores were dissimilar from each other, it will be shown later in this chapter an explanation of the behavior of the pore with regard to the PC.

3.3.3.1 Thermal study of the soft protein corona using ITC

A complementary technique for the characterization of the corona was used: The MicroITC. This technique provides thermodynamic information about the superficial interactions between MSN and HSA. A HSA solution was titrated into a nanoparticle solution in the sample cell at 37 ºC to simulate the physiological medium. This process allows the formation of both soft and hard PC. The difference in temperature of the sample cell was monitored. If the reaction is endothermic, heat needs to be provided to the sample cell and a positive signal is obtained. On the other hand, if the sample in the cell emits heat, a negative signal is obtained[163].

When analyzing the first step, the endothermic one, a positive value of heat during the formation of the complex indicates that this interaction (protein-NP) is an enthalpically unfavorable (entropically driven) process. This means that the reaction takes place spontaneously since the change in entropy is positive. In this process the disruption of the water bound to the NP surface was energy dependent.

$$\Delta G = \Delta H - T\Delta S$$

Equation 1: Third Law of Thermodynamics.

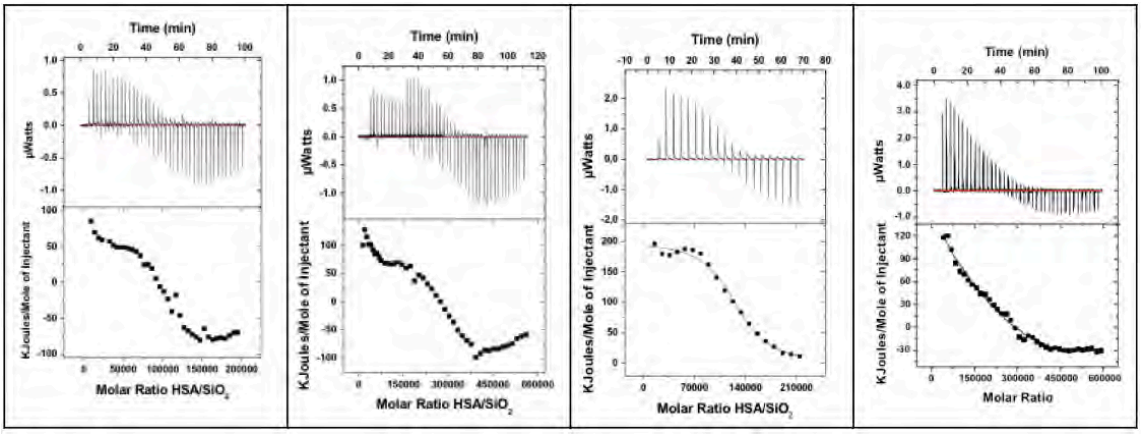

Figure 35: Thermograms of the ITC titrated with HSA.

3.3.4 Correlation between synthetic identity and biological identity

To study the relationship between synthetic identity and the biological identity, and to elucidate which property of the MSN is more important for the PC formation, the properties of the MSN and of the protein corona were correlated. Due to, this correlation the ideal application for the MSN-PC complex.

3.3.4.1 Correlation between protein corona and AR and pore size

Collectively from data, it can be concluded that the pore size and the aspect ratio excerpts a great influence on the formation of the protein corona. This effect can be explained depends on the aspect ratio but mostly the size pore. Some authors claim that the highly curved surfaces of NPs affect protein-protein interactions. Proteins adsorbed on highly curved NPs tend to undergo fewer changes in conformation than those adsorbed on less curved surfaces. In this work this concept was extrapolated and explained as the pore size effect. The orientation of the protein to form the PC was found to be exclusively dependent on the specific protein structure and the geometrical fitting for a specific surface. For that reason, the curvature, which is function of the aspect ratio, plays a crucial role, e.g. S101 with a rod-shape, AR of 1.940, even though it has a pore size of 34.9, the PC was a small. Even so, due to the HSA uses several helical sites from different domains to fit perfectly onto the MSN surface, the size pore is the most important factor. This fact can be observed because nanoparticles almost spherical have more differences in the PC by changing the pore size.

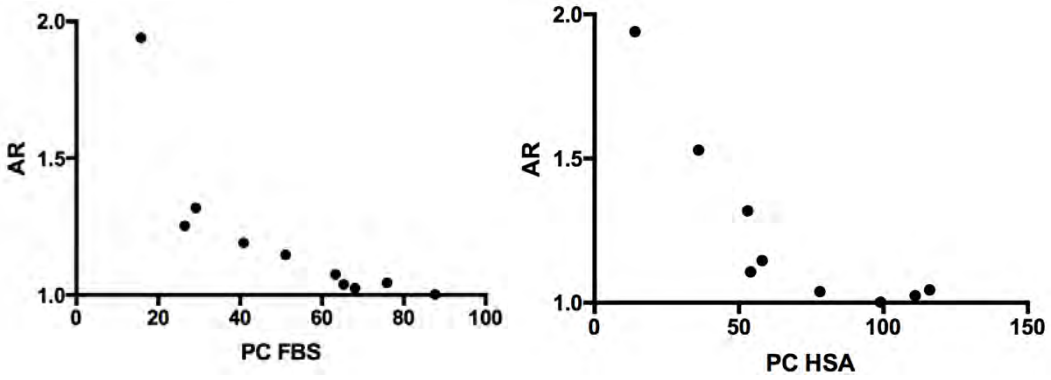

Figure 36: Relationship between AR and PC (FBS or HSA).

Even so, it can be observed the coexistent dependence on the amount of proteins that form the hard PC (BCA assay) besides the pore size. Due to, the primary bound monolayer of HSA, which are attached to the nanoparticle surface, uses several helical sites from different domains to fit perfectly onto the MSN surface[164].

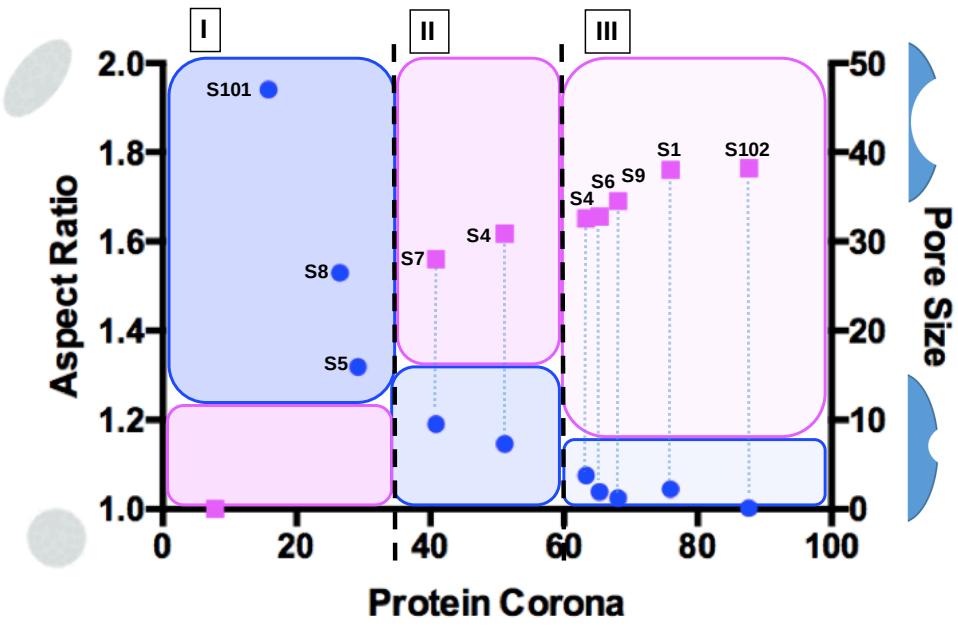

Figure 37: Relationship between pore size, PC and AR. The samples were grouped in three blocks (I, II, III) depending on their properties.

As depicted in Figure 37, samples can be grouped into three groups according to their pore size and AR. The group I was composed by nanoparticles with a defined rod-shape and thus an AR higher that 1.3; at the same time these nanoparticles had different pore size. This group of nanoparticles showed few proteins in the PC, and although the AR was different enough among them, there were not huge differences within their PC. MSNs arranged in group II have a shape close to the spherical and a pore size between 28 and 31 Å. In this group, the difference in the PC can be explained both because of the AR and the pore size. The last group was the one showing the greatest influence of pore size in PC. This III group clusters spherical nanoparticles with a pore size larger than 32.2 Å and an AR smaller than 1.07. The larger the pore size was, the higher increase in the PC was observed. The hard PC, formed by proteins strongly bound the nanoparticle surface, is directly affected by the surface properties, in this case by the pores. Therefore, it has been here demonstrated the huge influence of the pore size on the formation of the hard protein corona.

3.3.4.2 Correlation between pore size and nanoDSC and ITC

The conformation of the absorbed proteins is different from their original or native conformation[165]. Conformation of adsorbed proteins is more altered in the presence of charged or hydrophobic nanomaterials. The change in the conformation allows the correlation between the free proteins and the quantity of protein that forms the protein corona. From inspection of the thermograms, it is possible to obtain the melting

temperature (T_m) of each protein corona, which shows a linear correlation with its corresponding quantity of PC[166]. The higher is the quantity of protein forming the whole PC, both soft and hard PC, the more instable this protein is, so smaller becomes the T_m. This observation maybe due to the higher amount of protein is accumulated on the MSN's surface, the more density of charges and hydrophobicity turn out, so more protein with conformational changes are there.

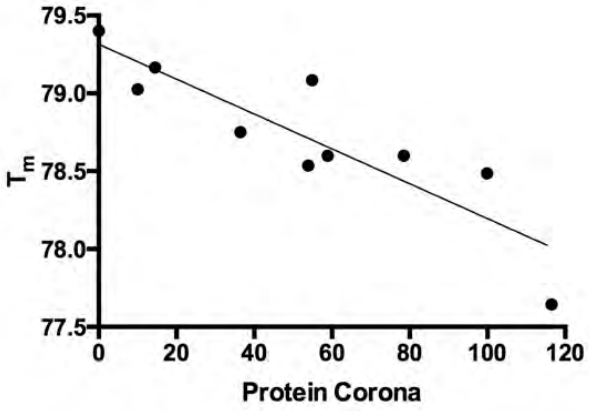

Figure 38: Linear relationship between T_m and PC

On the other hand, it can be observed in the DSC thermogram a widening of the base of the peak (Figure 31). This fact can be explained because of the presence of two types of layers that form the protein corona, the hard and the soft PC, widely described in 3.3.1 section. Plotting the temperature at which proteins start to denaturize together with the temperature at which the last native protein co-exists with denatured proteins compared to the protein corona provides a graphic which evidences two different behaviors of the proteins[167].

We hypothesize that the first peak is due to the external proteins, which are more exposed to the medium and the disruption of their native form result in less stable proteins, the so-called soft protein corona. The second peak is hypothesized to correspond to the fact that, as time goes by, proteins begin to fit in the pores. This allows the formation of a highly stable protein corona composed of the proteins internalized in the pores, known as the hard protein corona. Thus, a high temperature by reason of the denaturing of these proteins is observed in the plot. The effect of the two factors can be understood as the presence of two peaks[164,168,169]. In the other one which the picks appear at a higher temperature was because the presence of the pores. The pore allows the stabilization of the protein because of its packaging within it. This can be represented as a deconvolution of the peak of the DSC as a representation of the influence of the two

effects, surface and pores, understanding as the soft and hard PC (Figure 41). The percentage of proteins that form the pore's layer or surface's layer will determine the final T_m.

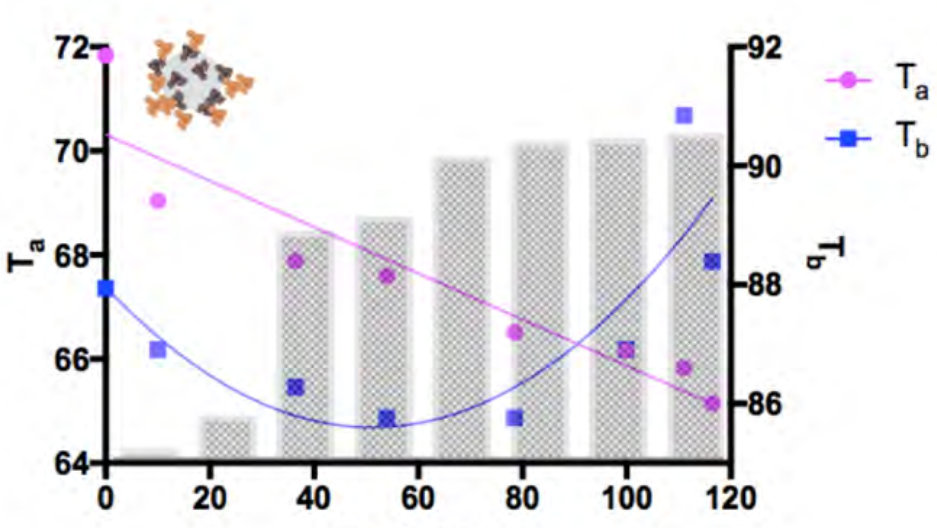

Figure 39: Relationship between Ta, Tb and PC.

Analyzing the ITC's thermograms, we hypothesize that the increase in entropy of the system, the first step, was due to the release of a highly ordered solvent molecules (water) from the interface to the medium could compensate the unfavorable enthalpy contribution. The second step displays exothermic peaks. It is reported in the literature that the curvature of nanoparticle affects the exothermic peak. In this case, the exothermic peaks vary with the pore size[170,171]. The higher the pore size was, the bigger was the exothermic peak. The nanoparticle which have a pore big enough to fit and stabilize the protein play a more important role in the formation and the structure of the protein corona[172,146]. The sample of the compact nanoparticle, without pore, confirms the above mentioned behavior since there was only the surface effect. Complementary to the DSC data, the endothermic peaks correspond to the first PC formation, the soft PC; on the other hand, the exothermic peaks, which were pore depending, are representative of the hard PC.

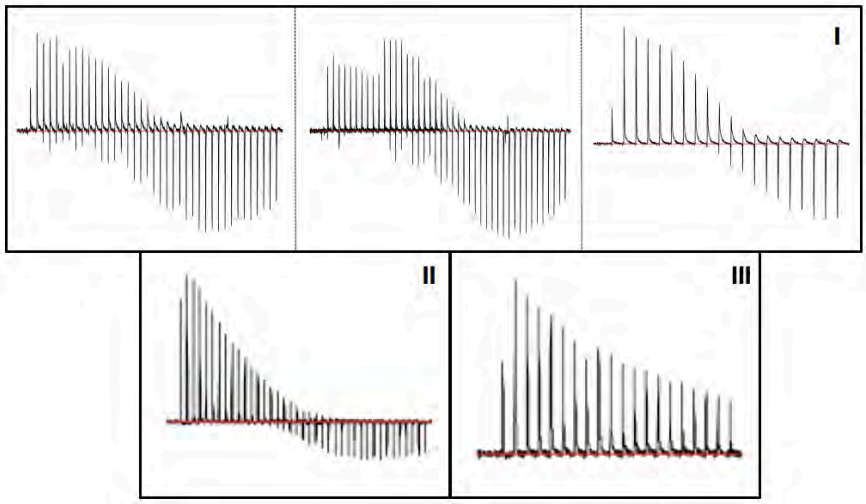

Figure 40: Thermograms of MSN from different blocks (I, II, III).

According to the behavior depending on the pore size, human serum albumin was titrated over different samples: four different nanoparticles with pore sizes, three of which form part of the first group of pore size (38.8, 38.4, 36) and other one of the second group (30.9 Å) and nanoparticles without pore. The thermograms shown in Figure 40, and demonstrate that the adsorption of the protein has two step process. In the first one, the protein approaches to the surface and binds loosely in its native state at random positions on the surface of the nanoparticle. In the second one, the protein can undertake conformational changes and form non-covalent protein-nanoparticle bounds that help to stabilize the protein into the pore and, therefore, leading to a stronger adsorption[173].

The comparison between the two techniques allows the understanding of the composition of the PC, the formation (ITC) and the stability and denaturalization (DSC). In the ITC the rate of the exothermic part, which correspond to the effect of the pores, respect the whole heat change (exothermic and endothermic) was from top to bottom and from left to right, following a descending order in the pore size 48.4% 40% 29%. The last one was the nanoparticle which do not have pore. This can be compared with the deconvolution of the peak of the DSC as a representation of the influence of the two effects, surface and pores, where the surface effects would be represented by the peak displaced to the left and the pore effects to the right. The same influence would be with comparable values, 47.4 % 40.7% 33.2% (15.2%). Through these two techniques it can be understood at the same time both the behavior of the PC and the discrimination of the soft corona in the surface and the hard corona stabilized in the pores.

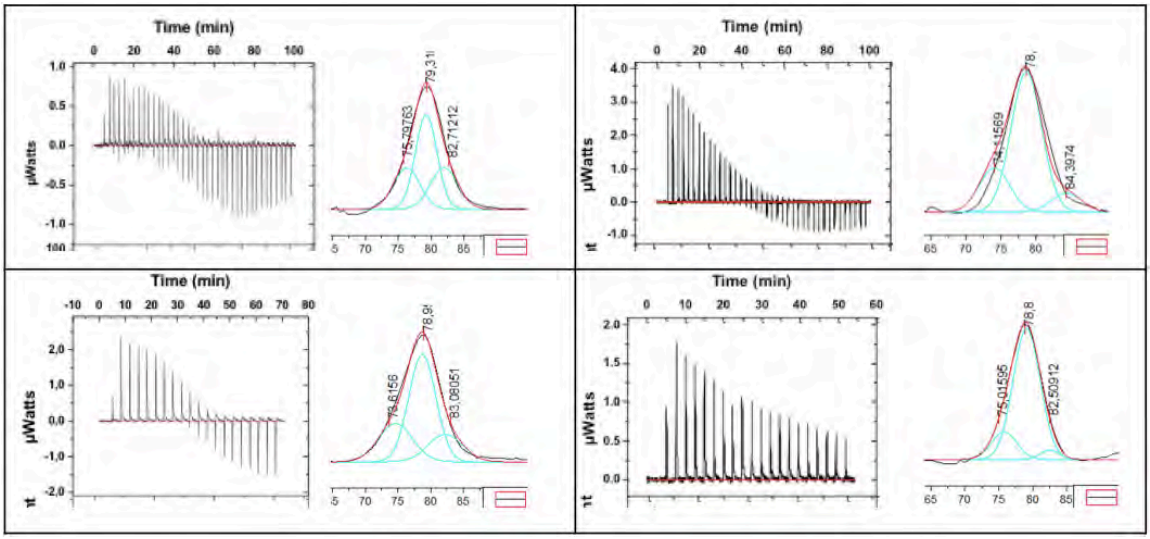

Figure 41: Relationship between ITC thermograms and deconvoluted DSC thermograms.

To sum up, the utilization of nanoDSC and MicroITC allows the understanding of the mechanism through which the protein corona was formed, to achieve the optimal application, as a targeting, gatekeeper or protein release, in function of the ratio pore-protein size.

3.3.5 Study of the behaviour of a small protein versus different MSN pore sizes

Interestingly, when a small protein was chosen the relationship between this small protein and the pore size would be different. Lysozyme (Lys) was used as a model protein, whose dimension is comparable in size to 34 Å, and 14.3 kDa. In Figure 42 four DSC thermograms are shown, two of them of HSA, and the others two of Lys. Regarding the HSA, it was previously discussed the effect of the pore and the relationship between the pore and the albumin size. This relationship makes that, even though T_m was smaller than that of the free albumin, the base of the peak widens practically equidistance from the center, due to the equal participation of the pore and the surface in the formation of the PC. On the other hand, in the case of the lysozyme, the pore was much bigger than the protein. This makes that the presence of the pore has a greater effect on the formation of the PC. For that reason, the peak shifts to the right, making the protein more stable.

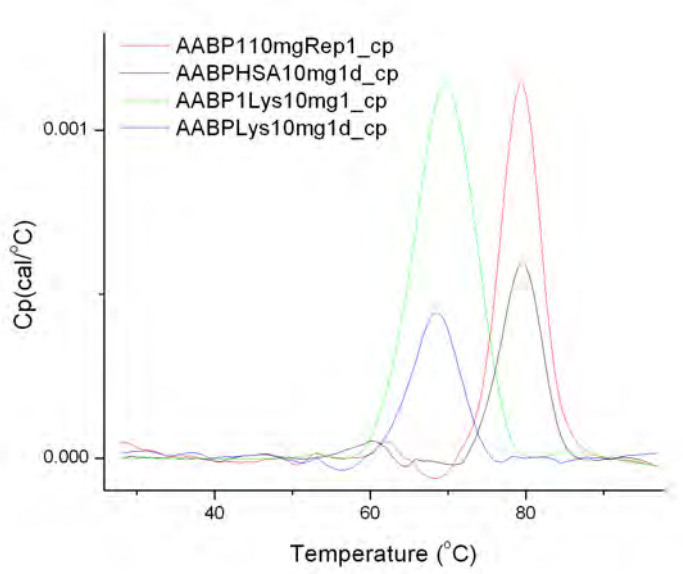

Figure 42: Comparison of the behavior of lysozyme and albumin regarding S1.

Focusing solely on the lysozyme regarding different pore sizes, the interaction between lysozyme with S1 with a pore size of 38.8 Å, S4 of 34.2 Å and S5 of 28.8 Å was studied. The result is shown in, Figure 43, where it can be seen how in S5 NPs the lysozyme was not allowed to enter inside the pore, and practically only the surface had effect in the PC formation (the peak shifts to the left). In this case NPs can be used for target some organ. S4 NPs have a pore size where the lysozyme fits widely, so this fitting confers stability to the protein (the peak shifts to the right). S4 can be used for block the pore, and avoid a pre-release not desirable. Lastly, in S1 NPs the pore is too big and the protein can enter completely inside the pore, so the PC formation is influenced by the surface and the pore at the same time (the base of the peak widens). In this case, as the protein can enter entirely inside the pore it can used for release it.

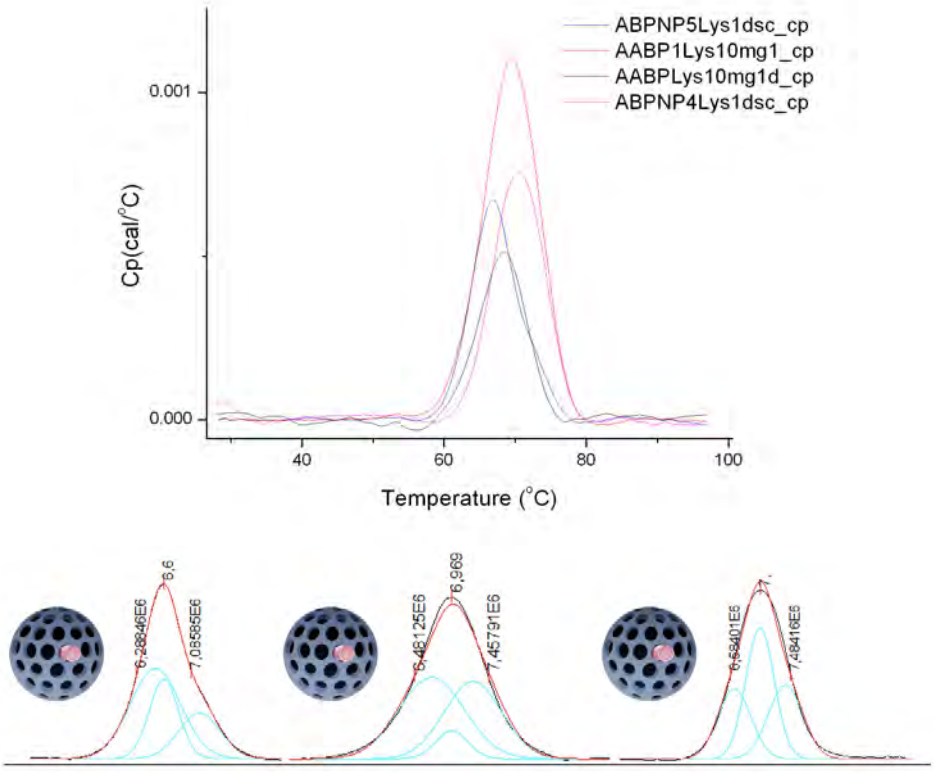

Figure 43: Lys DSC thermograms depending on the pore size and their deconvolution.

It should be noticed that, by expanding the upper limit of the pore size, it can be observed that once the pore size was considerably greater than that of the proteins, the T_m becomes greater than that of the free protein. This implies that when proteins enter completely within the pore (for being released from the nanoparticle), the protein stability increases as does the percentage of proteins that fit inside the pore, i.e. the hard PC is greater than soft. In the case of S1 nanoparticles with HSA, only the first layer of hard protein corona enters the pore. Thus, the percentage of proteins with respect to the global PC was smaller as compared to the case of lysozyme. On the other hand, looking at the deconvolution of the DSC peaks, where it can be seen these peak displacements, in S5 (small pore) the deconvolution shows a clear shift to the left; S1 shows two big peaks in the left and in the right (corresponding to surface and pore, respectively); and S4 shows also two peaks but smaller than those from S1 (their pore is not as big as S1).

3.3.6 Study of the behaviour of a big protein versus different MSN pore sizes

The study of different proteins, albumin and lysozyme, with different protein-pore size relationships has been performed, evidencing the importance of this relationship. In the experiments carried out, the protein could have several behaviors, ranging from

fitting into the pore until entire penetration to settled on the surface of the MSN. Here, the aim was to check the behavior of a protein far larger than the pores of the nanoparticles. According to the aforementioned hypothesis, it was expected that the proteins that form the PC will be destabilized due to the "only" interaction with the surface. This interrelation yields a complex could be used to target.

For this experiment, glucose oxidase (GO) was employed as it can be considered a big protein if compared to the pore size. GO is 40-50 x 120-140 x 80-90 Å, whereas the pore size of S1 is 38.8 Å (Figure 44).

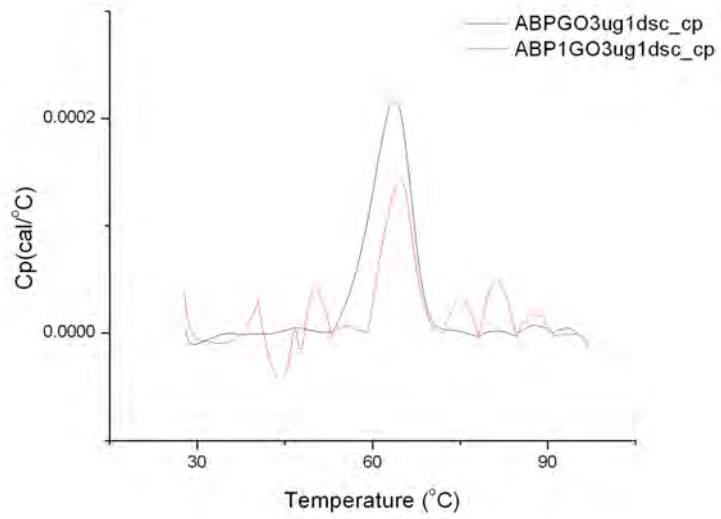

Figure 44: DSC thermogram of the GO.

As predicted, the peak of the GO was shifted to the left, being the T_m smaller than for the free GO, due to the participation of the surface in the PC destabilization. The GO was not allowed to fit into the pore because of its size. The thermogram was similar to the one in Figure 34 (nanoparticles without pores), since for GO the pore of S1 was as small as if it did not even exist.

The difference between the protein corona that is formed using only surface or using both surface and pore factors has also an influence on the quantity of proteins that form these PCs. The smaller the protein is, the more amount of it can fit in the pore, so higher quantity of protein will compose the protein corona.

Table 6: Protein corona of different proteins

	Lys	*HSA*	*GO*
PC	209	116	0,64

3.3.7 Study of the evolution of the protein corona formation over time

In order to corroborate this hypothesis, the denaturation of PC formed at different time points was studied using the nanoDSC. MSN were incubated with HSA at 5 minutes, 30 minutes, 2 hours, 10 hours and 24 hours. In Figure 45 is observed that, as time goes by, the T_m shows a shift of the peak to the right and it becomes higher, thus corroborating the protein fitting inside the NP pore. This observed change related to the protein fitting inside the pore can be explained through the different conformations that HSA acquires over time. It has been corroborated that in a first stage the protein forms a layer with a random conformation on the surface of the nanoparticle and in a second stage it acquires different conformations that allow its entrance to the pore.

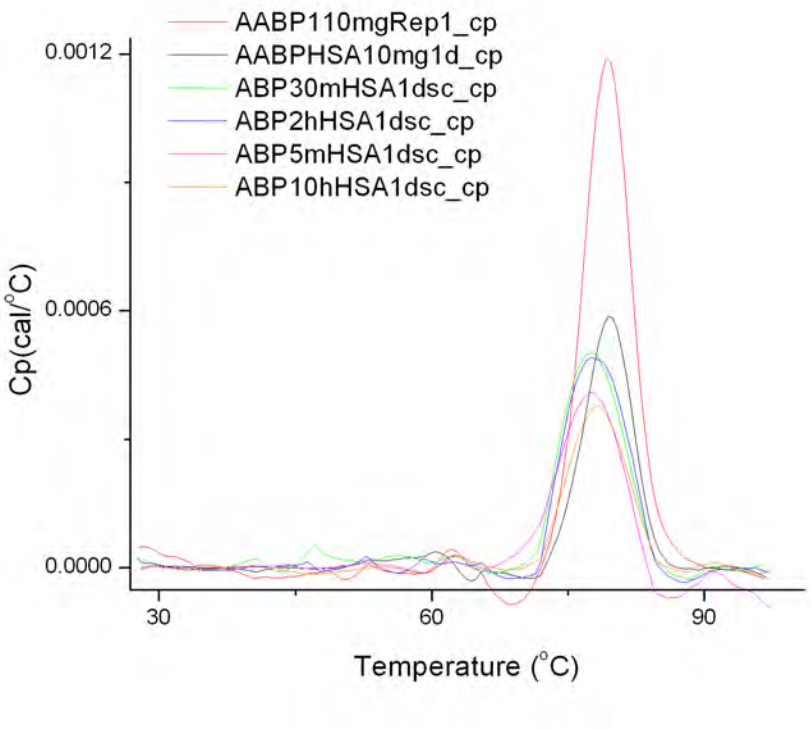

Figure 45: DSC thermograms of S1 and the evolution of the PC over time.

Regarding the height of the peak, the amount of proteins is directly related to the height of the peak. Thus, the higher peaks correspond to higher amounts of proteins inside the nanoparticle pores (hard PC) (Figure 46).

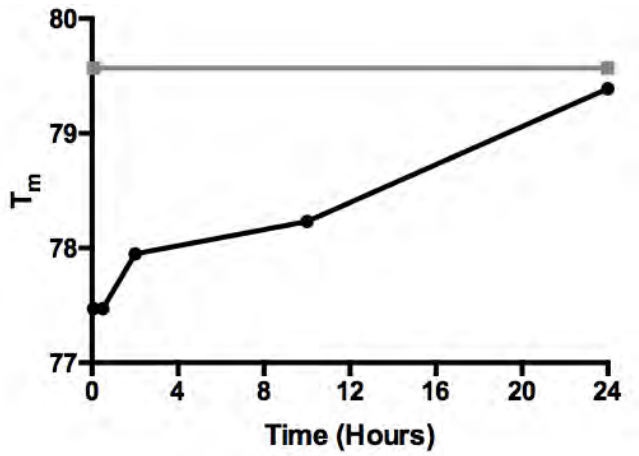

Figure 46: Evolution of the PC over time

3.3.7.1 Influencing of the pore size in the PC's formation regarding the protein size

In order to know the stability of this protein-pore binding, the nanoparticles were first incubated 24 h in HSA and then 5 minutes, 10 hours or 24 h in FBS, during which time protein competition will occur, having corroborated the differences between the first stage (random conformation on the surface) and the second stage (acquires different conformations).

In Figure 47 the first lane in each gel corresponds to the protein corona formed only with an incubation of HSA during 24h and the last one to the PC incubating with only FBS also during 24h. The three lanes in the middle are the different PC formed when incubating first 24h in HSA and then 5', 10h and 24h in FBS, respectively.

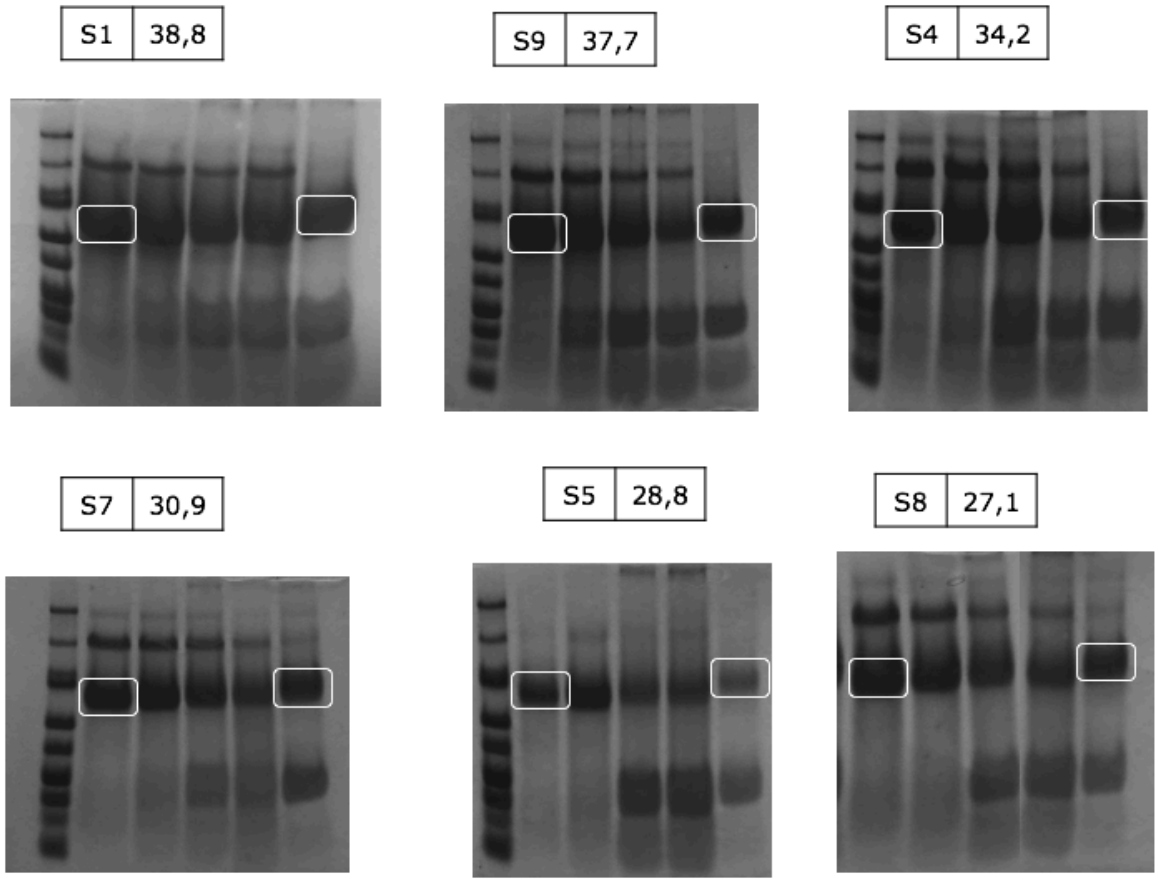

Figure 47: Protein exchange study. SDS-Page of the MSN with different pore sizes incubated with HSA 24h (left lane) and then re-incubated at different times (5', 10h and 24h, lanes 2 to 4) with FBS. The last lane corresponds to MSN only incubated 24h with FBS.

The difference between albumin from FBS and from HSA is that bovine is 1 kDa larger than human, so it remains more retained and it is possible to see which albumin of the HSA-PC is replaced by the bovine. Figure 47 shows that the smaller is the pore, the shorter time it is needed to replace the albumin. That means that when the pore is big enough to fit the protein, this protein will remain more easily in this bound state than the protein that is bound on the surface.

Here it can be observed how the nanoparticles with a pore size in which the protein can fitted remain more time forming part of the PC. This was suitable for act as a gatekeeper and for avoid the undesirable pre-release.

On the other hand, nanoparticles with different pore size were incubated in HSA with FITC conjugated. After the respective washes, MSNs with the fluorescent corona were incubated in HSA and the HSA-FITC that remained as PC was quantified in order to prove the stability of the protein corona as function of the pore size.

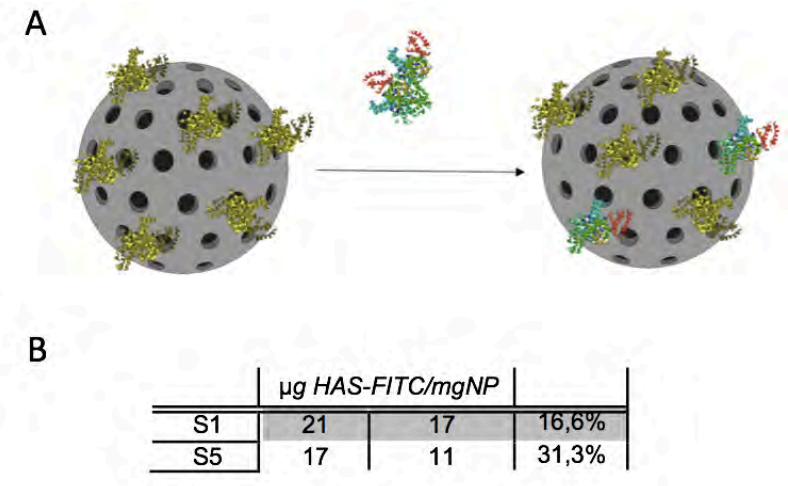

Figure 48: Replacement of the HSA that forms the PC using FTIC-HSA.

It was observed that the protein fitted in the pore (S1) suffers a replacement of 16.6% of its proteins, while the MSN with pore not big enough to accommodate the proteins (S5) suffers a replacement of 31.3%, almost twice. Thus, it demonstrated that the fit proteins were more stable to the replacement than the proteins in the surface.

3.3.8 Composition determination of the PC using proteomics

Following the previous results in which was observed that depending on the time the proteins that forms the protein corona can be replaced for other proteins of the new media regarding the pore size of the MSN. In order to study which protein were replaced, a proteomic assay was made with S1 and S5, pore size of 38.8 Å and 28.8 Å respectively, incubated 24 h in HSA and subsequently 24h in FBS, and only 24h in FBS. The results are expressed in percentage of the score of each protein with respect to the score of the most abundant ones. The following table shows these results:

Table 7: The three most abundant proteins in the PC through proteomic assay.

S1				S5			
FBS		**HSA + FBS**		**FBS**		**HSA + FBS**	
BSA	31.4	HSA	32.2	ApoAI	34	ApoAI	23.9
TRFE_B	24.5	BSA	13.6	BSA	14.5	HSA	18.7
TRFE_B2	23.8	ApoAI	12.2	Glyco_B	10.9	BSA	13.9

The percentages of abundance of the three most abundant proteins in each PC were compared among samples. The molecular weight of these proteins in kDa were: BSA 69.2, TRFE 77.6, TRFE2 77.7, HSA 69.3, ApoAI 30.3 and Glyco_B 38.4.

The results showed that the in PC formed on S1 incubating with FBS the most abundant protein was albumin, while in the case of S5 was ApoA1. The naturally-occurring formation of a PC when incubating NPs in FBS renders a PC composed of proteins which can be fitted in the pore. The proteins that form the PC in S1 nanoparticles had a MW of 69.2, 77.6 and 77.7 kDa, while in S5 were 30.3, 69.2 and 38.4 kDa in MW.

On the other hand, nanoparticles pre-incubated 24h in HSA were allowed to form an unnatural PC composed only of HSA. During the following 24h in FBS, the PC suffers a replacement of the HSA by proteins that are present in the FBS. When this happens, S1 shows a 32.2% of HSA, remaining as the most abundant protein in the PC, while in S5 it shows a 18.7%, not being the most abundant one. In the case of S5 the most represented protein is the ApoI, coming from the incubation in FBS.

3.3.9 Microscopy of the PC: CryoTEM

DSC thermograms show the range of temperature at which the proteins from the PC were denatured. Using that, it is possible to heat nanoparticles with a PC formed until a temperature at which the surface proteins are denatured but the proteins inside the pore remain folded, and it can be observed using a negative staining microscopy. In this case, nanoparticles were heated to 77 ºC. A quantification through BCA assay shows that the initial nanoparticles had 97.9 µg/mg NP of PC and the nanoparticles once heated at 77 °C, had 46.4 µg/mg NP. It can be observed in Figure 49 and Figure 50 that the behavior was different in each case.

In Figure 49 it can be observed the MSN with the entire PC formed. The surface seems grainy due to the presence of the PC in the surface, the complex matrix of the PC made that the absorption of the electrons along the samples was different. On the other hand, in Figure 50 the sample was homogeneous because of the fact that the surface was only composed of the material of the nanoparticle. In this case the protein was located inside the pore.

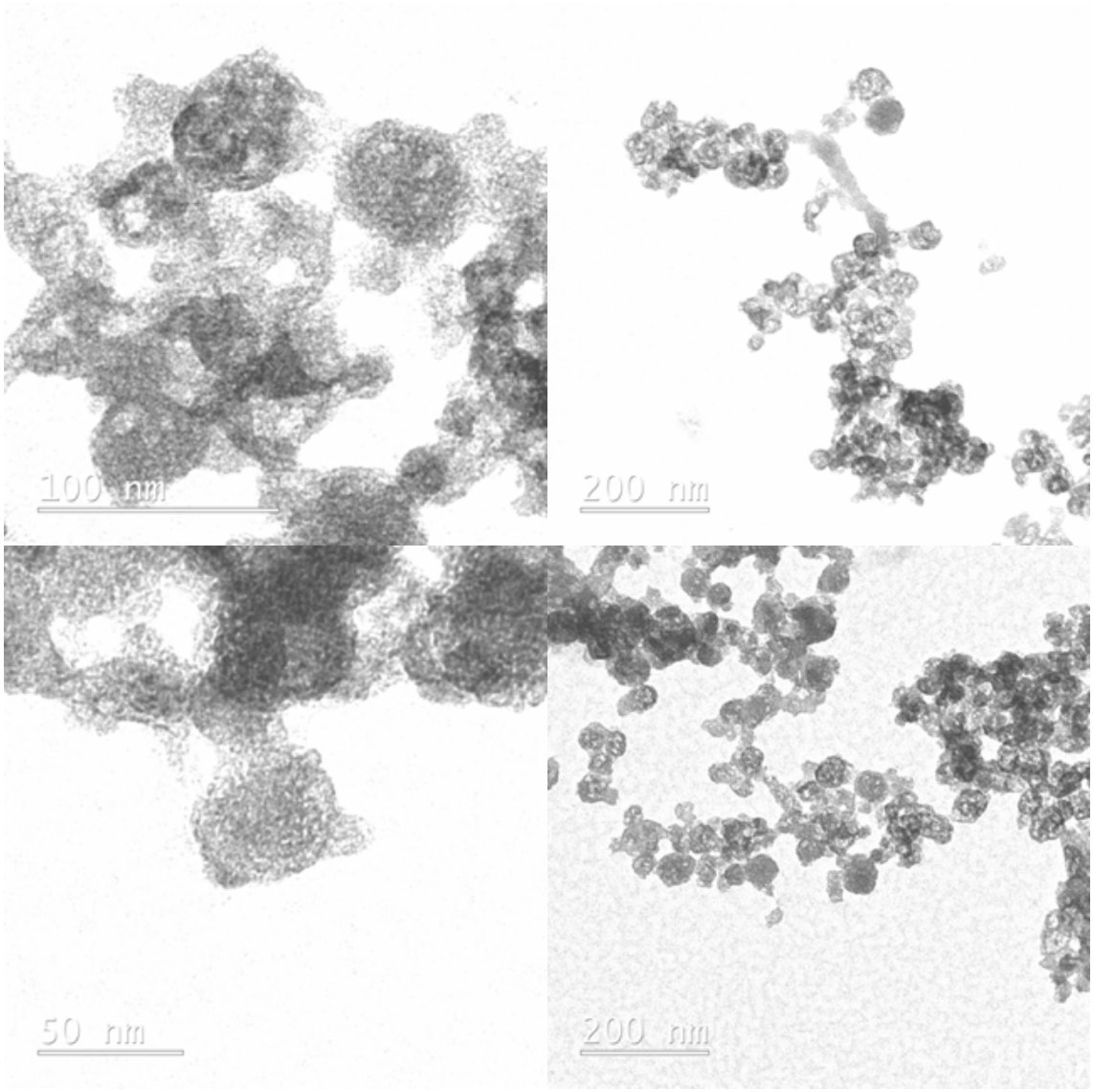

Figure 49: Images obtained from the TEM of the nanoparticles with protein corona.

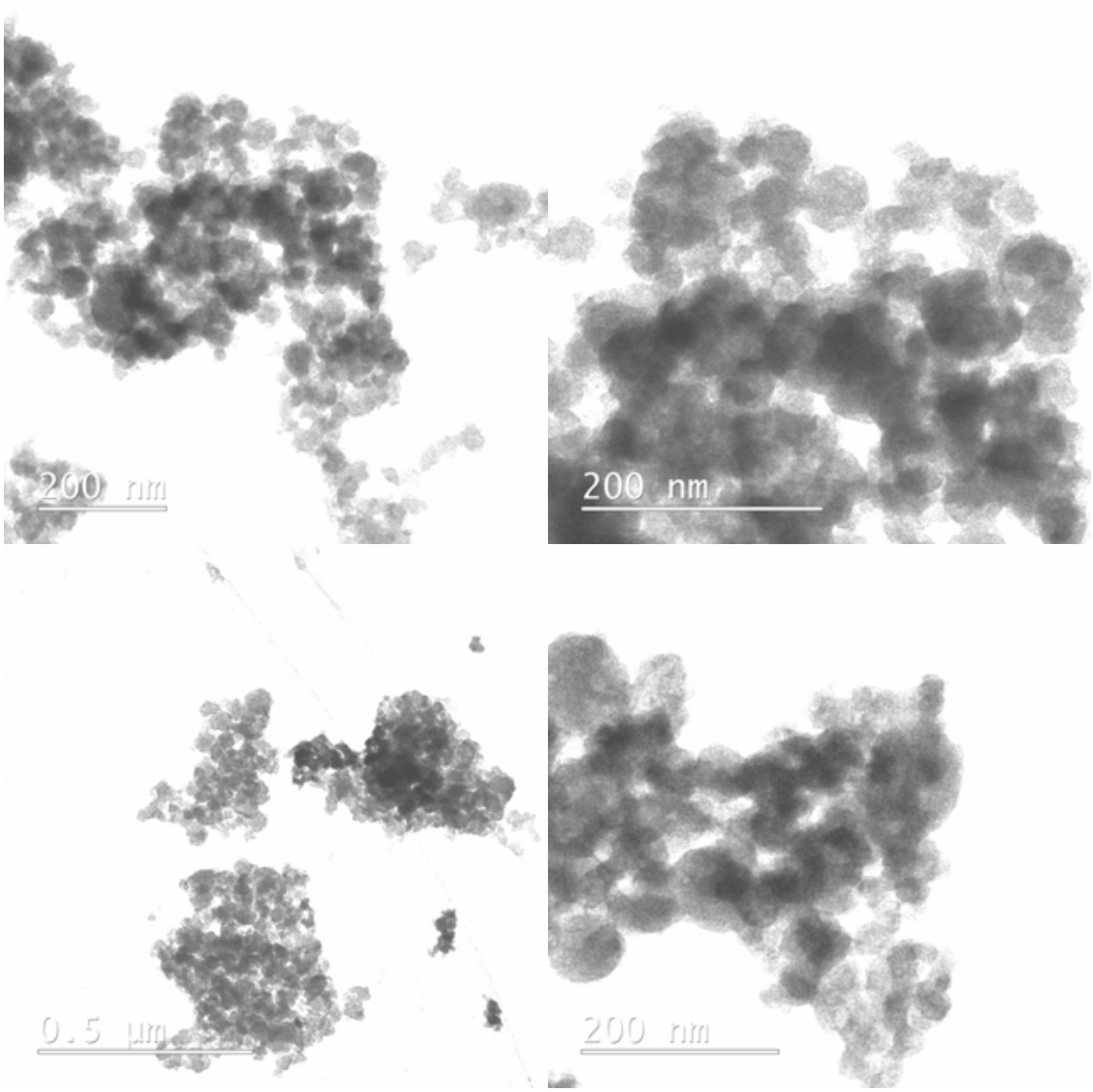

Figure 50: Images obtained from the TEM of the nanoparticles with protein corona and heated at 77 ºC

3.4 Concluding remarks

The results of this chapter prove that different mesoporous silica nanoparticles can render different types of protein coronas due to their different physiochemical properties. The differences in the synthetic identities characterized in chapter II allows the formation of a variety of biological identities.

The utilization of these techniques in a new way allows the intelligent design of MSN regarding the protein that is wanted to use in order to plug the pore for its utilization as a drug delivery system. If the protein is inside the pore it will be more stable and so it will have a controlled release until reaching the therapeutic target.

It could be concluded that proteins that have a size capable of entering in the pore will be stabilized. If the protein has a size which can just fit inside the pore, the layer that forms the stabilized proteins will be small (the case of HSA with S1). This can be seen using the ITC where it is appreciated that less than 50% represents the protein inside the pore (exothermic part). On the other hand, it has been seen that the T_m of samples in which albumin was forming PC was lower than the T_m of free albumin. This is due to the fact that more than 50% of the whole PC is on the MSN surface, which has been proved to be more destabilized than the free HSA (Figure 51). The cases of MSN with a small pore size show that it has less portion within the pore (ITC), although the T_m was closer to the T_m of free albumin since it also forms less protein corona.

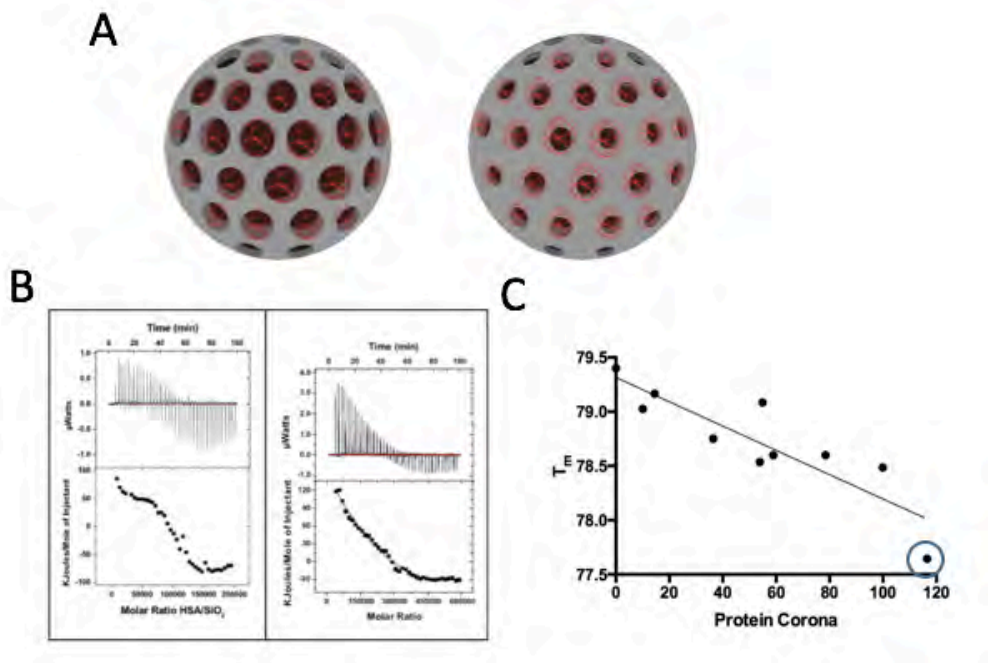

Figure 51: Concluding remarks of the chapter III. A) Schematic representation of the gatekeeper B) ITC thermograms C) Linear relationship between T_m and PC.

The utilization of the lysozyme allows increase the pore-protein ratio window. In which it was observed as if the pore size was much greater than that of the protein, the pore factor was higher, with which the amount of proteins that form the PC increases, and the stabilization was observed with the large displacement of the peak of the DSC to the right, even increasing the T_m with respect to the free one.

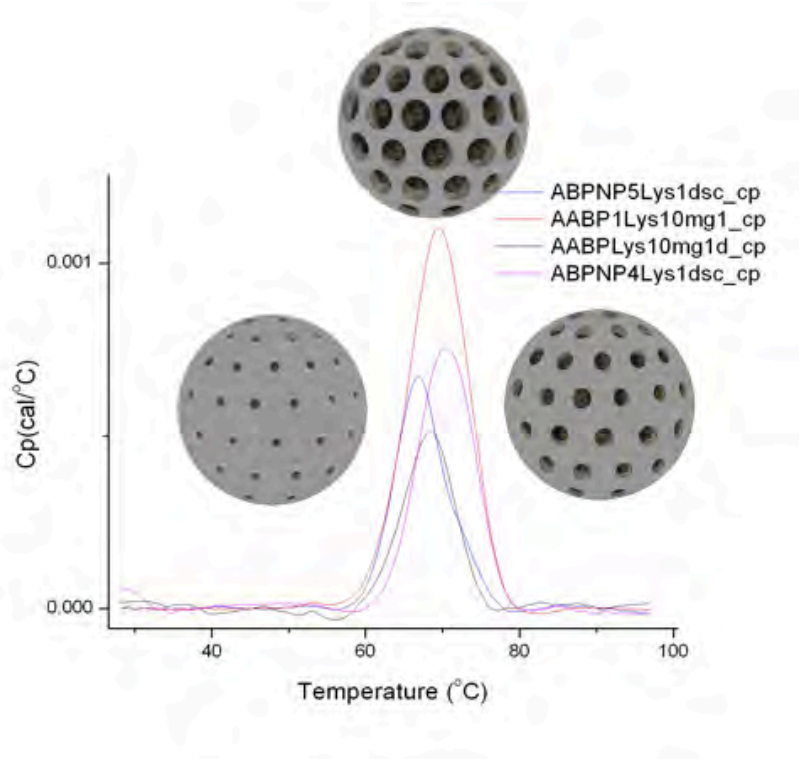

Figure 52: Concluding remarks of the chapter III. DSC thermograms of the lysozyme.

In short, with the range of synthetic identities characterized in the previous chapter, in this one, it is hypothesized the behaviour of the proteins that forms PC regarding the pore size. Also, here it determines the application of the MSN-PC complex in correlation to the relationship between pore and protein size. Proteins in these systems can be used for targeting, for blocking the pores and avoid de pre-release or for being released from the nanoparticle. Consequently, in the next chapter studied drugs will be loaded and released of MSN in order to known the release profile according to the formed PC, as well as it should be studied the physiological response in front of cells lines, as the bioavailability and the cytotoxicity.

3.5 References

(2) Ferrari, M. Nanovector Therapeutics. *Curr. Opin. Chem. Biol.* **2005**, *9* (4), 343–346.

(4) Albanese, A.; Walkey, C. D.; Olsen, J. B.; Guo, H.; Emili, A.; Chan, W. C. W. Secreted Biomolecules Alter the Biological Identity and Cellular Interactions of Nanoparticles. *ACS Nano* **2014**, *8* (6), 5515–5526.

(29) Lazarovits, J.; Chen, Y.; Sykes, A.; Chan, W. C. W. Nanoparticle – Blood Interactions : The Implications on Solid Tumour Targeting. *Chem. Commun.* **2015**, *51*, 2756–2767.

(32) Mahmoudi, M.; Lohse, S. E.; Murphy, C. J.; Fathizadeh, A.; Montazeri, A.; Suslick, K. S. Variation of Protein Corona Composition of Gold Nanoparticles Following Plasmonic Heating. *Nano Lett.* **2013**, *14* (1), 6–12.

(34) Flanagan, M. B.; Lundqvist, M.; Stigler, J.; Cedervall, T.; Bergga, T. The Evolution of the Protein Corona around Nanoparticles : A Test Study. *ACS Appl. Nano Mater.* **2011**, *5* (9), 7503–7509.

(35) Vilanova, O.; Mittag, J. J.; Kelly, P. M.; Milani, S.; Dawson, K. A.; Ra, J. O. Understanding the Kinetics of Protein − Nanoparticle Corona Formation. *ACS Appl. Nano Mater.* **2016**, *10*, 10842–10850.

(36) Lee, B. Protein Corona : A New Approach for Nanomedicine Design. *Int. J. Nanomedicine* **2017**, *12*, 3137–3151.

(37) Ritz, S.; Schöttler, S.; Kotman, N.; Baier, G.; Musyanovych, A.; Kuharev, J.; Landfester, K.; Schild, H.; Jahn, O.; Tenzer, S.; et al. Protein Corona of Nanoparticles: Distinct Proteins Regulate the Cellular Uptake. *Biomacromolecules* **2015**, *16* (4), 1311–1321.

(49) Wang, H.; Thorling, C. A.; Liang, X.; Bridle, K. R.; Grice, J. E.; Zhu, Y.; Crawford, D. H. G.; Xu, Z. P.; Liu, X.; Roberts, M. S. Diagnostic Imaging and Therapeutic Application of Nanoparticles Targeting the Liver. *J. Mater. Chem. B* **2015**, *3* (6), 939–958.

(50) Surendran, S. P.; Thomas, R. G.; Moon, M. J.; Jeong, Y. Y. Nanoparticles for the Treatment of Liver Fibrosis. *Int. J. Nanomedicine* **2017**, *12*, 6997–7006.

(63) Yu, M. K.; Park, J.; Jon, S. Targeting Strategies for Multifunctional Nanoparticles in Cancer Imaging and Therapy. *Theranostics* **2012**, *2* (1), 3–44.

(78) Tu, J.; Boyle, A. L.; Friedrich, H.; Bomans, P. H. H.; Bussmann, J.; Sommerdijk, N. A. J. M.; Jiskoot, W.; Kros, A. Mesoporous Silica Nanoparticles with Large Pores for the Encapsulation and Release of Proteins. *ACS Appl. Mater. Interfaces* **2016**, *8*, 32211–32219.

(85) Balcells, L.; Fornaguera, C.; Brugada-Vilà, P.; Guerra-Rebollo, M.; Meca-Cortés, Ó.; Martínez, G.; Rubio, N.; Blanco, J.; Santamaría, J.; Cascante, A.; et al. SPIONs ' Enhancer Effect on Cell Transfection: An Unexpected Advantage for an Improved Gene Delivery System. *ACS Omega* **2019**, *4*, 2728–2740.

(119) Mudshinge, S. R.; Deore, A. B.; Patil, S.; Bhalgat, C. M. Nanoparticles : Emerging Carriers for Drug Delivery. *Saudi Pharm. J.* **2011**, *19* (3), 129–141.

(123) Hamidi, M.; Azadi, A.; Ra, P. Hydrogel Nanoparticles in Drug Delivery. *Adv. Drug Deliv. Rev.* **2008**, *60*, 1638–1649.

(133) Singh, R.; W. Llillard Jr, J. Nanoparticle.Based Targeted Drug Delivery. *Exp Mol Pathol* **2012**, *86* (3), 215–223.

(134) Hadjidemetriou, M.; Al-Ahmady, Z.; Mazza, M.; Collins, R. F.; Dawson, K.; Kostarelos, K. In Vivo Biomolecule Corona around Blood-Circulating, Clinically Used and Antibody-Targeted Lipid Bilayer Nanoscale Vesicles. *ACS Nano* **2015**, *9* (8), 8142–8156.

(135) An, F. F.; Zhang, X. H. Strategies for Preparing Albumin-Based Nanoparticles for Multifunctional Bioimaging and Drug Delivery. *Theranostics* **2017**, *7* (15), 3667–3689.

(136) Slack, S. M.; Horbett, T. A. The Vroman Effect. *ACS Symp. Ser.* **1995**, No. 5, 112–128.

(137) Bartczak, D.; Vincent, P.; Goenaga-Infante, H. Determination of Size- and Numer-Based Concentration of Silica Nanoparticles in a Complex Biological Matrix by on-Line Techniques. 2–6.

(138) Rosenholm, J. M.; Sahlgren, C.; Lindén, M. Towards Multifunctional, Targeted Drug Delivery Systems Using Mesoporous Silica Nanoparticles - Opportunities & Challenges. *Nanoscale* **2010**, *2* (10), 1870–1883.

(139) Gao, Y.; Che, X.; Zheng, C.; Hou, K.; Qu, X.; Liu, Y.; Zhu, Z. Effect of an Albumin-Coated Mesoporous Silicon Nanoparticle Platform for Paclitaxel Delivery in Human Lung Cancer Cell Line A549. *J. Nanomater.* **2016**.

(140) Ma, Z.; Bai, J.; Wang, Y.; Jiang, X. Impact of Shape and Pore Size of Mesoporous Silica Nanoparticles on Serum Protein Adsorption and RBCs Hemolysis. *ACS Appl. Mater. Interfaces* **2014**, *6*, 2431–2438.

(141) Sarparanta, M.; Bimbo, L. M.; Rytkoänen, J.; Mäkilä, E.; Laaksonen, T. J.; Laaksonen, P.; Nyman, M.; Salonen, J.; Linder, M. B.; Hirvonen, J.; et al. Intravenous Delivery of Hydrophobin-Functionalized Porous Silicon Nanoparticles: Stability, Plasma Protein Adsorption and Biodistribution. *Mol. Pharm.* **2012**, *9* (3), 654–663.

(142) Beck, M.; Mandal, T.; Buske, C.; Lindén, M. Serum Protein Adsorption

Enhances Active Leukemia Stem Cell Targeting of Mesoporous Silica Nanoparticles. *ACS Appl. Mater. Interfaces* **2017**, *9* (22), 18566–18574.

(143) Tang, F.; Li, L.; Chen, D. Mesoporous Silica Nanoparticles: Synthesis, Biocompatibility and Drug Delivery. *Adv. Mater.* **2012**, *24* (12), 1504–1534.

(144) Peng, Q.; Zhang, S.; Yang, Q.; Zhang, T.; Wei, X.; Jiang, L. Biomaterials Preformed Albumin Corona , a Protective Coating for Nanoparticles Based Drug Delivery System. *Biomaterials* **2013**, *34* (33), 8521–8530.

(145) Ferrari, M. Frontiers in Cancer Nanomedicine: Directing Mass Transport through Biological Barriers. *Trends Biotechnol.* **2010**, *28* (4), 181–188.

(146) Winzen, S.; Schoettler, S.; Baier, G.; Rosenauer, C.; Mailaender, V.; Landfester, K.; Mohr, K. Complementary Analysis of the Hard and Soft Protein Corona: Sample Preparation Critically Effects Corona Composition. *Nanoscale* **2015**, *7* (7), 2992–3001.

(147) Reddy, L. H.; Couvreur, P. Nanotechnology for Therapy and Imaging of Liver Diseases. *J. Hepatol.* **2011**, *55* (6), 1461–1466.

(148) Castillo, O.; Neyoy, H.; Soria, J.; García, M.; Valdez, F. Dynamic Fuzzy Logic Parameter Tuning for ACO and Its Application in the Fuzzy Logic Control of an Autonomous Mobile Robot. *Int. J. Adv. Robot. Syst.* **2013**, *10* (1), 85–96.

(149) Lam, P. L.; Kok, S. H. L.; Gambari, R.; Kok, T. W.; Leung, H. Y.; Choi, K. L.; Wong, C. S.; Hau, D. K. P.; Wong, W. Y.; Lam, K. H.; et al. Evaluation of Berberine/Bovine Serum Albumin Nanoparticles for Liver Fibrosis Therapy. *Green Chem.* **2015**, *17* (3), 1640–1646.

(150) Minardi, S.; Pandolfi, L.; Taraballi, F.; De Rosa, E.; Yazdi, I. K.; Liu, X.; Ferrari, M.; Tasciotti, E. PLGA-Mesoporous Silicon Microspheres for the in Vivo Controlled Temporospatial Delivery of Proteins. *ACS Appl. Mater. Interfaces* **2015**, *7* (30), 16364–16373.

(151) Hames, B. D. *Gel Electrophoresis of Proteins: A Practical Approoach*; 1998.

(152) Walczyk, D.; Baldelli Bombelli, F.; Monopoli, M. P.; Lynch, I.; Dawson, K. . What the Cell “Ss” in Bionanoscience. *J. Am. Chem. Soc.* **2010**, *132*, 5761–5768.

(153) Walker, J. M. *The Protein Protocols Handbook*; 1996.

(154) Baumann, R.; Bodard, G.; Cayless, H.; Sosin, J.; Viglianti, R. Integrating Digital Papyrology. *Digit. Humanit. 2011* **2010**, 2011–2020.

(155) Ebert, D. D.; Nobis, S.; Lehr, D.; Baumeister, H.; Riper, H.; Auerbach, R. P.; Snoek, F.; Cuijpers, P.; Berking, M. The 6-Month Effectiveness of Internet-Based Guided Self-Help for Depression in Adults with Type 1 and 2 Diabetes Mellitus. *Diabet. Med.* **2017**, *34* (1), 99–107.

(156) Bunjes, H.; Unruh, T. Characterization of Lipid Nanoparticles by Differential

Scanning Calorimetry, X-Ray and Neutron Scattering. *Adv. Drug Deliv. Rev.* **2007**, *59* (6), 379–402.

(157) Mainardes, R. M.; Gremião, M. P. D.; Evangelista, R. C. Thermoanalytical Study of Praziquantel-Loaded PLGA Nanoparticles. *Rev. Bras. Ciências Farm.* **2006**, *42* (4), 523–530.

(158) Levitas, V. I.; Samani, K. Melting of Nanoparticles. *Nat. Commun.* **2011**, *2*, 284–286.

(159) Calorimetry, D. S. Differential Scanning Calorimetry; First and Second OrderTransitions in Polymers Purpose. *DSC Polym.* 1–7.

(160) Walkey, C. D.; Chan, W. C. W. Understanding and Controlling the Interaction of Nanomaterials with Proteins in a Physiological Environment. *Chem. Soc. Rev.* **2012**, *41* (7), 2780–2799.

(161) Lang, B. E.; Cole, K. D. Unfolding Properties of Recombinant Human Serum Albumin Products Are Due To Bioprocessing Steps. *Biotechnol. Prog* **2014**, *00* (00).

(162) Yenilmez, E. D.; Tuli, A. *New Perspectives in Prenatal Diagnosis of Sickle Cell Anemia*; 2016.

(163) Nasir, I.; Lundqvist, M.; Cabaleiro-Lago, C. Size and Surface Chemistry of Nanoparticles Lead to a Variant Behavior in the Unfolding Dynamics of Human Carbonic Anhydrase. *Nanoscale* **2015**, *7* (41), 17504–17515.

(164) Khan, S.; Gupta, A.; Chaudhary, A.; Nandi, C. K. Orientational Switching of Protein Conformation as a Function of Nanoparticle Curvature and Their Geometrical Fitting. *J. Chem. Phys.* **2014**, *141* (8).

(165) Cedervall, T.; Lynch, I.; Lindman, S.; Berggård, T.; Thulin, E.; Nilsson, H.; Dawson, K. A.; Linse, S. Understanding the Nanoparticle – Protein Corona Using Methods to Quantify Exchange Rates and Affinities of Proteins for Nanoparticles. **2007**, *104* (7).

(166) Hamborg, M.; Jorgensen, L.; Bojsen, A. R.; Christensen, D.; Foged, C. Protein Antigen Adsorption to the DDA/TDB Liposomal Adjuvant: Effect on Protein Structure, Stability, and Liposome Physicochemical Characteristics. *Pharm. Res.* **2013**, *30* (1), 140–155.

(167) Setyawati, M. I.; Tay, C. Y.; Docter, D.; Stauber, R. H.; Leong, D. T. Understanding and Exploiting Nanoparticles' Intimacy with the Blood Vessel and Blood. *Chem. Soc. Rev.* **2015**, *44* (22), 8174–8199.

(168) Kharazian, B.; Hadipour, N. L.; Ejtehadi, M. R. Understanding the Nanoparticle-Protein Corona Complexes Using Computational and Experimental Methods. *Int. J. Biochem. Cell Biol.* **2016**, *75*, 162–174.

(169) De Paoli Lacerda, S. H.; Park, J. J.; Meuse, C.; Pristinski, D.; Becker, M. L.; Karim, A.; Douglas, J. F. Interaction of Gold Nanoparticles with Common Human Blood Proteins. *ACS Nano* **2010**, *4* (1), 365–379.

(170) Zhang, X.; Zhang, J.; Zhang, F.; Yu, S. Probing the Binding Affinity of Plasma Proteins Adsorbed on Au Nanoparticles. *Nanoscale* **2017**, *9* (14), 4787–4792.

(171) Geras, A. Leading Manual Test Efforts with Agile Methods. *Proc. - Agil. 2008 Conf.* **2008**, *104* (7), 245–251.

(172) Loregian, A.; Sinigalia, E.; Mercorelli, B.; Palù, G.; Coen, D. M. Binding Parameters and Thermodynamics of the Interaction of the Human Cytomegalovirus DNA Polymerase Accessory Protein, UL44, with DNA: Implications for the Processivity Mechanism. *Nucleic Acids Res.* **2007**, *35* (14), 4779–4791.

(173) Wang, B.; Zhang, L.; Bae, S. C.; Granick, S. Nanoparticle-Induced Surface Reconstruction of Phospholipid Membranes. *Proc. Natl. Acad. Sci.* **2008**, *105* (47), 18171–18175.

Chapter IV. Physiological response

This page left blank intentionally

4.1 Introduction

In the previous chapter, taking advantage of MSN with different pore sizes, it was optimized the usage of the complexes formed by such MSN and protein coronas. It was demonstrated that according to the size ratio between pores and proteins, the different PCs of MSN could be employed as gatekeepers, for targeting or even to be self-released from the nanoparticles. At this point, the potential therapeutic application of these complexes wanted to be studied. Cancer, that is considered as a 21st century disease, was chosen.

Cancer is characterized by growth of abnormal cells in the body forming tumours. Tumours are characterized by massive cell division, which is no longer controlled as it is in normal tissue. Healthy, normal cells stop dividing when they get in contact with another cell, a mechanism known as contact inhibition, whereas cancerous cells lose this ability. The success of chemotherapy to kill cancer cells depends on its capacity to halt cell division[174]. Usually, chemotherapeutic drugs' mechanism of action relies on damaging the RNA or DNA that dictates the cell to copy its own genetic material for cell division. For instance, 5-fluoruracil is an antimetabolite that interferes with DNA and RNA synthesis by mimicking the building blocks necessary for synthesis at very specific phases in the cell cycle. If the cells are unable to divide, then they die. The faster the cells are dividing, the more likely it is that chemotherapy will kill them, causing the tumour shrink. Drugs can also induce cell suicide (self-death or apoptosis). Chemotherapeutic drugs can also be antitumor antibiotics, which act during multiple phases of the cell cycle and are considered cell-cycle specific. Doxorubicin is one of the most commonly used antitumor antibiotics[175,176,177].

Unfortunately, chemotherapy cannot distinguish between cancerous and normal, healthy cells. Chemotherapeutic drugs will act killing all cells that are rapidly dividing. The "normal" cells that are most affected by chemotherapy are blood cells, cells in the mouth, stomach and bowel, and hair follicles, resulting in low blood counts, mouth sores, nausea, diarrhoea, and/or hair loss. Different drugs may affect different parts of the body[178,179]. This unwanted collateral damage can be avoided using nanoparticles systems which encapsulate the drug and release it specifically in the damage tissue. Once nanoparticles arrive in the target organ, the drug is released, preventing healthy tissues from being damaged during the travel within the body[180,181,182].

However, the translation of nanoparticles to the clinic for cancer therapy is hampered by the limited stability in biological fluids of most nanomaterials. As mentioned before, the incorporation of nanoparticles in the bloodstream causes a strong reaction with serum proteins, lipids, membranes, cells, DNA, different organelles and small molecules, forming a shell of aggregated compounds onto the NPs' surface known as the "protein corona". This protein corona alters the size and interfacial composition of a nanomaterial, giving it a biological identity that is distinct from its initial synthetic identity. This is the reason why many of the questions regarding the biocompatibility and biodistribution of MSNs *in vivo* still remain unanswered. The comprehension of the PC formation and composition bring MSN together to their use as drug delivery systems.

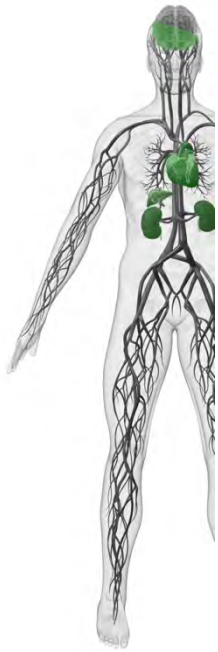

Figure 53: Biodistribution of nanoparticles.

The correlation between the synthetic identity and biological identity was deeply analysed in chapter III. Yet, medical applications of nanoparticles require the understanding of their interactions with living systems in order to control their physiological response, such as cellular uptake and cytotoxicity. The identity of the proteins that form the PC plays a key role in the physiological response. For instance, the mechanisms of uptake will be determined by this biological identity of the nanoparticle, varying from entering into cells via a receptor-mediated or caveolin-mediated endocytosis pathway. That is why, in this work, the effect of the corona composition on nanoparticle uptake has been investigated, by studying the impact of different PC on cell uptake results. Also, the cytotoxicity has been analysed, aimed at

finding differences between healthy and cancerous cells, minimizing the collateral damage in the healthy ones.

The following step has been studying the capacity of loading the nanoparticles with a drug and the capacity of releasing it from the MSN once inside the cell. The MSN have to be able to incorporate enough quantity of drug to, once the NP is inside the tumour cell, release it and cause the cell death.

To sum up, after the previous design of MSN with defined properties and the knowledge of the influence of the PC formation, the relationship between the drug and the MSN with the PC must be studied. At the same time, the cellular uptake and the viability of the target cells need to be analysed.

4.1.1 Objectives

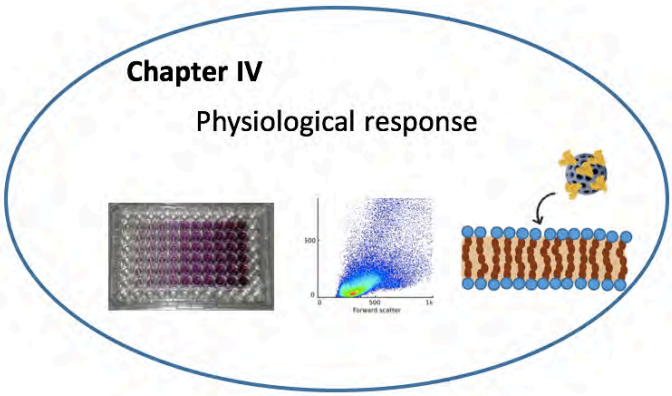

Figure 54: Graphical abstract of Chapter IV.

In order to achieve this objective, the following tasks were proposed:

- To assess the effect of the loading and release profile of the studied drugs regarding the formed PC.
- To analyse the uptake of nanoparticles depending on the proteins of the surface in different cell lines.
- To compare the differences in cytotoxicity of nanoparticles loaded with the drugs and with a PC.

4.2 Materials and methods

4.2.1 Uptake procedure

Cells were seeded in 96 well plate at $12*10^5$ cell/ well. After 24h, uptake experiment was carried using different samples of MSN. Briefly, MSN were performed as previously described using FITC. Then, cells were incubated with nanoparticles using DMEM supplemented. After that, nanoparticles were removed, cells were washed twice with PBS 1X and cells were trypsinized with 100 µl of trypsin and 200 µL of completed medium for flow cytometry analysis.

4.2.2 Uptake (Albumin-FITC)

10 mg of HSA-FITC in a total volume of 1 mL (PBS). Samples were mixed carefully, to avoid protein denaturation due to mixing, and incubated 24 hours at 37 °C. Purification of hard corona was carried out by centrifuging samples at 13000 rpm for 13 minutes and including three washing steps in the purification procedure. Samples were first centrifuged and supernatants (SN) were discarded and 1 mL of fresh PBS was added to suspend nanoparticles. Procedure was repeated 3 additional times, in order to wash nanoparticle solution from non-attached protein present in solution. Then, the methodology of the uptake was performed. After the necessary 24 h, cells were lysed by sonication, and the fluorescents proteins were separated centrifuging. The amount of HSA-FITC was analysed with a UV–Vis absorption spectrophotometer at 490 nm.

4.2.3 Live and dead assay

Cells were grown in 96-well plates at an initial seeding density of 12000 cells/well in 200 µL growth medium. Cells were grown for 24 h, and then different MSN were added and incubated during 3h. Nanoparticles with protein corona were formed as the methodology in chapter II. Then, nanoparticles were removed, cells were washed once with PBS 1X and 100 µL of 120 µM solution fluorescein diacetate (FDA) was added. q h post-addition, the medium was removed, cells were washed with PBS, and cells were trypsinized with 100ul of trypsin and 200 µL of completed medium for flow cytometry analysis. Cell viability was expressed as a relative percentage compared with untreated cells.

4.2.4 DOX loading and release of the MSN

4.2.4.1 DOX loading in MSN

To 15 mg MSN in 30 mL MeOH and 7 mg (12 mmol) of DOX were added. The solution was left 24 h at room temperature. Then, MSNs were washed extensively, until no red supernatant was obtained. Supernatant was collected and measured by UV-Vis to assess the quantity of DOX loaded at 490 nm, which was near 8 %.

4.2.4.2 Release

In vitro release experiments were performed at pH=7.4, pH=6.3 and pH=5. For each release study, 1 mL of PBS was first added to 1 mg of MSNs and maintained at 37 ◦C, while being stirred at 100 rpm. Briefly, protein coronas were performed as previously described using different types of proteins. Release medium was removed for analysis at specific time intervals by centrifuging at 12000 rpm for 30 min and placing solid residues into identical volumes of fresh buffer solution. The amount of released was analyzed with a UV–Vis absorption spectrophotometer at 490 nm for DOX.

4.2.4.3 DOX in presence of HSA according to the pH

2 mg of MSN load with DOX were suspended in 500 µL of PBS at a pH of 7.31 and 6.44. Then, 5 mg of HSA were added and mixed carefully.

4.2.5 5-Fluorouracil loading and release of the MSN

4.2.5.1 5-FU loading in MSN

To 36 mg MSN (S1) in 25 mL MeOH and 20 mg (26 mmol) of 5-FU were added. The solution was left 24 h at room temperature. Then, MSNs were washed extensively. Supernatant was collected and measured by UV-Vis to assess the quantity of 5-FU loaded at 266 nm, which was near 45 %.

4.2.5.2 Release

In vitro release experiments were performed at pH=7.4, pH=6.3 and pH=5. For each release study, 1 mL of PBS was first added to 1 mg of MSNs and maintained at 37 ◦C, while being stirred at 100 rpm. Briefly, protein coronas were performed as previously described using different types of proteins. Release medium was removed for analysis at specific time intervals by centrifuging at 12000 rpm for 30 min and placing solid residues into identical volumes of fresh buffer solution. The amount of released was analyzed with a UV–Vis absorption spectrophotometer at 266 nm for 5-FU.

4.2.5.3 MTT assay

MSN toxicity was measured using MTT assay (Sigma-Aldrich) at 24 and 48 hours post nanoparticle addition and 5 hours and 2 days after incubation. MTT assay measures the activity of living cells via mitochondrial dehydrogenase activity. Briefly, MTT stock solution (5 mg/mL) was added to each culture well, being assayed to equal one-tenth of the original culture volume and incubated for 3 h. After that, DMSO was added in an amount equal to the original culture volume. Finally, the cell viability was determined by measuring the absorbance at 570 nm using a microplate reader (Elx808 Biotek Instrument Ltd, USA). Cell viability was expressed as a relative percentage compared with untreated cells.

4.3 Results and discussion

In the previous chapter, the PC formation was studied depending on the pore size. Consequently, to fight against the cancerous tumour, MSNs were loaded by one of the most popular drug in cancer chemotherapy, Doxorubicin (DOX).

4.3.1 DOX loading on MSN

For this therapeutic application, the size ratio between MSN and PC that was picked up was that one when the protein fits inside the pore. This way, not only the spontaneous pre-release that can cause several side effects was avoided but also the targeting to a certain organ could be more effective.

First, S1 are the nanoparticles which the albumin fits better inside their pore were chosen for the preliminary study. The chosen drug was Doxorubicin (DOX). Doc is a cytotoxic anthracycline antibiotic isolated from cultures of Streptomyces *peucetius var. caesius*. Doxorubicin binds to nucleic acids, presumably by specific intercalation of the planar anthracycline nucleus with the DNA double helix[175]. Also, as discussed above, it has been demonstrated that liver cancer cells' display an overexpression of specific human serum albumin receptors, which internalize large amounts of HSA through the mechanism of caveolae-mediated endocytosis.

MSNs with amines at the porous surface of the NP present an excellent advantage, which is that at basic pH, amino moieties would not be protonated and cationic DOX would be easily absorbed. While in an acid pH, amines would protonate preventing the electrostatic binding from taking place and as a consequence, DOX release would be boosted[183,184,185]. To this end, first of all, DOX absorption inside MSNs porous must be studied. The drug loading of S1 is quantified by the difference between the amount of DOX present in the supernatant (released) and that added initially in the reaction (total). The loading of DOX inside S1 NP is about 8.5% in PBS medium.

Afterward, the release study was performed. First, nanoparticles loaded with DOX were incubated in HSA and FBS to form the protein corona. The nanoparticles without protein corona, MSN naked, were also incubated with PBS to emulate the same conditions and to be able to compare all the samples. After 24 hours, the washes were performed and MSN were suspended in 1 mL of PBS. At different time points MSN were centrifuged and the DOX in the supernatant was quantified through its absorbance. Then, 1 mL of new PBS was added and incubated longer time. Taking into account that pH values at cancerous tissues (pH=6.5) are lower than in blood and normal tissues

(pH=7.4), pH sensitivity can be used to control release systems in cancer applications. Therefore, two pH were studied, 6.44 as acidic pH and 7.31 as a physiological medium.

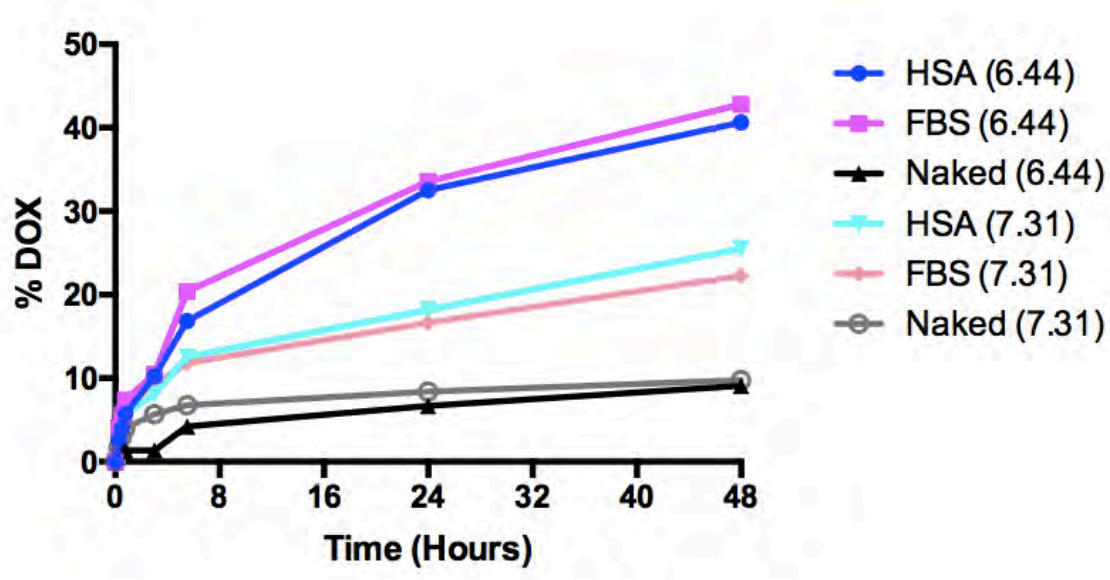

Figure 55: Differences in the DOX release depending on the protein that forms the PC.

The amount of DOX released from the MSN with respect to the incubation time were represented in Figure 55. As expected, the medium at pH 6.4 suffers a greater release of DOX than the respective one at pH 7.3. The behaviours regarding HSA and FBS corona were similar, due to FBS is composed mostly by albumin. Unexpectedly, instead of the PC clogging the release of the DOX, it suffers a much greater release than in the naked nanoparticles.

To rule out a possible experimental error, some HSA was added to MSN already loaded with DOX at different pH. It can be observed in Figure 56 that the sample with the addition of HSA suffers a massive release of DOX as compared to the sample without HSA. The unwanted release of the DOX from the MSN can explain why with a HSA PC the release was higher than naked.

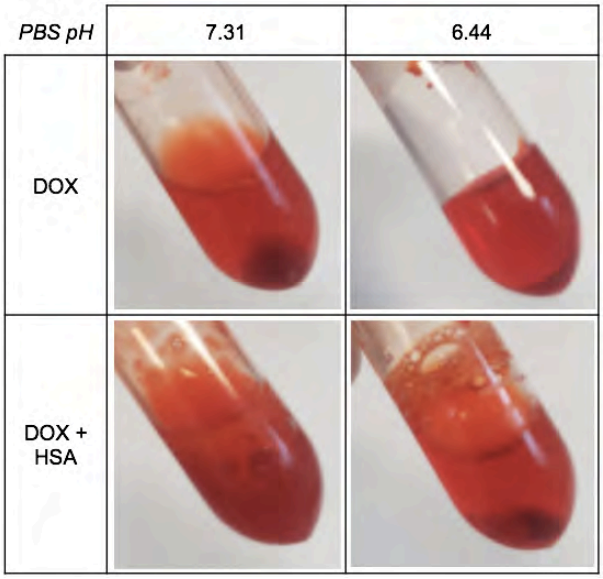

Figure 56: DOX behaviour with respect to HSA and pH.

This occurs due to the binding of doxorubicin to HSA via hydrophilic and hydrophobic contacts with stable complexes. The drug-protein binding involves several amino acids residues, which stabilize by H-bonding network. Drug interaction alters protein's secondary structure for HSA causing a partial protein destabilization.

A commercial form for doxorubicin is Doxil, a liposome version of this drug. That is, Doxil is the drug doxorubicin encapsulated in a liposome. Liposomes have on their surface a substance to protect themselves from detection by the body's immune system and to increase the time that Doxil is circulating in the blood. By enclosing a drug in the complex it is possible to get close to the tumour and the encapsulated drug doxorubicin becomes able to work against the tumour cells[49].

The clogging by others proteins which do not suffer this destabilization effect were studied using aprotinin and fibronectin. Aprotinin is a bovine pancreatic trypsin inhibitor, that is used as medication administered by injection to reduce bleeding during complex surgery, such as heart and liver surgery[186]. Fibronectin mediates a wide variety of cellular interactions with the extracellular matrix and plays important roles in cell adhesion, migration, growth and differentiation[186]. The size of aprotinin is 6.5 kDa while fibronectin is 220 kDa.

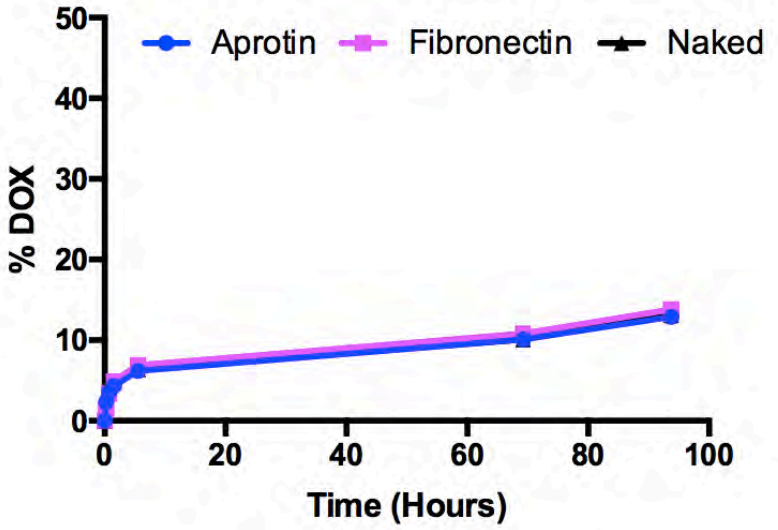

Figure 57: Release of DOX when nanoparticles are incubated with aprotinin and fibronectin.

It can be observed in Figure 57 that neither aprotinin or fibronectin can block the DOX release, since no differences with the naked nanoparticles were observed. Aprotinin is too small and fibronectin too big to fit inside the pore. For that reason, the relationship between the pore and the protein size is so important as detailed in chapter III.

Then, the dependence of the release of DOX with the pH and the nature of the corona formation were summarized in Figure 58.

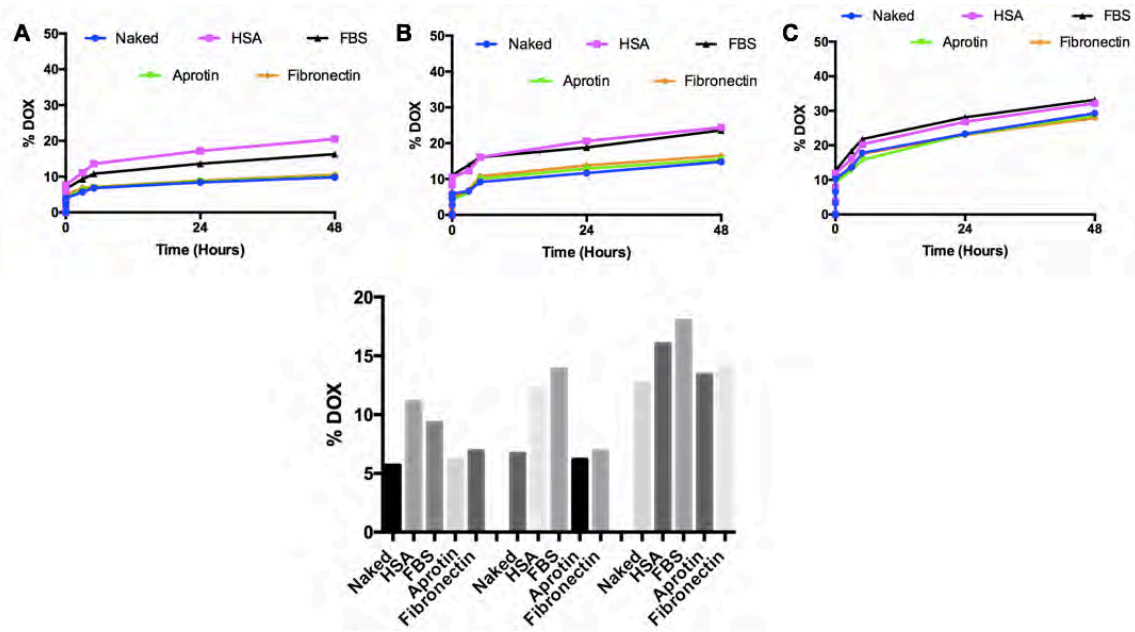

Figure 58: Summary of pH and proteins with respect to the DOX release. From left to right the release was made in pH 7.31, 6.44 and 5.

In Figure 58, it can be observed that HSA and FBS induce a more abrupt release with respect to the aprotinin and fibronectin coronas, due to the albumins' destabilization because of the presence of DOX. Every release was increased with the acidification of the medium.

4.3.2 5-Fluorouracil loading on MSN

The drugs which have chemical structures similar to DOX are less stable in the presence of HSA, including for example camptothecin. The destabilisation is explained due to these agents are found to hydrolyze rapidly in the presence of HSA. The lactone-carboxylate equilibrium for each structure went almost completely (96-99%) to the right, the carboxylate form of camptothecin have a preferential binding by HSA[28]. For that reason, it was chosen a drug with a different chemical structure, as is the case of 5-Fluorouracil (5FU).

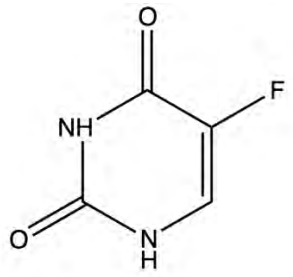

Figure 59: 5-fluorouracil structure.

Again, MSN were loaded with the drug, in this case with 5-FU. The methodology used was the same as for DOX (see Materials and methods). The 5-FU loading was higher with respect to DOX, due to the fact that the size of 5-FU is lower, and this facilitates its adsorption through the MSN matrix. Here, three nanoparticles were chosen: S1, S4 and S5. It can be observed in Figure 60 that the bigger was the pore, the higher amount of 5-FU entered in the MSN. Nanoparticle S1, with a pore size of 38.8 Å, had a loading of about 44.7% (w/w); S4, with a pore size of 34.2 Å, loaded about the 34.2% of 5-FU supplied; and finally, S5 of 28.8 Å pore size loaded a 17.3%.

A

B

	S1	S4	S5
5-FU loaded (%)	44.7	34.2	17.3
Pore Size	38.8	34.2	28.8

Figure 60: 5-FU loading in the MSN depending on the pore size.

The release of 5-FU in S1 was studied regarding two pH: the physiological one and one acidic that simulates the pH of a tumour. Finally, in Figure 61 it can be observed that albumin, not being destabilized by 5-FU, can block the release, being it more controlled. In the same way, the release in acid pH was higher.

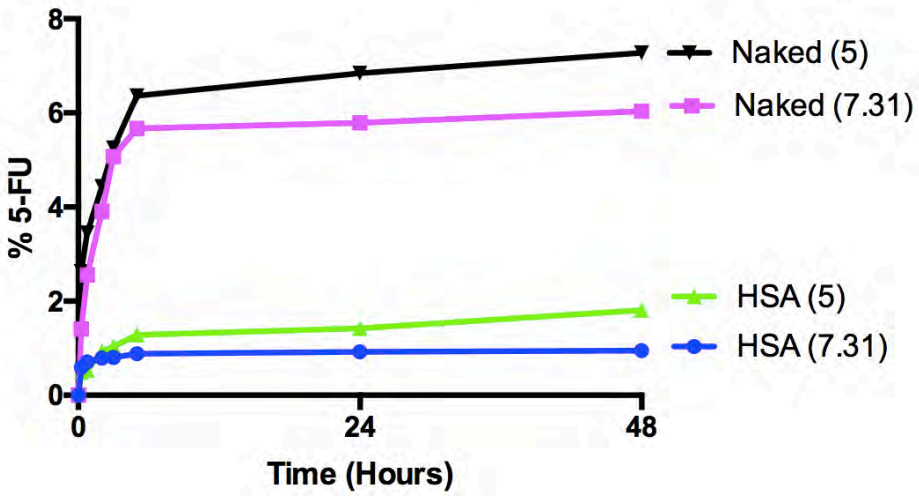

Figure 61: 5-FU release of the MSN S1 regarding two pH (5 and 7.31).

Regardless of the pH, in order to prove in this system, the clogging of the pore to avoid the DOX pre-release, a lysozyme PC was made on the MSN loaded with DOX (see materials and methods). Lysozyme (Lys) was used as a model protein, whose dimension is comparable in size to 34 Å, and 14.3 kDa. In Figure 62 (A) it can be observed that, while the albumin blocks the 5-FU release in S1 nanoparticles, lysozyme due to their small size cannot be so effective. On the other hand, it was also probed the capacity of Lys blocking in S4 and S5 which has a smaller pore, although the blocking

of proteins remains ineffective. In Figure 62 (B), it can be observed the total charge of the nanoparticle, being decremented as the pore is smaller. The blocking of albumin in S1 (even having a loading greater than S4 and S5) is so effective that the release of the drug is even lower than S4 and S5 without protein. This corroborates the importance between the ratio of the pore size with the protein corona in the release of a drug and its use in a controlled release.

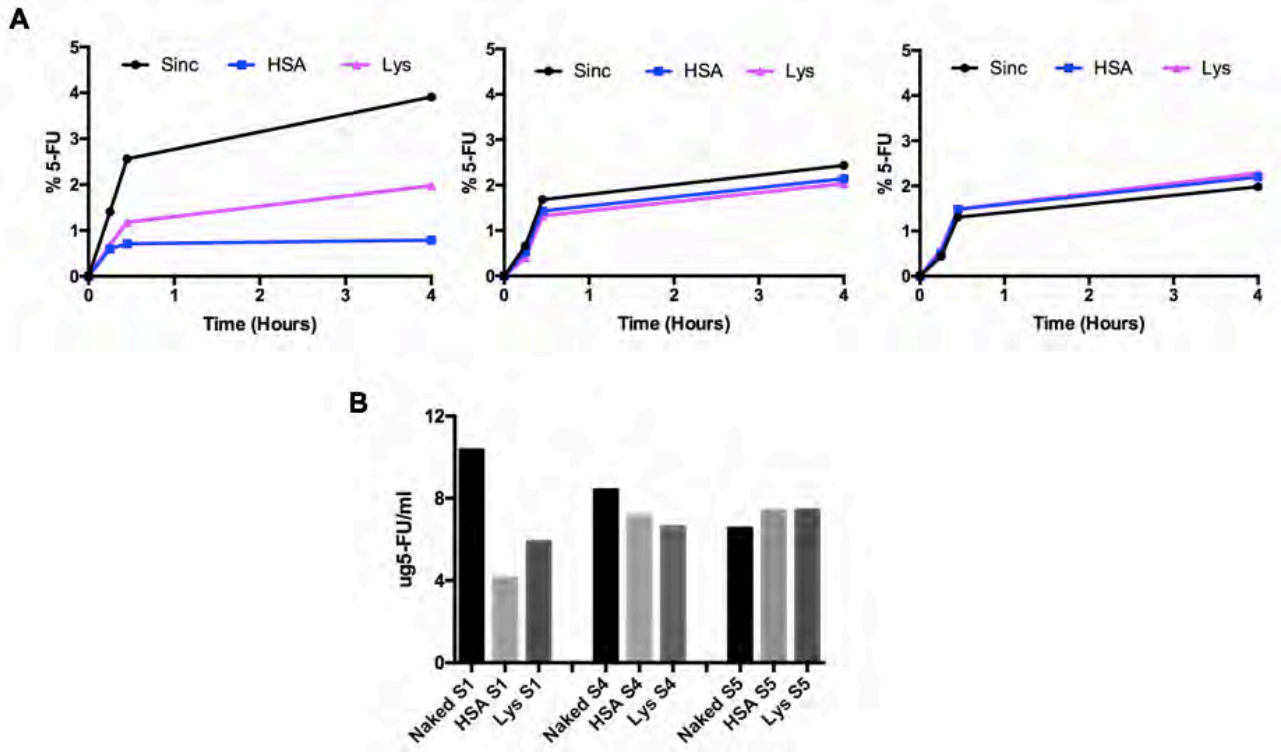

Figure 62: Comparison of the 5-FU release regarding pH and pore sizes. A) From left to right the plotted samples were S1, S4 and S5. B) The initial rate of release of each sample, in the same order as in graphs A.

4.3.3 Cell Viability studies

5-Fluoruracil is a drug, which belongs to the category of chemotherapeutic drugs called antimetabolites. When the cells incorporate 5-FU into the cellular metabolism, they are unable to divide. 5-Fluoruracil is classified as a pyrimidine analogue because it interferes with DNA and RNA synthesis by mimicking the building blocks necessary for their synthesis. For that reason, the study of the cell viability was necessary. This work is aimed at improving the treatment for liver cancer. Consequently, two cell lines were chosen, being one from hepatic cells, AML12, and the other from hepatic carcinoma, HepG2, for possible comparison. HepG2 is an immortalized cell line consisting of human liver carcinoma cells. The same experiment was carried out on AML12 cells, a healthy

cell line from hepatocytes (not tumorigenic), in order to be allowed to compare the results.

Firstly, in Figure 63 in can be observed the comparison of the cell viability of the two cell lines. The samples were S1, S1 with an albumin corona, S1 loaded with 5-FU with and without PC, and 5-FU. Nanoparticles loaded with the drug, regardless of the PC, showed less toxicity to healthy cells (AML12) than to cancerous cells (HepG2), being it a great advantage. Furthermore, when comparing nanoparticles with the free 5-FU not only is the viability of the healthy cells higher, but also the mortality of cancer cells is similar. Regarding the sample S1 without PC or drug, as seen in the internalization, when entering cells massively it produces a slight toxicity. The analogue with HSA shows less toxicity due to the loss of positive charge and thereby decreased cell uptake.

A

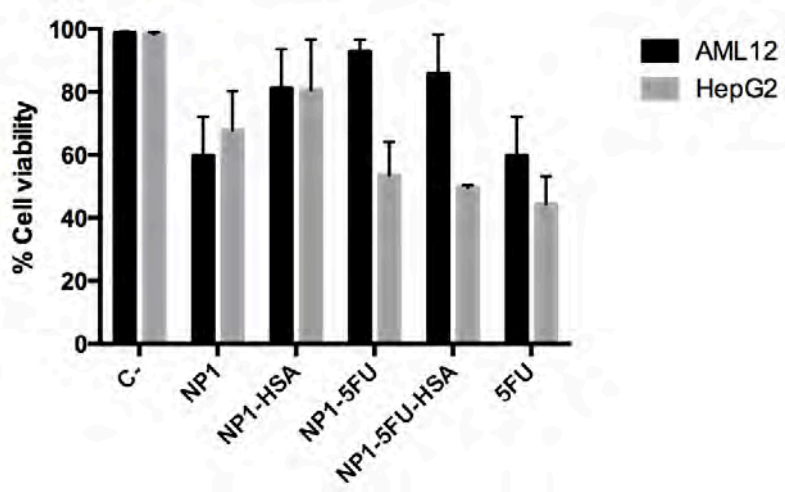

B

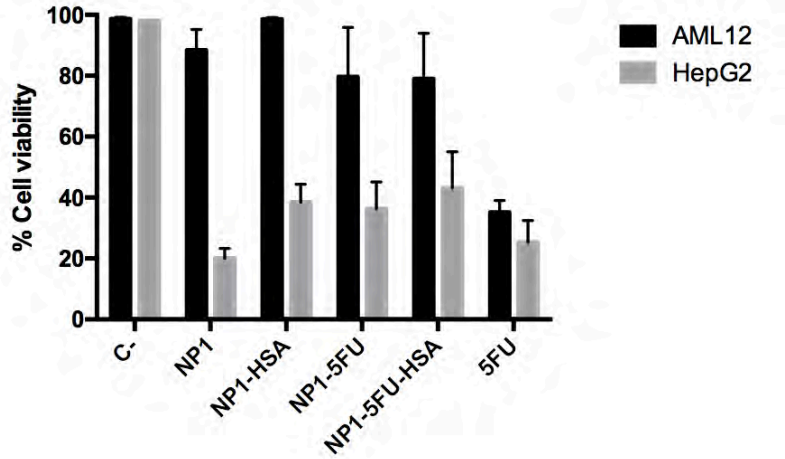

Figure 63: MTT assay at 3 (A) and 5 days (B). In black AML12 cells and in grey HepG2 cells.

In an *in vivo*, the cell uptake once nanoparticles are administrated into the body lasts a few hours. For that reason, it was studied the cell viability of cells exposed to 2.5 µg MSN/mL of NPs during 5 hours and then incubated for 24 hours. It can be observed in Figure 64 that, although in general cell viability of cancer cells (HepG2) was a slightly higher than that of healthy cells (AML12), when comparing the free 5-FU condition. This showed higher absorption, consequently less quantity can be injected. The side effects would decrease because of the less toxicity in the neighbouring tissues.

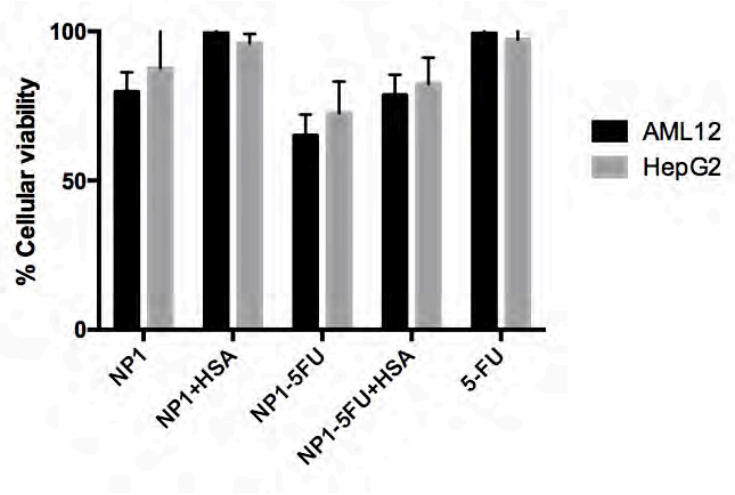

Figure 64: MTT assay at 24h after a 5h-time incubation of the MSN with HSA. Results correspond to mean ± SD values of at least three replicates.

The amount of drug administrated is decisive in the design of the any experiment. Hence, the cell viability regarding different concentrations of 5-FU was studied. In this case, the chosen concentrations were 0.5 mg 5-FU/ml, 0.05 mg 5-FU/ml and 0.0015 mg 5-FU/ml. Figure 65 shows the interesting result that in healthy cells higher concentrations of the drug (0.5 mg 5-FU/ml and 0.05 mg 5-FU/ml) cause more mortality than the same amount of drug encapsulated in the MSN, indistinctly with or without PC. 0.0015 mg 5-FU/ml concentration is comparable to the results obtained in Figure 64. On the other hand, no significant difference is observed in the tumours cells. At this point, it can be concluded that it is possible to administer higher amount of drug if it is encapsulated in MSN. Also the clogged with the albumin will prevent the premature release and that will target MSN to the liver.

A

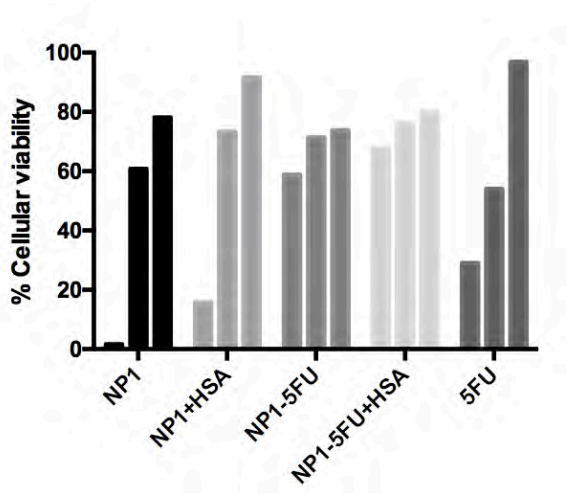

B

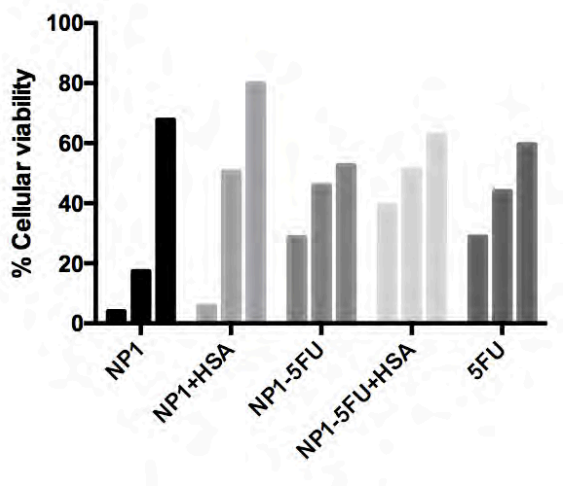

Figure 65: MTT assay on AML12 and HepG2 cell lines. For each sample the three bars correspond to 0.5 mg 5-FU/ml, 0.05 mg 5-FU/ml and 0.0015 mg 5-FU/ml, respectively.

4.3.4 Cellular Uptake

Nanoparticles used for drug delivery have to be allowed to both enter inside the cell and release the drug. For that reason, using nanoparticles with their surface modified with FITC, the cellular uptake was studied. In this case, for analyse the suitable conditions for biological experiments HeLa cells were chosen since they are widely studied and well-known cells. The analysis of the PC formed on the different MSN samples was studied in this chapter regarding its physiological response. Firstly, the cellular uptake was determined through flow cytometer analysis using four differentiated enough samples of MSN. Some of them were incubated in FBS and others were

delivered to cells naked. Two concentrations of MSN in the cell medium were studied: 5 µg MSN/ml and 25 µg MSN/ml.

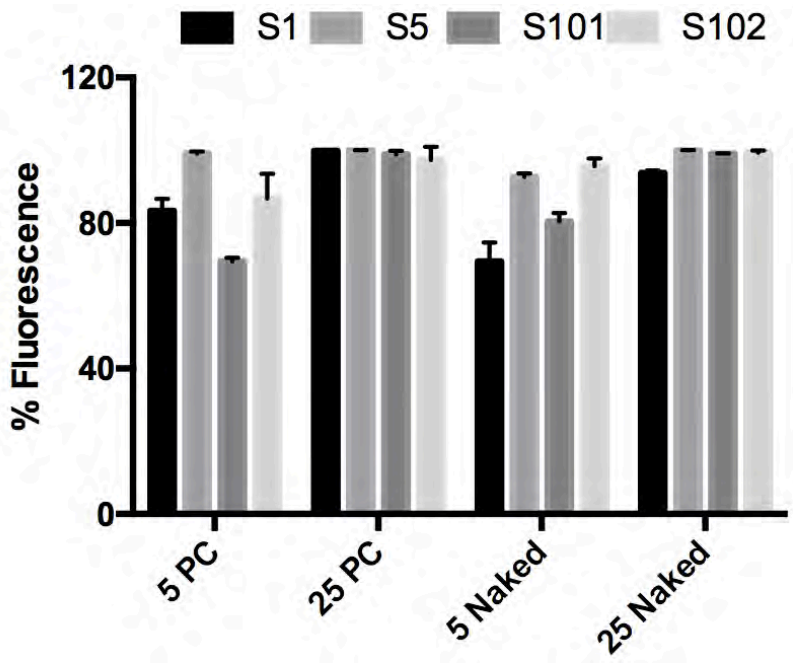

Figure 66: FACS analysis of the different MSN samples (S1, S5, S101, and S102) uptake on HeLa cells at different nanoparticles concentrations. Results correspond to mean ± SD values of at least three replicates. PC= nanoparticles incubated 24h in FBS to form a Protein Corona; Naked= nanoparticles without this treatment.

Then, the cellular uptake was analysed, using the live-cell microscopy of the IncuCyte® system. In contrast to real-time cell analysis which estimates cell numbers, attachment and viability based on the impedance measurements across the bottom of the wells, live-cell microscopy allows the observation of cell uptake in real time. Using this methodology, it can be determined which samples have a greater cell uptake using nanoparticles with FITC on the surface. In this case it was also used the cell line HeLa due to their sturdiness. In Figure 67, it can be observed that S101 has the highest uptake followed by S5, S102 and S1. By analysing the results, it can be determined that the less PC there is, the more internalization results. This minimize the excessive cellular uptake.

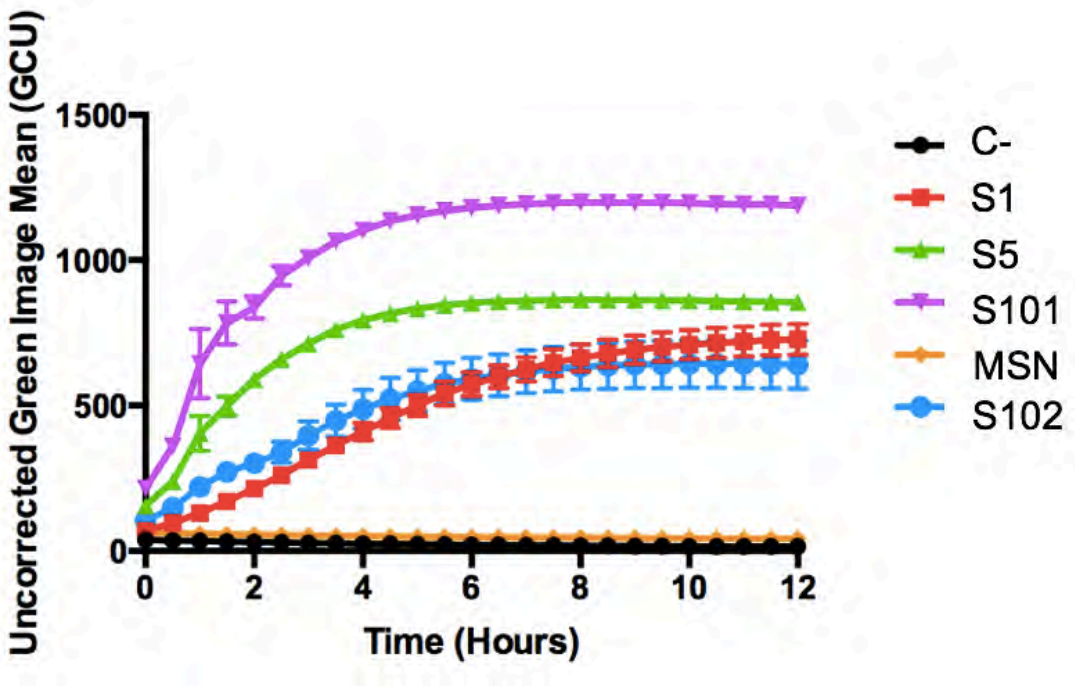

Figure 67: Cell uptake of MSN with FITC over time.

These results corroborate both cellular uptake and the experiment of the uptake using HAS-FITC. The cellular uptake is depending on the surficial charge, i.e. on the protein corona formed.

Once the conditions were optimized, the cellular uptake was studied using HepG2 and AML12 cells. The uptake was determined from the different samples of MSN without any pre-treatment, and also with the pre-formed PC (HSA and FBS corona).

A

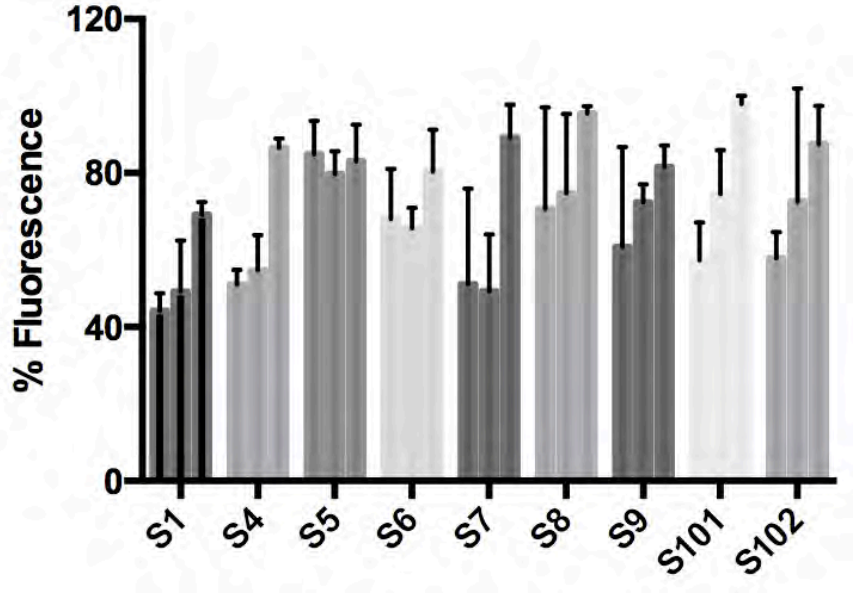

B

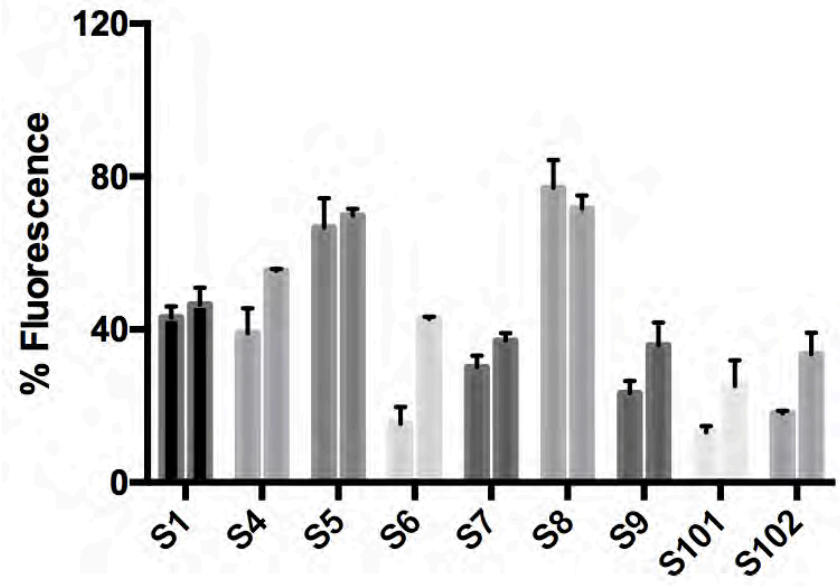

Figure 68: FACS analysis of the different MSN samples uptake on (A) HepG2 and (B) AML12 cell lines at 2.5 mg/mL nanoparticles concentration. From the left to the right the sample were naked, with FBS PC and with HSA PC, respectively (in the case of AML12 without FBS PC sample). Results correspond to mean ± SD values of at least three replicates

The obtained results are shown in Figure 68. In both cell lines and for every sample, the uptake is higher for MSN naked than for MSN with PC. Probably because of the positive charge of the nanoparticles. Negatively charged proteins adsorbed on positive MSN surface reduce the resulting zeta potential of such MSN surfaces. Thus, there is an expected decrease in the uptake due to charge repulsions with the negatively charged cellular membrane. It should be noted that excessive uptake is detrimental to cellular viability.

In order to corroborate these uptake results, samples S1, S5, S8, S9 and S102, as a representation of the different pore sizes, were incubated with albumin-FITC. After allowing the cell uptake to take place, cells were washed and lysed. Then, FITC in the supernatant was quantified, and charted in Figure 69. The more PC there was on the surface of the MSN, the less was the uptake. According to the results of the cellular uptake obtained with flow cytometry analysis, the less positive is the surface, the modest the smaller uptake appears. Sample S1 was the MSN with more proteins, so it resulted in the one with less uptake; on the other hand, samples S5 and S8, had less PC and, consequently, the highest uptakes.

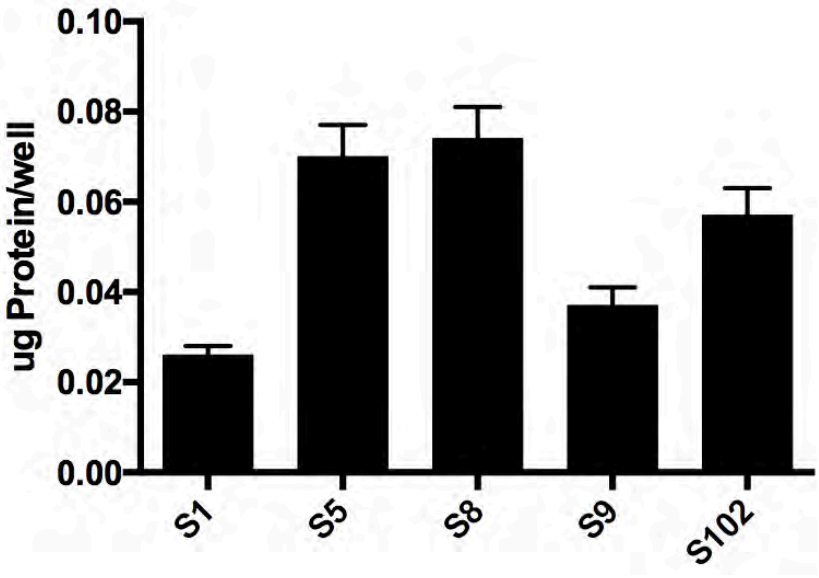

Figure 69: Quantification of the albumin-FITC of the different MSN samples (S1, S5, S8, S9 and S102) uptake on HeLa cells. Results correspond to mean ± SD values of at least three replicates.

Finally, although was widely studied, it was necessary prove the non-toxicity of the MSNs. For all of the viability experiments, $12*10^3$ HeLa cells per well were seeded in 96-well plates. S1, S4, S5, S6, S7, S8, S9 S101 and S102 at 2.5 µg MSN/mL concentration were added to cells and let 24h incubating at 37 ºC with 5% CO_2. A live and dead method was used for the determination of the cellular viability (see Materials and methods). Viability results are represented in Figure 70. As expected, mesoporous silica nanoparticles did not present cytotoxicity.

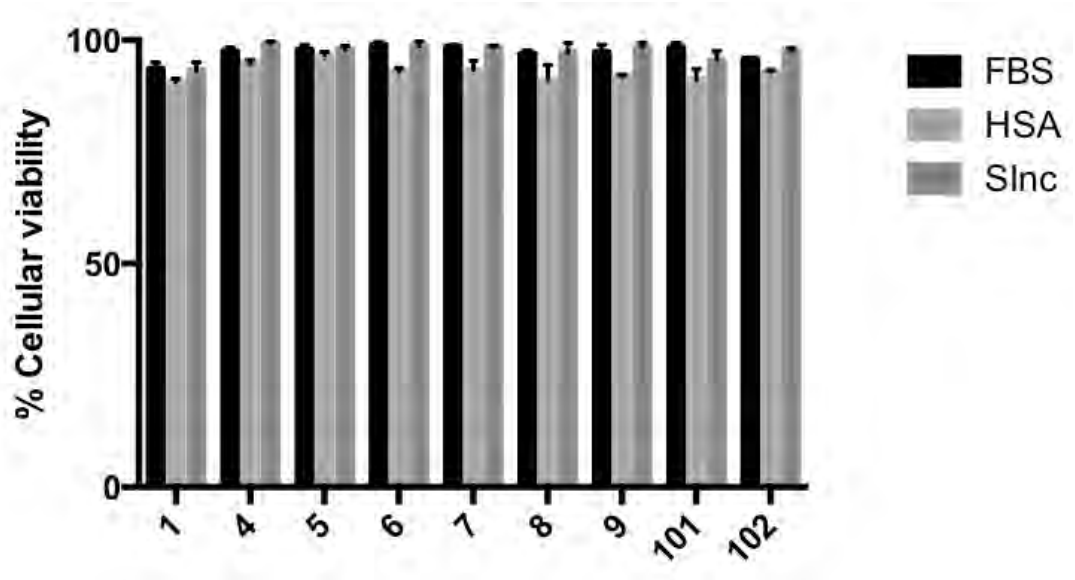

Figure 70: Cellular viability assay using the live and dead (L&D) of the different MSN samples (S1, S4, S5, S6, S7, S8, S9, S101, and S102) uptake on HeLa cells at different nanoparticles concentrations. Results correspond to mean ± SD values of at least three replicates.

4.4 Concluding remarks

Previously in Chapter II and III, it has been described that differences in synthetic identity, as the aspect ratio and the pore size, render different biological identities i.e. differences in the protein corona formation, which can be determined their application. The new identity dependent of the proteins absorbed in the surface determines the physiological response. For that reason, in this chapter the influence of the PC regarding the cellular behaviour has been studied.

Firstly, it is moved on to loading the nanoparticle with doxorubicin. Here it is demonstrated that DOX loaded in a MSN with an albumin as a PC does not work, due to DOX interaction alters protein secondary structure for HSA causing a partial protein destabilization. A boost release is observed because of the albumin interaction. This is not desired and, for that reason, the drug is changed by using another drug, 5-Fluorouracil, with a different chemical structure. This change allows an increase in the drug loading and the blocking of the pre-release in the pore caused by the albumin.

The clogging of the pore through the albumin corroborates the results of the nanoDSC and ITC in the Chapter III. Albumins is capable of blocking the release of the drug when it is allowed to fit in the pore. Nanoparticles which its pore is not big enough to fit albumin present a release similar to the nanoparticles without PC. At the same this this blocking will make that the organs and tissues through which the nanoparticle passes to reach the target organ will not be damaged. The using of albumin as a PC will at the same time be useful for targeting the liver, organ by which it is attracted, due to the liver cancer cells' overexpression of specific human serum albumin receptors and their ability to internalize large amounts of HSA through the mechanism of caveolae-mediated endocytosis (Chapter I).

Then, MSN load with 5-FU present lower toxicity in healthy cells (AML12) than in tumour cells (HepG2), contrary to the free 5-FU. That means that cancer cells will be attacked, and consequently killed, more than normal cells. This behaviour with respect to nanoparticles loaded with 5-FU and with albumin in the surface will be used to target the liver.

Lastly, the influence in the cellular uptake is proved. MSN with proteins in the surface suffer a decrease of the uptake. This can be explained due to both the cellular membrane and the albumin in the surface are negative, so they are repulsed, losing internalization capacity. Nevertheless, the uptake of nanoparticles without proteins is too

massive, making the reduction of the internalization better for the therapeutic purpose. This cellular uptake is checked as a non-toxic through the live and dead assay.

To sum up, in this chapter it is corroborated that the complex formed by MSN with a pore size big enough to fit albumin as a PC and loaded with 5-FU is both promising for drug delivery and for liver cancer targeting. This fact is due to the preference in internalization in tumours cells against healthy cells. At the same time that the plugging of the pore avoiding a premature release avoids the damage of the cells through which the vector passes. These results suggest that we have developed efficient complexes with promising characteristics to treat cancer. Showing that active targeting and efficient release of 5-FU are a key factor to obtain a successful therapeutic advance.

4.5 References

(175) A. Smajlovic , S. Hasanbašic , M. Biberovic , A. Džuzdanovic, Z. M. 5-Fluorouracil and Doxorubicin Interactions With Human Serum Albumin At Mild Acidic. *Pharmacia* **2015**, *18* (1), 22–29.

(176) Cairns, R. A.; Harris, I. S.; Mak, T. W. Regulation of Cancer Cell Metabolism. *Nat. Rev. Cancer* **2011**, *11*, 85.

(177) Kennecke, H.; Yerushalmi, R.; Woods, R.; Cheang, M. C. U.; Voduc, D.; Speers, C. H.; Nielsen, T. O.; Gelmon, K. J OURNAL OF C LINICAL O NCOLOGY Metastatic Behavior of Breast Cancer Subtypes. **2019**, *28* (20), 3271–3277.

(178) Gordon, K. B.; Tajuddin, A.; Guitard, J. Hand-Foot Syndrome Associated with Liposome-Encapsulated Doxorubicin Therapy. *Cancer Res.* **1995**, *75* (8), 2169–2173.

(179) Chaffer, C. L.; Weinberg, R. A. A Perspective on Cancer Cell Metastasis. *Science (80-.).* **2011**, *331* (6024), 1559 LP-1564.

(180) Manzano, M.; Vallet-Regí, M. Ultrasound Responsive Mesoporous Silica Nanoparticles for Biomedical Applications. *Chem. Commun.* **2019**, *55* (19), 2731–2740.

(181) Zhang, J.; Yuan, Z. F.; Wang, Y.; Chen, W. H.; Luo, G. F.; Cheng, S. X.; Zhuo, R. X.; Zhang, X. Z. Multifunctional Envelope-Type Mesoporous Silica Nanoparticles for Tumor-Triggered Targeting Drug Delivery. *J. Am. Chem. Soc.* **2013**, *135* (13), 5068–5073.

(182) Grosjean, R.; Delacroix, S.; Gouget, G.; Beaunier, P.; Ersen, O.; Ihiawakrim, D.; Kurakevych, O.; Portehault, D. High Pressures Pathway toward Boron-Based Nanostructured Solids. *Dalt. Trans.* **2017**, *47* (23), 7634–7639.

(183) Meng, H.; Xue, M.; Xia, T.; Zhao, Y.-L.; Tamanoi, F.; Stoddart, J. F.; Zink, J. I.; Nel, A. E. Autonomous in Vitro Anticancer Drug Release from Mesoporous Silica Nanoparticles by PH-Sensitive Nanovalves. *J. Am. Chem. Soc.* **2010**, *132* (36), 12690–12697.

(184) Muhammad, F.; Guo, M.; Qi, W.; Sun, F.; Wang, A.; Guo, Y.; Zhu, G. PH-Triggered Controlled Drug Release from Mesoporous Silica Nanoparticles via

Intracelluar Dissolution of ZnO Nanolids. *J. Am. Chem. Soc.* **2011**, *133* (23), 8778–8781.

(185) Nakazawa, J.; Smith, B. J.; Stack, T. D. P. Discrete Complexes Immnolilized onto Click-SBA-15 Silica: Controllable Loadings and the Impact of Surface Coverage on Catalysis. *J. Am. Chem. Soc.* **2013**, *134* (5), 2750–2759.

(186) Mosher, D. *Fibronectin*, Elsevier.; 2012.

Chapter V. Conclusions

This page left blank intentionally

Conclusions

Mesoporous silica nanoparticles have been synthesized with optimized pore sizes for the fitting of specific proteins which avoid the pre-release of loaded drugs. The system is simultaneously efficient for the preferably uptake to hepatic cancerous cells as compared to healthy hepatic ones.

Firstly, MSN have been synthesized with different synthetic properties using a design of experiences.

- A DOE has been used to obtain monodisperse mesoporous silica nanoparticles with defined properties and elucidate the factors with higher influence in their synthesis. This opens the door to the design of MSN with specific properties for desired applications

- Surface chemistry was applied to the samples in order to evaluate the capacity of change in their synthetic identity. For these modifications isothiocyanate, BOC, PEG and oleyl group were employed. Results have shown that it is possible to obtain different synthetic identities through these surface modifications.

The incubation of the different synthetic identities in protein-rich mediums led to the obtaining of various biological identities. The protein corona of these nanoparticles has been developed, quantified, characterized, and tested.

- NanoDSC and ITC have been used for the characterization of the relationship between the sizes of MSN's pores and proteins forming the PC. These techniques have allowed the understanding of the protein's behaviour with regard to MSN pores.

- The use of nanoDSC and ITC can determine the percentage of proteins forming the PC which are inside the pore and, consequently, stabilized

- Proteins that have sizes small enough to enter inside the pore are stabilized there. Conversely, proteins that are adsorbed on the NP surface are destabilized by the same surface.

In vitro proof of concept of the influence of the surface identity in the physiological response has been studied. Different cells lines have been tested to determine the effect of the PC in the cellular uptake and cytotoxicity of MSN.

- *In vitro* assays demonstrated the decreasing in the uptake of MSN when having PC in their surface. In addition, the quantification of proteins internalised by cells was achieved using HSA-FITC and corroborated that the less proteins were in the surface the more nanoparticles entered in the cells.

- As widely reported in bibliography, our *in vitro* assays demonstrated that MSN do not show significant cytotoxicity in HeLa cells.

- NPs loaded with DOX showed an interaction between this drug and HSA, causing a partial protein destabilization and subsequently the undesirable premature release of DOX. As a consequence, a boost in the release of DOX was observed because of the mentioned interaction.

- This undesired destabilization of the albumin due to the interaction with the drug can be solved using a drug that does not affect negatively the HSA structure, such as 5-FU. The blocking of the loaded drug (5-FU) controlled by HSA was possible when the ratio between protein and pore size was adequate. If the pore was big enough to fit the protein, the system presented a release similar to the nanoparticles without PC.

- MSN loaded with 5-FU present a lower toxicity in healthy cells (AML12) than in tumour cells (HepG2) as compared to the drug administrated without any nanoparticle. This means that cancer cells will be attacked and, consequently killed, with higher affinity than normal cells.

This page left blank intentionally